USER MANUAL

CR-SIM SOFTWARE v 4.0

Radar Science Group
radarscience.weebly.com

mariko.oue@stonybrook.edu
pavlos.kollias@stonybrook.edu

CONTENT

LIST OF TABLES

LIST OF FIGURES

1 Introduction

The **CR-SIM** uses the inputs from the high resolution **W**eather **R**esearch and **F**orecasting Model (**WRF**), for microphysical schemes MP_PHYSICS=8 (Thompson scheme), MP_PHYSICS=10 (Morrison double-moment scheme), MP_PHYSICS=9 (Milbrandt and Yau double-moment scheme), MP_PHYSICS=20 (bin explicit scheme), and MP_PHYSICS=50 (Predicted particle properties scheme) and computes "idealized" forward modeled scanning (or vertical-pointing) radar observations (Figure 1) and profiling lidar observables. The latest version can use the inputs from the **ICO**sahedral **N**on-hydrostatic general circulation model (**ICON,** MP_PHYSICS=30) and the **R**egional **A**tmospheric **M**odeling **S**ystem (**RAMS**, MP_PHYSICS=40), **S**ystem for **A**tmospheric **M**odeling (**SAM**, MP_PHYSICS=70 for bin microphysics, MP_PHYSICS=75 for Morrison double-moment scheme), and NCAR Cloud Model 1 (CM1, MP_PHYSICS=80). The microphysical packages currently implemented in the CR-SIM are shown in Table 1. The idea behind CR-SIM is to create an accurate radar forward model operator consistent with WRF microphysics (now integrating ICON and RAMS 2-moment microphysics) that converts the model variables into the form of radar observations and thus to enable the direct comparison between WRF output and radar and lidar observations. Simulated radar and lidar observables are applied to produce additional products (e.g. multi-sensor cloud location) in post processing. The CR-SIM can be applied in order to reproduce characteristic (polarimetric) signatures commonly found in (polarimetric) radar/lidar observations and examine the performance of different microphysical schemes and also to examine the assumptions related to scattering characteristics of observed cloud and precipitation systems.

Table 1: The microphysical packages currently implemented in the CR-SIM

MP_PHYSIC	Model	Microphysical scheme	Hydrometeor Types	Scattering Type Names (Default configuration; see Table 17 for more information)
9	WRF	Milbrandt and Yau double-moment scheme	Cloud Rain Ice Snow Graupel Hail	"cloud" "rainb" "ice_ar0.20" "snow_ar0.60" "gh_ryzh" "gh_ryzh"
10 **[101 if hail instead of graupel is defined]**	WRF	Morrison double-moment scheme	Cloud Rain Ice Snow Graupel OR Hail	"cloud" "rainb" "ice_ar0.20" "snow_ar0.60" "gh_ryzh"
8	WRF	Thompson scheme	Cloud Rain Ice Snow Graupel	"cloud" "rainb" "ice_ar0.20" "snow_ar0.60" "gh_ryzh"
50	WRF	Predicted Particle Properties (P3) scheme	Cloud Rain Small ice Unrimed Ice Graupel Partially rimed Ice	"cloud" "raina" "smallice" "unrimed_ice_ar0.60" "graupel" "partrimedice_ar0.60"
30	ICON	Seifert and Beheng 2-moment microphysical scheme	Cloud Rain Ice Snow Graupel Hail	"cloud" "rainb" "ice_ar0.20" "snow_ar0.60" "gh_ryzh" "gh_ryzh"
40	RAMS	2-moment microphysical scheme	Cloud Rain Ice Snow Graupel Hail Drizzle Aggregates	"cloud" "rainb" "ice_ar0.20" "snow_ar0.60" "gh_ryzh" "gh_ryzh" "cloud" "snow_ar060"
75	SAM	Morrison 2-moment microphysical scheme	Cloud Rain Ice Snow Graupel	"cloud" "rainb" "ice_ar0.20" "snow_ar0.60" "gh_ryzh"
80	CM1	Morrison 2-moment microphysical scheme	Cloud Rain Ice Snow Graupel	"cloud" "rainb" "ice_ar0.20" "snow_ar0.60" "gh_ryzh"
	Spectral bin-explicit schemes			
20	WRF	fast spectral-bin microphysics scheme	Cloud Rain Ice Snow Graupel Hail	"cloud" "rainb" "ice_ar0.20" "snow_ar0.60" "gh_ryzh" "gh_ryzh"

70	SAM	spectral-bin microphysics scheme	Cloud Rain Ice Snow Graupel Hail	"cloud" "rainb" "ice_ar0.20" "snow_ar0.60" "gh_ryzh" "gh_ryzh"

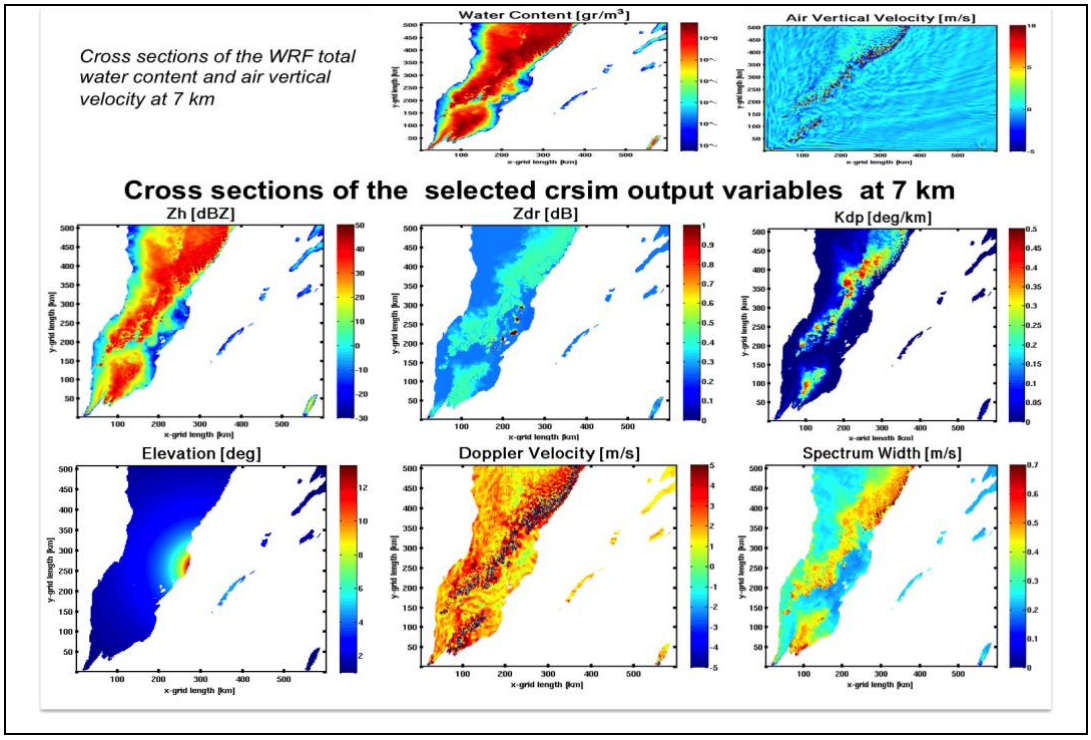

Figure 1: Illustration of the CR-SIM output: cross section of the selected CR-SIM output variables at 7 *km*.

The CR-SIM is written in FORTRAN and uses as input the WRF prognostic mass and number variables in the case of double-moment microphysics schemes or the explicit (bin) microphysics for the bin explicit scheme. The list of needed WRF input variables and the exact format of the CR-SIM input are given in Sections 3.2 and 4.1, while the details about the WRF microphysical schemes used by CR-SIM are described in Sections 4.2 and 4.3.

The CR-SIM employs the T-matrix method for computation of scattering characteristics for cloud water, cloud ice, rain, snow, graupel and hail and allows the

specifications of the following radar frequencies for scattering calculations: 3 *GHz*, 5.5 *GHz*, 9.5 *GHz*, 35 *GHz* and 94 *GHz*.

Given the particles size distributions (explicit or reconstructed from the provided PSD moments), polarimetric radar variables can be calculated if the scattering amplitudes are known. The complex scattering amplitudes are pre-computed and stored as look-up tables (LUTs) for equally spaced particle sizes using the Mishchenko's T-matrix code for a non-spherical particle at a fixed orientation (Mishchenko, 2000) and for elevation angles from 0° to 90° with a spacing of 1°, for specified radar frequencies, temperatures and different possibilities of particles densities and aspect ratios. A hydrometeor class for which the look-up tables were pre-built by setting a fixed number of assumptions prior to running the T-matrix is referred as the "scattering type". Each hydrometeor category present in the WRF output has to be assigned to the corresponding scattering type in the Configuration File. For example, if the oblateness of raindrops is assumed to change with size according to Brandes et al. (2002), the scattering type that has to be chosen is "*rainb*", while, if it is assumed that the rain aspect ratio increases with size as in Andsager et al. (1999), the assigned scattering type would be "*raina*". The details about the built look-up tables and present scattering types are given in Section 4.4. This approach involving the assigning of the specific scattering type to each WRF hydrometeor class in the Configuration File allows an addition of the new look-up tables without the need to change the CR-SIM source code.

It is worth noting that some particle characteristics needed to simulate polarimetric variables such as the shape or the statistical properties of the particle orientations are not explicitly specified in the WRF. Thus, certain assumptions have to be made, based on much available information as possible. For example, the mean canting angles of all hydrometeors are assumed to be 0°. This is a reasonable assumption and it enables the use of Ryzhkov et al. (2011) formulations for computation of polarimetric variables and especially the use of simple expressions for the angular moments, which in turn make possible that the width of 2D Gaussian distribution of canting angle that is different for various hydrometeor species can be specified in a case-by-case basis in the Configuration

File. Detailed information of T-matrix calculations and the method used in computing the scattering characteristics is given in Sections 4.4 and 4.5.

The polarimetric variables simulated include reflectivity at vertical and horizontal polarization, differential reflectivity, specific differential phase, specific attenuation at horizontal and vertical polarization, specific differential attenuation, linear depolarization ratio, cross-correlation coefficient and backscatter differential phase (Section 4.5). The simulated variables also include reflectivity weighted velocity, mean Doppler velocity and spectrum width. The computation of fall velocities is consistent to the computational method used in the specific WRF, ICON, and RAMS microphysical packages (Sections 4.2 and 4.3). The complete list of output variables is given in Tables 6 and 7 (Section 3.3.1). The output produced by the CR-SIM is a set of NetCDF files, one per each hydrometeor's specie, and the one for the total hydrometeor.

If you use the CR-SIM software to simulate WRF data used in publication, an acknowledgment would be appreciated. If you have any comments, suggestions for improvements, bug fixes or you need help to interface CR-SIM with your model output, please contact us (mariko.oue@stonybrook.edu; pavlos.kollias@stonybrook.edu).

ACKNOWLEDGMENT

We would like to thank Ms. Aleksandra Tatarević, the original lead developer of CR-SIM. We would also like to thank Dr. H. Morrison, Dr. Z. Feng and Dr. J. Fan for providing the WRF output data and for their valuable comments, suggestions and encouragement. Our thanks are extended to Dr. M. Mech, Dr. P. Marinescu, Dr. T. Yamaguchi, and Dr. J. Peters for providing the ICON, RAMS, SAM, and CM1 output data, respectively, and for their valuable comments. The ICON LES data was produced within the "High Definition Clouds and Precipitation for advancing Climate Prediction" project, which is funded by the

German Federal Ministry of Education and Research within the framework program "Research for Sustainable Development (FONA)", under the FKZ: FKZ: 01LK1211A/C. We also would like to thank Dr. J. Vivekanandan for his Mueller-matrix-based code and M. I. Mishchenko for making his T-matrix codes public and freely available for research purposes. We also thank Dr. Dié Wang for incorporating the P3 microphysics, Dr, Kwang-Min Yu for optimizing the code, Dr. Kwonil Kim and Mr. Bernat P. Treserras for their contributions to surface backscatter calculations.

2 Installation

2.1 Programming language and dependencies

The coding language is a superset of Fortran 95 standard that includes all of the extensions supported by GNU Fortran. We tested CR-SIM compilation with the GCC version 4.7.2 20121015 (Red Hat 4.7.2-5).

Libraries(dependencies)

- gcc (GCC) 4.7.2 20121015 (Red Hat 4.7.2-5)
- GNU Autoconf 2.63
- GNU Automake 1.11.1
- NETCDF-C v4.4.1.1– C library needed to write NetCDF files
- HDF5 v1.8.16 – library needed by NetCDF
- NETCDF–FORTRAN v4.4.4 – Fortran library needed to write NetCDF files
- NCCMP – This library is optional and is a tool to perform numerical comparisons between two given NetCDF products and used only for testing purposes. Download is available on http://nccmp.sourceforge.net/. Version used is 1.8.2.0.

2.2 Configuration, compilation and installation

Get the latest version of the Fortran CR-SIM release. The source file is named crsim_[release version].tar.gz. The following steps are required to install, compile and run the CR-SIM software on a Linux platform:

1. Unpack the model by typing the following:

   tar –zxvf crsim_[release version].tar.gz

The main directory structure of the distribution package is shown in Table 2.

Table 2: Main distribution of the CR-SIM directories

Name	***Description***
crsim-[release_version]	model root
src	Source code
etc	configuration file
bin	binary file (executable)
share/crsim/aux	Scattering lookup tables and other auxiliary files
share/crsim/test	Test data and test scripts and reference data sets obtained on the developer machine
doc	CR-SIM documentation

The directory **share/crsim/aux/** is a default location for the scattering look-up tables and other auxiliary data files. The scattering look-up tables must be downloaded from https://doi.org/10.5281/zenodo.13345093 (Oue, 2024) before running crsim. For more details, see Section 4.4.

Main distribution of *f90 files in the distribution source directory is shown in Table 3.

Table 3: The list of CR-SIM FORTRAN source files

Name	***Description***
crsim.f90	Main code
crsim_subrs.f90	The collection of subroutines needed for computation of forward radar variables
ReadConfParameters.f90	It contains subroutine for reading and storing information given in the Configuration File
ReadInpWRFFile.f90	The collection of subroutines for reading the WRF input NetCDF data files
WriteOutNetcdf.f90	The collection of subroutines for writing the output NetCDF data files
crsim_luts_mod.f90	Module that contains stored information related to LUTs
crsim_mod.f90	Module that contains a number of subroutines for defining, (de-) allocating, and nullifying (or setting to the missed value) real data types used for computation of the crsim radar variables
wrf_rvar_mod.f90	Module that contains a number of subroutines for defining, (de-) allocating, and nullifying (or setting to the missed value) data types associated to the input WRF data fields

wrf_var_mod.f90	Module that contains the same types and routine as wrf_rvar_mod.f90 but in double precision
ReadInpRAMSFile.f90	The collection of subroutines for reading the RAMS and SAM data files
crsim_subrs_postprocess.f90	The collection of subroutines needed for computation of virtual observational variables (e.g., ARSCL, LWP)
postprocess_mod.f90	Module that contains subroutines for defining, (de-) allocating, and nullifying (or setting to the missed value) data types used for computation of the virtual observational variables
phys_param_mod.f90	Module that contains physical parameters and constants used throughout the CR-SIM.
crsim_subrs_airborne.f90	The collection of subroutines for computing parameters related to airborne radar simulations.

2. Go to the top level directory of the newly created *crsim-[release version]*
3. Configure the build by defining following:

   NETCDF=<netcdf4_library_location>
   NETCDF_FORTRAN=<netcdf_fortran_library_location>
   NCCMP=<NCCMP_library_location>
   INSTDIR=<installation_directory>

and run the configure script as follows:

./configure —with-netcdf=$NETCDF —with-netcdf-fortran=$NETCDF_FORTRAN —with-nccmp=$NCCMP —prefix=$INSTDIR

A sample call is as follows:

```
./configure —with-netcdf=/storage2/starbuck/packages/netcdf —with-

netcdf_fortran=/storage2/starbuck/packages/netcdf —with-nccmp=/usr/local/bin —

prefix=/storage2/starbuck/itest
```

Note that the NCCMP is not a mandatory library. If this library is not found (either on the system or on the specified path), the configure script will issue a warning saying that one or more tests will fail because the comparison between the reference output data sets and the output created on your system during the test runs will not be possible.

4. Possible options when invoking “configure”

--disable-openmp

The OpenMP library is mandatory for CR-SIM and it is enabled by default. However, user can reject OpenMP support and run the code serially by specifying the option “—disable-openmp” when invoking “configure”.

--without-preloadlut

The default compilation flag is “-D__PRELOAD_LUT__” which accelerates the code by loading all the scattering lookup tables (LUTs) in memory before the main computation part and is supported with OpenMP. However, user can disable this flag in configuration time by specifying the option “—without-preloadlut”.

This option should be specified in situation when there is a concern that there is not enough memory in user system to store the LUT data.

If “—without-preloadlut” is specified when invoking “configure”, the option “—disable-openmp” has also to be specified. If not, the configure script will report an error and stop configuration.

Our recommendations

- The configuration options MP_PHYSICS=20, MP_PHYSICS=50, and MP_PHYSICS=70 are not yet **fully** supported with OpenMP. You may specify “—without-preloadlut —disable-openmp” in configure time. However, it is possible and recommendable to execute the code in the standard configuration – with OpenMP and including “-D__PRELOAD_LUT__” compilation option – although the configuration options MP_PHYSICS=20, MP_PHYSICS=50, or MP_PHYSICS=70 (Section 3.1, Table 5) are planned to be used when executing the CR-SIM. To do so you have to be aware that the

configuration parameter OMPThreadNum has to be equal to one (See Section 3.1 and Table 5 for more details).

- If you want to use this software with differently specified options in configure time, you have to repeat the procedure *configure –>make –> make install* described here. Before doing so we recommend to enter to the source directory (src) and type "make clean" which will remove all *.o and *.mod files.

5. Build the executable by typing

   make

   This creates the executable file crsim under ./bin/.

6. Check the build with:

   make check

7. Install the software in the directory specified by "—prefix" argument:

   make install

   This will install the following:

- Executable crsim in the bin directory:
  <installation_directory>/bin/crsim

- Configuration file in the etc directory:
  <installation_directory>/etc/ PARAMETERS

- Software license, the README file and INSTALL.txt will be produced in share/crsim/ directory
  <installation_directory>/share/crsim/LICENSE
  <installation_directory>/share/crsim /README
<installation_directory>/share/crsim/ INSTALL.txt

- CRSIM Software User Manual in share/doc/crsim/ directory:
  <installation_directory>/share/doc/crsim/crsim_*v*.pdf

- Auxiliary data (contained in the directories LLUTS3, P3 and SBM_20) in the share/crsim/aux/ directory:

installation_directory>/share/crsim/aux/LLUTS3/
installation_directory>/share/crsim/aux/P3/
installation_directory>/share/crsim/aux/SBM_20/

- Test data, test scripts and test configuration files in the share/crsim/test directory:
  <installation_directory>/share/crsim/test/

8. Run the tests using the executable and input/output data files from the directory specified by "—prefix" argument

   make installcheck

   Those test runs include MP-10, MP-50, and MP-40. Note that these test runs use OpenMP for MP-10 and MP-40. If OpenMP was disabled at the compilation, the test runs may be failure.

2.2.1 Important notice when running the test scripts

You can execute the tests scripts either from the distribution directory (***make check***) or from the installation directory (***make installcheck***). You can also do this manually: go to the test directory (**share/crsim/test/** and/or **<installation_directory>/share/crsim/test/** and execute the test script(s) you see there. For example, to execute the test run with Morrison's double moment scheme (MP_PHYSICS=10), execute the test1:

sh test1.sh

The scripts testing the different options when running the CR-SIM will be progressively added in CR-SIM package. Note that these test runs use OpenMP for MP-10 (test 1) and MP-40 (test 3). If OpenMP was disabled at the compilation, the test runs may be failure.

To run the test scripts, you must download the test input and output files from https://doi.org/10.5281/zenodo.13346381. The dataset includes:

- **crsimtest1_inp_MP10.tar.gz** includes input files for Test-1 with the microphysical option MP10 (WRF Morrison microphysics)
- **crsimtest2_inp_MP50.tar.gz** includes input files for Test-2 with the microphysical option MP50 (WRF P3 microphysics)
- **crsimtest3_inp_MP40.tar.gz** includes input files for Test-3 with the microphysical option MP40 (RAMS Morrison microphysics)
- **crsimtest1_out_ref_MP10.tar.gz** includes example output files for Test-1 with the microphysical option MP10 (WRF Morrison microphysics)
- **crsimtest2_out_ref _MP50.tar.gz** includes example output files for Test-2 with the microphysical option MP50 (WRF P3 microphysics)
- **crsimtest3_out_ref _MP40.tar.gz** includes example output files for Test-3 with the microphysical option MP40 (RAMS Morrison microphysics)

The sample input files (crsimtest*_inp_*tar.gz) must be untared under ./inp, and the input model data and configuration files will be under [model name]_MP[microphysics option]/. The sample output files (crsimtest*_out_ref_*tar.gz) must be untared under ./out_ref

2.3 Execution

The general convention for invoking a model is via a command shell. The general format of the calling command is as follows:

```
executable configuration_file input_file_1,input_file_2,input_file_3  output_file
```

The first argument is the name of the binary (or executable shell-script). The first block is the name of the configuration file. The next group of command-line argument is a comma-separated list of input data file names while the last group of command-line arguments is the name of the main output data file. “input_file_2,input_file_3” will be required as needed for microphysics scheme. Note that: (1) each block is separated by a single blank space, and (2) file names shall not include blank spaces.

The existence of a configuration file is mandatory. Prior to the crsim execution, you have to edit the configuration file (PARAMETERS). For more details about Configuration File, see Section 3.1.

An example for the command line argument structure is given bellow:

***crsim* ConfigurationFile WRFInputFile,WRFmpInputFile OutFile**

where "***crsim***" is the name of executable and the meaning of the other command line arguments is given in Table 4. Please note that the **WRFmpInputFile** is the mandatory input only when configuration parameters MP_PHYSICS is equal to 20, 40, or 70; in all other cases the execution can be simply invoked with:

***crsim* ConfigurationFile WRFInputFile OutFile**

where it is implicitly assumed that the content of **WRFInputFile** is identical to content of **WRFmpInputFile,** so duplication of files in the command line is avoided.

Table 4: CR-SIM command line arguments

Command Line Parameter	***Format***	***Aim***	***Description***
ConfigurationFile	ASCII	Mandatory Input	Configuration file. The input configuration parameters are described in Section 3.1)
WRFInputFile	NetCDF	Mandatory Input	This file is the same for all microphysical packages and contains the environmental variables needed (like temperature, pressure, etc.). are read. For the complete list of the required variables, see Section 3.2). It is recommended that it also contains the prognostic 2-moments variables (mass and total number concentration) for existing hydrometeor categories.
WRFmpInputFile	NetCDF (exception: ASCII for	Optional Input (exception: Mandatory input for	MP_PHYSICS=20: The name of the spectral WRF NetCDF input file with explicit microphysics; MP_PHYSICS=40: The name of the RAMS header text file; MP_PHYSICS=70: The name of the SAM text file describing mass and diameter bins;

	MP_PHYSICS=40 or 70)	MP_PHYSICS= 20, 40, and 70)	MP_PHYSICS=75: The name of the SAM NetCDF file for profile data; or with the prognostic 2-moments variables (mass and total number concentration) for existing hydrometeor categories for all other microphysical packages. It can be omitted from the command line if the prognostic moments are already present in the WRFInputFile.
ProfileInputFile	NetCDF	Optional Input for MP_PHYSICS=75	MP_PHYSICS=70: The name of the SAM NetCDF file for profile data
OutFile	NetCDF	Output	The name of the main output file. The main output file is the one that refers to the CR-SIM output for the total hydrometeor content. The 5 (for MP_PHYSICS=8, 10, 75, 80, and 20), 6 (for MP_PHYSICS=9, 30 and 50), 8 (for MP_PHYSICS=40), or 2 (for MP_PHYSICS=70) additional output files will be created for each hydrometeor class. Per default, they will have extensions "_cloud", "_rain", "_ice", "_snow", " _graupel", "_hail", "drizzle", and "aggregate" (for MP_PHYSICS=8, 9, 10, 30, 40, 70, 75, 80, and 20) or "_cloud", "_rain", "_smallice", "_unrimedice", "_graupel", and "_parimedice" (for MP_PHYSICS=50) before the extension.

An example script is given in the test directory "run_crsim.sh". It demonstrates how to execute the code via command line arguments. You would only need to edit the names of configuration, input and output file. Prior to the crsim execution, you have to edit the configuration file (etc/PARAMETERS).

2.4 Processor Speed

A significant effort has been devoted to an increase of the processor speed. This is achieved via partial parallelization of the CR-SIM and modification of the way how the scattering libraries are assessed by the reading routines.

The OpenMP library is mandatory library for CR-SIM 3.xx releases. The processing speed will depend on number of OpenMP threads used and this number is configurable (see Table 5 for more details).

The simulation run time has been speeded up by the "-D__PRELOAD_LUT__" compilation option. This option turns on preloading all scattering lookup tables at the beginning of the processing and before all major computational blocks. In this loading on memory, only necessary LUT files are accessed from the file system. Therefore, file accessing time from file system is importantly reduced. In addition, this option is supported with OpenMP parallelization. In other words, when compiled with the "-D__PRELOAD_LUT__" option, OpenMP is automatically used. Note that both options are the default option in configure time.

With "-D__PRELOAD_LUT__" compile flag, the code can be significantly accelerated, but, on another side, enough memory would be needed in user system to store the LUT data.

However, user can disable this flag by specifying the option "—without-preloadlut" in configure time.

If "—without-preloadlut" is specified when invoking "configure", the option "—disable-openmp" has also to be specified. If not, the configure script will report an error and stop configuration.

3 I/O structure

3.1 CR-SIM Input configuration parameters

The format of the configulation file is updated for CR-SIM V4.0. The parameters that have to be edited in the Configuration File (PARAMETERS) are listed in Table 5. The crsim/etc directory includes some examples of the configuration file.

Table 5: CR-SIM configuration parameters

Variable	*Description*
OMPThreadNum	The number of OpenMP threads. OpenMP parallelization works only when "__PRELOAD_LUT__" flag is on (See 2.2 and 2.4). If negative, it would be set to 1 and if too large, it would be set to maximal number of OpenMP threads in User system. It is reset to one in the case of not supported microphysics (MP_PHYSICS =20 and MP_PHYSICS =50).
It	Selected time step in the WRFInputFile for which the CR-SIM will be executed. Per default, it=1.
Ix_start, ix_end	The starting and ending indices of the domain in **x**-direction (E-W) defining a subdomain to be extracted from WRFInputFile for the CR-SIM simulation. If the first index is negative, all grid points in E-W direction are considered. Both ix_start, ix_end refer to the WRF "mass" grid points, i.e. where the mass variables are defined.
Iy_start, iy_end	The starting and ending indices of the domain in **y**-direction (S-N) defining a subdomain to be extracted from WRFInputFile for the CR-SIM simulation. If the first index is negative, all grid points in S-N direction are considered. Both iy_start, iy_end refer to the WRF "mass" grid points, i.e. where the mass variables are defined.
Iz_start, iz_end	The starting and ending indices of the domain in z-direction (vertical) defining a subdomain to be extracted from WRFInputFile for the CR-SIM simulation. If the first index is negative, all vertical levels are considered.
MP_PHYSICS	The model microphysics scheme. Possible options are 8, 9, 10, 20, 30, 40, 50, 70, 75, and 80 (See Table 1 for more details). Due

	to the code architecture, it is straightforward to add other MP_PHYSICS options.
Ixc, iyc	Horizontal indices of the scanning radar's position. Radar can be placed at any horizontal grid point in the WRFInputFile, independently of the horizontal extent of the extracted scene defined by the indices ix_start, ix_end, iy_start and iy_end. The options ixc <=-999 or iyc <= -999 are reserved for down looking radar at airplane flying either along x axis at y=yc and scanning perpendicularly from -90 to +90 or along y axis at x=xc and scanning perpendicularly from -90 to +90.
Zc	Height of the radar in meters. Per default zc=0 meters.
Hydro_luts(5) for MP_PHYSICS=8, 10, 20, 75, and 80 OR hydro_luts(6) for MP_PHYSICS=9, 30 and 50 OR hydro_luts(8) for MP_PHYSICS=40 OR hydro_luts(2) for MP_PHYSICS=70	Names of scattering species assigned to hydrometer classes. The number of scattering species has to be equal to 5 for MP_PHYSICS=8, 10, 20, 75, and 80, equal to 6 for MP_PHYSICS=9, 30 and 50, equal to 8 for MP_PHYSICS=40, or equal to 2 for MP_PHYSICS=70. The names of scattering species are order sensitive and have to correspond to cloud, rain, ice, snow, graupel, and hail for MP_PHYSICS=8, 9, 10, 30, 20, 70, 75, and 80 (cloud, rain, small ice, unrimed ice, graupel and partial rimed ice for MP_PHYSICS=50), respectively, and plus drizzle(7) and aggregate(8) for MP_PHYSICS=40. Note that the names of scattering species correspond to directory names in the scattering LUTs. See Table 15 for the full list of scattering species that might be assigned to different hydrometeor categories.
Thr_mix_ratio(5) for MP_PHYSICS=8, 10, 20, 75, and 80 OR thr_mix_ratio(6) for MP_PHYSICS=9, 30 and 50 OR thr_mix_ratio(8) for MP_PHYSICS=40 OR thr_mix_ratio(2) for MP_PHYSICS=70	The minimum thresholds of the input mixing ratio for the crsim simulation. The input values of mixing ratios <= than specified threshold will be set to 0. Order has to be 1-cloud, 2-rain, 3-ice, 4-snow, 5-graupel and 6 –hail (1-cloud, 2-rain, 3-small ice, 4-unrimed ice, 5-graupel and 6–partial rimed ice for MP_PHYSICS=50), and 7-drizzle and 8-aggregate for MP_PHYSICS=40.
horientID(5) for MP_PHYSICS=8, 10, 20, 75, and 80 OR horientID(6) for MP_PHYSICS=9, 30 and 50 OR horientID(8) for MP_PHYSICS=40 OR horientID(2) for MP_PHYSICS=70	Choice of the distribution of particle orientation for 5 (MP_PHYSICS=8, 10, 20, 75, and 80), 6 (MP_PHYSICS=9, 30 and 50) 8 (MP_PHYSICS=40), or 2 (MP_PHYSICS=70) hydrometeor classes. The order is the same as for thr_mix_ratio. Possible values of this parameter are: =1 for fully chaotic orientation=2 for random orientation in horizontal plane and=3 for two-dimensional axisymmetric Gaussian distribution of orientation with zero mean and sigma standard deviation. The default value of horientID is 3 for all hydrometeors.
Sigma(5) for MP_PHYSICS=8, , 20, 75, and 80 OR	The width in degrees of the 2D Gaussian distribution of orientation with zero mean for 5 (MP_PHYSICS=8, 10, 20, 75, and 80), 6 (MP_PHYSICS=9, 30 and 50), 8

sigma(6) for MP_PHYSICS=9, 30 and 40 OR sigma (8) for MP_PHYSICS=40 OR sigma (2) for MP_PHYSICS=70	(MP_PHYSICS=40), or 2 (MP_PHYSICS=70) hydrometeor classes. The order is the same as for thr_mix_ratio. The default values are 10° for cloud, rain and ice and 40° for dry snowflakes, unrimed ice, partial rimed ice, graupel and hail. This option is valid only if horientID=3 for specific hydrometeor category and is disregarded otherwise.
Freq	Radar frequency in *GHz*. Possible values are 3 *GHz*, 5.5 *GHz*, 9.5 *GHz*, 35 *GHz* and 94 *GHz*.
Elev	Elevation given in degrees. It can be negative (Option 1) or set to any value in the range -90°-90° (Option 2). Option 1, scanning mode: If elev<=-999 elevation of each grid point is determined relatively to the position of radar origin (determined with ixc, iyc and zc). Option 2, fixed elevation: If elev is -90≤elev≤90 (Option 2), then each WRF grid point will be "observed" at this fixed value of elevation. For example, elev=90 for vertically pointing mode, or elev=60 for the case where each WRF grid point is observed at elevation of 60 degrees. The position of the radar origin is disregarded in the option 2.
radID	=1 to turn off the computation of polarimetric variables. In this output would consist of reflectivity, mean Doppler velocity, reflectivity weighted velocity, spectrum width and specific attenuation. ≠1 the full polarimetric output is written See Section 3.3 for more details.
Theta1	Radar beamwidth (i.e. one-way angular resolution) in degrees
Dr	Radar range resolution in meters
ZMIN	Value of coefficient ZMIN in relation dBZ_min(*dBZ*)=ZMIN(*dBZ*)+20 log10 (range in *km*)
ceiloID	Whether (ceiloID=1) or not (ceiloID=0) to introduce cloud lidar (ceilometer, *fr*=905 *nm*)
mplID	Whether (mplID>0) or not (mplID=0) to introduce micro pulse lidar (MPL, mplID=1 for *fr*=353 *nm*, mplID=2 for *fr*=532 *nm*)
aeroID	Whether (aeroID>0) or not (aeroID=0) to introduce aerosol backscatter into MPL backscatter
aero_tau	Cloud optical depth used to normalize aerosol extinction profile, if negative, do not normalize
aero_lidar_ratio	Constant for aerosol lidar ratio
spectraID	Whether (spectraID=1) or not (spectraID≠1) to introduce Doppler spectrum simulation
airborneID	Whether (airborneID ==1) or not (airborneID \=1) to introduce computing airborne radar variables ((surface backscatter and airplane radial \ velocity).

airborne_spd, airborne_azdeg, airborne_eldeg	Airplane speed (m/s) and az/el directions (degrees from north/ degrees from horizon). Ignored if airborneID \=1.
pulse_len	pulse length (m). default is 100 m. Ignored if airborneID \=1.
mwr_view	Microwave radiometer's field of view in degrees
mwr_alt	Altitude of microwave radiometer in meters

3.2 CR-SIM Input data

The list of required input files and its variables is shown in Table 6.

Table 6: List of input files and input variables

INPUT FILE	*VARIABLE*	*DIMENSION*	*UNITS*	*DESCRIPTION*
Naming convention	**MP_PHYSICS=8, 9, 10, 30, 20, and 50** Example: wrfout_d01_2011-05-20_08:00:00			
WRFInputFile	**RDX**	Time	m^{-1}	Inverse x grid length If this is not available, dx is read from global attribute (e.g. for ICON)
WRFInputFile	**RDY**	Time	m^{-1}	Inverse y grid length If this is not available, dy is read from global attribute (e.g. for ICON)
WRFInputFile	**XLAT**	west_east, south_north, bottom_top, Time	degree north	Latitude (south is negative)
WRFInputFile	**XLONG**	west_east, south_north, bottom_top, Time	degree east	Longitude (west is negative)
WRFInputFile	**U**	west_east_stag, south_north, bottom_top, Time	$m\ s^{-1}$	x-wind component
WRFInputFile	**V**	west_east, south_north_stag, bottom_top, Time	$m\ s^{-1}$	x-wind component
WRFInputFile	**W**	west_east, south_north, bottom_top_stag, Time	$m\ s^{-1}$	z-wind component
WRFInputFile	**TKE (TKE_PBL)**	west_east, south_north, bottom_top, Time	$m^2\ s^{-2}$	Turbulence kinetic energy

WRFInputFile	**PB**	west_east, south_north, bottom_top, Time	*Pa*	Base state pressure
WRFInputFile	**P**	west_east, south_north, bottom_top, Time	*Pa*	Perturbation pressure
WRFInputFile	**ALT**	west_east, south_north, bottom_top, Time	$m^3\ kg^{-1}$	Inverse density of dry air
WRFInputFile	**T**	west_east, south_north, bottom_top, Time	*K*	Perturbation potential temperature (theta-t0)
WRFInputFile	**PHB**	west_east, south_north, bottom_top_stag, Time	$m^2\ s^{-2}$	Base-state geopotential
WRFInputFile	**PH**	west_east, south_north, bottom_top_stag, Time	$m^2\ s^{-2}$	Perturbation geopotential
WRFInputFile	**QVAPOR**	west_east, south_north, bottom_top, Time	$kg\ kg^{-1}$	Water vapor mixing ratio
Naming convention	**MP_PHYSICS = 9, 10, 30** Example: wrfout_d01_2011-05-20_08:00:00			
WRFmpInputFile	**QCLOUD**	west_east, south_north, bottom_top, Time	$kg\ kg^{-1}$	Cloud water mixing ratio
WRFmpInputFile	**QRAIN**	west_east, south_north, bottom_top, Time	$kg\ kg^{-1}$	Rain water mixing ratio
WRFmpInputFile	**QICE**	west_east, south_north, bottom_top, Time	$kg\ kg^{-1}$	Ice mixing ratio
WRFmpInputFile	**QSNOW**	west_east, south_north, bottom_top, Time	$kg\ kg^{-1}$	Snow mixing ratio
WRFmpInputFile	**QGRAUP**	west_east, south_north, bottom_top, Time	$kg\ kg^{-1}$	Graupel mixing ratio
WRFmpInputFile	**QHAIL**	west_east, south_north, bottom_top, Time	$kg\ kg^{-1}$	Hail mixing ratio
WRFmpInputFile	**QNCLOUD**	west_east, south_north, bottom_top, Time	kg^{-1}	Cloud mass number concentration
WRFmpInputFile	**QNRAIN**	west_east, south_north, bottom_top, Time	kg^{-1}	Rain mass number concentration
WRFmpInputFile	**QNICE**	west_east, south_north, bottom_top, Time	kg^{-1}	Ice mass number concentration

WRFmpInputFile	**QNSNOW**	west_east, south_north, bottom_top, Time	kg^{-1}	Snow mass number concentration
WRFmpInputFile	**QNGRAUP**	west_east, south_north, bottom_top, Time	kg^{-1}	Graupel mass number concentration
WRFmpInputFile	**QNHAIL**	west_east, south_north, bottom_top, Time	kg^{-1}	Hail mass number concentration
Naming convention	**MP_PHYSICS = 8**			
WRFmpInputFile	**QCLOUD**	west_east, south_north, bottom_top, Time	$kg\ kg^{-1}$	Cloud water mixing ratio
WRFmpInputFile	**QRAIN**	west_east, south_north, bottom_top, Time	$kg\ kg^{-1}$	Rain water mixing ratio
WRFmpInputFile	**QICE**	west_east, south_north, bottom_top, Time	$kg\ kg^{-1}$	Ice mixing ratio
WRFmpInputFile	**QSNOW**	west_east, south_north, bottom_top, Time	$kg\ kg^{-1}$	Snow mixing ratio
WRFmpInputFile	**QGRAUP**	west_east, south_north, bottom_top, Time	$kg\ kg^{-1}$	Graupel mixing ratio
WRFmpInputFile	**QNRAIN**	west_east, south_north, bottom_top, Time	kg^{-1}	Rain mass number concentration
WRFmpInputFile	**QNICE**	west_east, south_north, bottom_top, Time	kg^{-1}	Ice mass number concentration
Naming convention	**MP_PHYSICS = 50** Example: P3_wrfout_d01_2011-05-20_08_00_00			
WRFmpInputFile	**QCLOUD**	west_east, south_north, bottom_top, Time	$kg\ kg^{-1}$	Cloud water mixing ratio
WRFmpInputFile	**QRAIN**	west_east, south_north, bottom_top, Time	$kg\ kg^{-1}$	Rain water mixing ratio
WRFmpInputFile	**QICE**	west_east, south_north, bottom_top, Time	$kg\ kg^{-1}$	Ice mixing ratio
WRFmpInputFile	**BRIM**	west_east, south_north, bottom_top, Time	$kg\ kg^{-1}$	Rime ice mass mixing ratio
WRFmpInputFile	**QRIM**	west_east, south_north, bottom_top, Time	$m^{-3}\ kg^{-1}$	Rime ice volume mixing ratio
WRFmpInputFile	**QNRAIN**	west_east, south_north, bottom_top, Time	kg^{-1}	Rain mass number concentration
WRFmpInputFile	**QNICE**	west_east, south_north, bottom_top, Time	kg^{-1}	Ice mass number concentration

Naming convention	**MP_PHYSICS = 20** Example: wrfout_d01_0001-01-01_00:00:00			
	Example: wrfSBM_d01_0001-01-01_00-00-00			
WRFmpInputFile	**ff1**i01-**ff1**i33	west_east, south_north, bottom_top, Time	*kg kg^{-1}*	33 variables with the bin mixing ratio for cloud and rain bins
WRFmpInputFile	**ff5**i01-**ff5**i33	west_east, south_north, bottom_top, Time	*kg kg^{-1}*	33 variables with the bin mixing ratio for ice and snow bins
WRFmpInputFile	**ff6**i01-**ff6**i33	west_east, south_north, bottom_top, Time	*kg kg^{-1}*	33 variables with the bin mixing ratio for graupel bins
Naming convention	**WRF_MP_PHYSICS_20_InputFiles(1)** Example: bulkradii.asc_s_0_03_0_9			
-	-	-	*cm*	Bin radius (the format is prescribed)
Naming convention	**WRF_MP_PHYSICS_20_InputFiles(2)** Example: bulkdens.asc_s_0_03_0_9			
-	-	-	*gr cm^{-3}*	Bin density (the format is prescribed)
Naming convention	**WRF_MP_PHYSICS_20_InputFiles(3)** Example: masses.asc			
-	-	-	*gr*	Bin mass (the format is prescribed)
Naming convention	**WRF_MP_PHYSICS_20_InputFiles(4)** Example: termvels.asc			
-	-	-	*cm sec^{-1}*	Bin terminal velocity (the format is prescribed)
Naming convention	**MP_PHYSICS=40** Example: a-A-2013-06-19-210000-g3.h5			
WRFInputFile	**Phony_dim_0**	dimension		nx and ny (nx=ny)
WRFInputFile	**Phony_dim_1**	dimension		nz
WRFInputFile	**GLAT**	nx, ny	*deg*	Latitude
WRFInputFile	**GLON**	nx, ny	*deg*	Longitude
WRFInputFile	**TOPT**	nx, ny	*m*	topography height
WRFInputFile	**PI**	nx,ny,nz	*J/(kg*K)*	PI = Exner function * Cp, where (Cp=1004 J/kg/K in RAMS) Exner-function = T/Θ = (p/p00)^(Rd/Cp), p00=1000 hPa
WRFInputFile	**PC**	nx,ny,nz	*J/(kg*K)*	Current perturbation Exner function (PI-prime)
WRFInputFile	**UC**	nx,ny,nz	*m s^{-1}*	Current U wind component
WRFInputFile	**VC**	nx,ny,nz	*m s^{-1}*	Current V wind component

WRFInputFile	**UWWC**	nx,ny,nz	$m\ s^{-1}$	Current W wind component
WRFInputFile	**THETA**	nx,ny,nz	K	Theta, potential temperature
WRFInputFile	**RV**	nx,ny,nz	$kg\ kg^{-1}$	Water vapor mixing ratio
WRFInputFile	**RCP**	nx,ny,nz	$kg\ kg^{-1}$	Cloud mixing ratio
WRFInputFile	**RDP**	nx,ny,nz	$kg\ kg^{-1}$	Drizzle mixing ratio
WRFInputFile	**RRP**	nx,ny,nz	$kg\ kg^{-1}$	Rain mixing ratio
WRFInputFile	**RPP**	nx,ny,nz	$kg\ kg^{-1}$	Ice mixing ratio
WRFInputFile	**RSP**	nx,ny,nz	$kg\ kg^{-1}$	Snow mixing ratio
WRFInputFile	**RAP**	nx,ny,nz	$kg\ kg^{-1}$	Aggregate mixing ratio
WRFInputFile	**RGP**	nx,ny,nz	$kg\ kg^{-1}$	Graupel mixing ratio
WRFInputFile	**RHP**	nx,ny,nz	$kg\ kg^{-1}$	Hail mixing ratio
WRFInputFile	**CCP**	nx,ny,nz	kg^{-1}	Cloud number concentration
WRFInputFile	**CDP**	nx,ny,nz	kg^{-1}	Drizzle number concentration
WRFInputFile	**CRP**	nx,ny,nz	kg^{-1}	Rain number concentration
WRFInputFile	**CPP**	nx,ny,nz	kg^{-1}	Ice number concentration
WRFInputFile	**CSP**	nx,ny,nz	kg^{-1}	Snow number concentration
WRFInputFile	**CAP**	nx,ny,nz	kg^{-1}	Aggregate number concentration
WRFInputFile	**CGP**	nx,ny,nz	kg^{-1}	Graupel number concentration
WRFInputFile	**CHP**	nx,ny,nz	kg^{-1}	Hail number concentration
Naming convention	**MP_PHYSICS=40** Example: a-A-2013-06-19-210000-head.txt			
Get information of DX and Z. If this file is not available, DX and Z are calculated from GLAT/GLON and P				
WRFmpInputFile	**__dentaxn**		m	dx (=dy) If this is not available, dx is calculated from dGLON/dGLAT.
WRFmpInputFile	**__ztn01**		m	Height If this is not available, dx is calculated from pressure.
Naming convention	**MP_PHYSICS=70, 75**			
WRFInputFile	**X**	dimension		nx

WRFInputFile	**Y**	dimension		ny
WRFInputFile	**Z**	dimension		nz
WRFInputFile	**P**	nx,ny,nz	*hPa*	Pressure
WRFInputFile	**U**	nx,ny,nz	$m\ s^{-1}$	Current U wind component
WRFInputFile	**V**	nx,ny,nz	$m\ s^{-1}$	Current V wind component
WRFInputFile	**W**	nx,ny,nz	$m\ s^{-1}$	Current W wind component
WRFInputFile	**TABS**	nx,ny,nz	*K*	Absolute temperature
WRFInputFile	**X**	nx	*m*	West-east distance
WRFInputFile	**Y**	ny	*m*	South-north distance
WRFInputFile	**Z**	nz	*m*	Height
WRFInputFile	**QV**	nx,ny,nz	$g\ kg^{-1}$	Water vapour mixing ratio
WRFInputFile	**NA**	nx,ny,nz	$\#\ cm^{-3}$	Aerosol number concentration
Naming convention	**MP_PHYSICS=70 Naming convention**			
WRFInputFile	**QC**	nx,ny,nz	$g\ kg^{-1}$	Cloud water mixing ratio
WRFInputFile	**QR**	nx,ny,nz	$g\ kg^{-1}$	Rain water mixing ratio
WRFInputFile	**NC**	nx,ny,nz	$\#\ cm^{-3}$	Cloud droplet number concentration
WRFInputFile	**NR**	nx,ny,nz	$\#\ cm^{-3}$	Rain droplet number concentration
WRFInputFile	**M01 – M36**	nx,ny,nz	$g\ kg^{-1}$	Mass mixing ratio at each bin
WRFInputFile	**N01 – N36**	nx,ny,nz	$\#\ cm^{-3}$	Droplet number concentration at each bin
Naming convention	**MP_PHYSICS=75 Naming convention**			
WRFInputFile	**QR**	nx,ny,nz	$g\ kg^{-1}$	Rain water mixing ratio
WRFInputFile	**QI**	nx,ny,nz	$g\ kg^{-1}$	Cloud ice mixing ratio
WRFInputFile	**QS**	nx,ny,nz	$g\ kg^{-1}$	Snow mixing ratio
WRFInputFile	**QN**	nx,ny,nz	$g\ kg^{-1}$	Non-precipitating hydrometeor mixing ratio (cloud water + cloud ice)
WRFInputFile	**QP**	nx,ny,nz	$g\ kg^{-1}$	Precipitating hydrometeor mixing ratio (rain + snow)
WRFInputFile	**NC**	nx,ny,nz	$\#\ cm^{-3}$	Cloud droplet number concentration
WRFInputFile	**NR**	nx,ny,nz	$\#\ cm^{-3}$	Rain droplet number concentration

WRFInputFile	**NI**	nx,ny,nz	*# cm^{-3}*	Cloud ice number concentration
WRFInputFile	**NS**	nx,ny,nz	*# cm^{-3}*	Snow number concentration
WRFInputFile	**NG**	nx,ny,nz	*# cm^{-3}*	Graupel number concentration
Naming convention	**MP_PHYSICS=70** Example: micro_taubin_info.txt (Get bin boundaries for mass and diameter (or radius).)			
WRFmpInputFile	**Mass**		*g*	Bin boundaries for mass
WRFmpInputFile	**Diameter**		*cm*	Bin boundaries for numer
Naming convention	**MP_PHYSICS=70, 75** (Get air density profile data.)			
ProfileInputFile (for MP_PHYSICS=70) ; WRFmpInputFile (for MP_PHYSICS=75)	**Z**	dimension		nz
	Time	dimension		nt
	Z	nz	*m*	Height
	RHO	nz, time	*kg m^{-3}*	Air density
Naming convention	**MP_PHYSICS=80**			
WRFInputFile	**ni**	dimension		nx
WRFInputFile	**nj**	dimension		ny
WRFInputFile	**nk**	dimension		nz
WRFInputFile	**prs**	nx,ny,nz	*Pa*	Pressure
WRFInputFile	**uinterp**	nx,ny,nz	*m s^{-1}*	Current U wind component
WRFInputFile	**vinterp**	nx,ny,nz	*m s^{-1}*	Current V wind component
WRFInputFile	**winterp**	nx,ny,nz	*m s^{-1}*	Current W wind component
WRFInputFile	**th**	nx,ny,nz	*K*	Potential temperature
WRFInputFile	**xh**	nx	*km*	West-east distance
WRFInputFile	**yh**	ny	*km*	South-north distance
WRFInputFile	**z**	nz	*km*	Height
WRFInputFile	**qv**	nx,ny,nz	*kg kg^{-1}*	Water vapour mixing ratio
WRFInputFile	**qc**	nx,ny,nz	*kg kg^{-1}*	Cloud water mixing ratio
WRFInputFile	**qr**	nx,ny,nz	*kg kg^{-1}*	Rain water mixing ratio
WRFInputFile	**qi**	nx,ny,nz	*g kg^{-1}*	Cloud ice mixing ratio

WRFInputFile	**qs**	nx,ny,nz	$g\ kg^{-1}$	Snow mixing ratio
WRFInputFile	**qg**	nx,ny,nz	$g\ kg^{-1}$	Graupel mixing ratio
WRFInputFile	**ncr**	nx,ny,nz	kg^{-1}	Rain water number concentration
WRFInputFile	**nci**	nx,ny,nz	kg^{-1}	Cloud ice number concentration
WRFInputFile	**ncs**	nx,ny,nz	kg^{-1}	Snow number concentration
WRFInputFile	**ncg**	nx,ny,nz	kg^{-3}	Graupel number concentration

Note that variable *ALT* (inverse density of dry air) is an optional input in the WRFInputFile. If not present, this variable is recomputed from *T*, *P*, *PB* and *QVAPOR* using the definition of the water vapor mixing ratio and equations of state for water vapor and dry air. The turbulence kinetic energy is named *TKE_PBL* for MP_PHYSICS=50, while *TKE* for other microphysics schemes.

The mass mixing ratio and number concentration for hail category are needed only for MP_PHYSICS=9. Cloud mass number concentration *QNCLOUD* for MP_PHYSICS=8, 10 and 50 is prescribed, so this variable is not required to be present in the WRF Input File. However, if *QNCLOUD* for MP_PHYSICS=8, 10, 50, and 80 is present in the input, it will be read by CR-SIM routines, and the prescribed value will be ignored. The *QRIM* and *BRIM* are presented only for MP_PHYSICS=50.

The MP_PHYSICS=40 reads RAMS files consisted of a data file (HDF5 format) and a header text file. The data has nx, ny, and nz dimensions, but does not have time dimension, and nx = ny. The dx (=dy) and heights are obtained from the text file, but if this file is not available, dx and height are calculated from latitude/longitude and pressure, respectively. The MP_PHYSICS=40 needs mass mixing ratio and number concentration for 8 hydrometeor categories (1-cloud, 2-rain, 3-ice, 4-snow, 5-graupel, 6-hail, 7-drizzle, and 8-aggregate). The drizzle and aggregate categories are considered as cloud and snow, respectively, for scattering calculation, and drizzle is involved in ceilometer and MPL simulations.

3.3 CR-SIM Output data

The name of the main output file is specified in the command line when executing the code. An additional number of output files will be created, for each hydrometeor category. Per default, they will have extensions "_cloud", "_rain", "_ice", "_snow", "_graupel" and "_hail" (for MP_PHYSICS=8, 9, 10, 30, 40, 20, 70 , and 75), and "_drizzle" and "_aggregate" (for MP_PHYSICS=40), or "_cloud", "_rain", "_smallice", "_unrimedice", "_graupel" and "_parimedice" (for MP_PHYSICS=50) before the extension ".nc".

The structure of the output file depends on how the parameters "radID" and "ceiloID" are specified in the Configuration File. If the parameter "radID" is equal to one, the computation of polarimetric variables is turned off. In this case, the CR-SIM output would consist of reflectivity, mean Doppler velocity, reflectivity weighted velocity, spectrum width and specific attenuation. If radID≠1, the full polarimetric output is written (Tables 7 and 8). The parameter "ceiloID" defines whether or not to include simulation of ceilometer measurements in the output. If this parameter is equal to one (ceiloID=1), the following cloud lidar variables are outputted in the main output file: true backscatter, measured backscatter, lidar extinction coefficient and the first cloud base observed by ceilometer (Table 8). Note that lidar output variables are reported only in the main output file, the one for the total hydrometeor content, and are not copied in the NetCDF files for hydrometeor species. Variables that are reported only in the main output file are listed in Table 9.

An example of variables included in global attributes field in created NetCDF file is given bellow. Note that the names of specific input files used in simulation are preserved.

```
// global attributes:
```

:**description** = “forward scanning radar simulator output” ;
:**model_version** = “crsim_v3.3” ;
:**WRF_input_file** = “wrfout_4simulator_2014-03-05_09:00:00” ;
:**MP_PHYSICS** = “10” ;
:**x_indices_of_WRF_extracted_scene** = “1 – 311” ;
:**y_indices_of_WRF_extracted_scene** = “1 – 312” ;
:**z_indices_of_WRF_extracted_scene** = “1 – 39” ;
:**scene_extracted_at_time_step** = “1” ;
:**radar_frequency** = “3.0 GHz” ;
:**x_and_y_indices_of_radar_position** = “120, 290” ;
:**height_of_radar** = “0.0 m” ;
:**scanning_mode** = “elevation is set to 90.0 degrees” ;
:**created_by** = “Aleksandra Tatarevic” ;
:**institute** = “http://wwww.clouds.mcgill.ca” ;

3.3.1 CR-SIM Output data file structure

The full list of ***crsim v4,0*** variables outputted in the NetCDF file in the case of the total hydrometeor content (main output file) and in the case of any specific hydrometeor category is given in Tables 7 and 8, respectively. Table 9 lists variables that are reported only in the main output file, and they are not repeated (copied) in the NetCDF output files for different hydrometeor categories.

Table 7: The structure of CR-SIM output NetCDF files for total hydrometer content

DIMENSION NAMES	Description	Comment
Nx	Number of grid boxes along the horizontal E-W axis	-
Ny	Number of grid boxes along the horizontal S-N axis	-
Nz	Number of grid boxes along the vertical axis at WRF resolution	-
Nht	Number of hydrometer species	-
One	=1	-
n_layers	Number of cloud layers for ARSCL =10,	*if arsclID=1*
Nfft	Number of FFT points for Doppler spectrum	*If spectraID=1*

VARIABLE	DIMENSION	UNITS	DESCRIPTION	Comment

xlat	[nx, ny]	*deg*	Latitude (north is positive)	*WRF variable (copied or routinely calculated)*
xlong	[nx, ny]	*deg*	Longitude (south is positive)	*WRF variable (copied or routinely calculated)*
Zhh	[nx, ny, nz]	*dBZ*	Reflectivity at hh polarization	
Zvv	[nx, ny, nz]	*dBZ*	Reflectivity at vv polarization	***Not computed if radID=1***
Zvh	[nx, ny, nz]	*dBZ*	Reflectivity at vh polarization	***Not computed if radID=1***
Zdr	[nx, ny, nz]	*dB*	Differential reflectivity	***Not computed if radID=1***
LDRh	[nx, ny, nz]	*dB*	Linear Depolarization Ratio	***Not computed if radID=1***
RHOhv	[nx, ny, nz]	-	Cross-correlation coefficient	***Not computed if radID=1***
DV	[nx, ny, nz]	$m\ s^{-1}$	Mean Radial Doppler Velocity, positive upward, away from the radar	
SWh	[nx, ny, nz]	$m\ s^{-1}$	Spectrum width due to hydrometeors	
SWt	[nx, ny, nz]	$m\ s^{-1}$	Spectrum width due to turbulence	
SWs	[nx, ny, nz]	$m\ s^{-1}$	Spectrum width due to wind shear	
SWv	[nx, ny, nz]	$m\ s^{-1}$	Spectrum width due to cross wind	
SWtot	[nx, ny, nz]	$m\ s^{-1}$	Total spectrum width (including all contributions)	
DV90	[nx, ny, nz]	$m\ s^{-1}$	Vertical Mean Doppler Velocity (el=90 deg), positive upward (away from the radar)	
RWV	[nx, ny, nz]	$m\ s^{-1}$	Reflectivity Weighted Velocity (w=0, elev=90), positive downward, towards the radar	
SWh90	[nx, ny, nz]	$m\ s^{-1}$	Spectrum width due to hydrometeor (elev=90 deg)	
Kdp	[nx, ny, nz]	$deg\ km^{-1}$	Specific Differential Phase	***Not computed if radID=1***
Adp	[nx, ny, nz]	$dB\ km^{-1}$	Specific Differential Attenuation	***Not computed if radID=1***
Ah	[nx, ny, nz]	$dB\ km^{-1}$	Specific Horizontal Attenuation	
Av	[nx, ny, nz]	$dB\ km^{-1}$	Specific Vertical Attenuation	***Not computed if radID=1***
diff_back_phase	[nx, ny, nz]	*deg*	Differential backscatter phase	***Not computed if radID=1***
Avap	[nx, ny, nz]	$dB\ km^{-1}$	Specific Water Vapor Attenuation	
Atot	[nx, ny, nz]	$dB\ km^{-1}$	Two-way total attenuation (Ah + Atot)	***Computed if elev=90 or -90***
ceilo_back_obs	[nx, ny, nz]	$m^{-1}\ sr^{-1}$	Attenuated cloud lidar true backscatter	***Computed if ceiloID=1***

ceilo_back_true	[nx, ny, nz]	*m^{-1} sr^{-1}*	Cloud lidar true backscatter	***Computed if ceiloID=1***
ceilo_ext	[nx, ny, nz]	*m^{-1} sr^{-1}*	Cloud lidar extinction coefficient	***Computed if ceiloID=1***
lidar_ratio	[nx, ny, nz]	-	Cloud lidar ratio	***Computed if ceiloID=1***
ceilo_first_cloud_base	[nx, ny]	*m*	Height of the first cloud base observed by ceilometer	***Computed if ceiloID=1***
spectra_zhh	[nfft, nx, ny, nz]	*dB/(m s^{-1})*	Doppler spectra at hh polarization	***Computed if spectraID=1***
spectra_zvv	[nfft, nx, ny, nz]	*dB/(m s^{-1})*	Doppler spectra at vv polarization	***Computed if spectraID=1 and radID≠1***
spectra_zvh	[nfft, nx, ny, nz]	*dB/(m s^{-1})*	Doppler spectra at vh polarization	***Computed if spectraID=1 and radID≠1***
Zsfc_Ocean	[nx, ny]	*dBZ*	Surface reflectivity over ocean	***Computed if airborneID=1 and radar height is above the ground (zc>0)***
Zsfc_Land_Coarse	[nx, ny]	*dBZ*	Surface reflectivity over coarse land (i.e. wet snow)	
Zsfc_Land_Flat	[nx, ny]	*dBZ*	Surface reflectivity over flat land (i.e. flat road)	
DV_airborne	[nx, ny, nz]	*m s^{-1}*	Radial airmotion related to airborne moving	***Computed if airborneID=1***
Zmin	[nx, ny, nz]	*dBZ*	Radar sensitivity limitation with range	
temp	[nx, ny, nz]	*deg C*	Temperature	*WRF variable (copied or routinely calculated)*
rho_d	[nx, ny, nz]	*kg m^{-3}*	Dry air density	*WRF variable (copied or routinely calculated)*
u	[nx, ny, nz]	*m s^{-1}*	U horizontal wind component	*WRF variable (copied or routinely calculated)*
v	[nx, ny, nz]	*m s^{-1}*	V horizontal wind component	*WRF variable (copied or routinely calculated)*
w	[nx, ny, nz]	*m s^{-1}*	Vertical air velocity	*WRF variable (copied or routinely calculated)*
elev	[nx, ny, nz]	*deg*	Elevation angle from horizontal (zenith=90 deg)	
azim	[nx, ny, nz]	*deg*	Azimuth angle (EAST=0 deg, NORTH=90 deg)	
range	[nx, ny, nz]	*m*	Radar range	Configuration variable (copied)
rad_freq	[one]	*GHz*	Radar frequency	Configuration variable (copied)
rad_beamwidth	[one]	*deg*	Radar antenna beam width	Configuration variable (copied)
rad_range_resolution	[one]	*m*	Radar range resolution	Configuration variable (copied)

rad_ixc	[one]	-	Index of position in x (x_scene coordinate) direction of radar origin	Configuration variable (copied)
rad_iyc	[one]	-	Index of position in y direction (y_scene coordinate) of radar origin	Configuration variable (copied)
rad_zc	[one]	*m*	Radar height	Configuration variable (copied)
height	[nx, ny, nz]	*m*	Height	*WRF variable (copied or routinely calculated)*
wcont	[nx, ny, nz]	$kg\ m^{-3}$	Water content	*WRF variable (copied or routinely calculated)*
x_scene	[nx]	*m*	Scene extent in E-W direction	
y_scene	[ny]	*m*	Scene extent in S-N direction	

Table 8: The structure of CR-SIM output NetCDF files per hydrometeor specie

DIMENSION NAMES	Description	Comment
nx	Number of grid boxes along the horizontal E-W axis	-
ny	Number of grid boxes along the horizontal S-N axis	-
nz	Number of grid boxes along the vertical axis at WRF resolution	-
nht	Number of hydrometer species	-
one	=1	

VARIABLE	DIMENSION	UNITS	DESCRIPTION	Comment
xlat	[nx, ny]	*deg*	Latitude (north is positive)	*WRF variable (copied or routinely calculated)*
xlong	[nx, ny]	*deg*	Longitude (south is positive)	*WRF variable (copied or routinely calculated)*
Zhh	[nx, ny, nz]	*dBZ*	Reflectivity at hh polarization	
Zvv	[nx, ny, nz]	*dBZ*	Reflectivity at vv polarization	***Not computed if radID=1***
Zvh	[nx, ny, nz]	*dBZ*	Reflectivity at vh polarization	***Not computed if radID=1***
Zdr	[nx, ny, nz]	*dB*	Differential reflectivity	***Not computed if radID=1***
LDRh	[nx, ny, nz]	*dB*	Linear Depolarization Ratio	***Not computed if radID=1***
RHOhv	[nx, ny, nz]	-	Cross-correlation coefficient	***Not computed if radID=1***
DV	[nx, ny, nz]	$m\ s^{-1}$	Mean Radial Doppler Velocity, positive upward, away from the radar	

SWh	[nx, ny, nz]	*m s^{-1}*	Spectrum width due to hydrometeors	
SWt	[nx, ny, nz]	*m s^{-1}*	Spectrum width due to turbulence	
SWs	[nx, ny, nz]	*m s^{-1}*	Spectrum width due to wind shear	
SWv	[nx, ny, nz]	*m s^{-1}*	Spectrum width due to cross wind	
SWtot	[nx, ny, nz]	*m s^{-1}*	Total spectrum width (including all contributions)	
DV90	[nx, ny, nz]	*m s^{-1}*	Vertical Mean Doppler Velocity (el=90 deg), positive upward (away from the radar)	
RWV	[nx, ny, nz]	*m s^{-1}*	Reflectivity Weighted Velocity (w=0, elev=90), positive downward, towards the raar	
SWh90	[nx, ny, nz]	*m s^{-1}*	Spectrum width due to hydrometeor (elev=90 deg)	
Kdp	[nx, ny, nz]	*deg km^{-1}*	Specific Differential Phase	***Not computed if radID=1***
Adp	[nx, ny, nz]	*dB km^{-1}*	Specific Differential Attenuation	***Not computed if radID=1***
Ah	[nx, ny, nz]	*dB km^{-1}*	Specific Horizontal Attenuation	
Av	[nx, ny, nz]	*dB km^{-1}*	Specific Vertical Attenuation	***Not computed if radID=1***
diff_back_phase	[nx, ny, nz]	*deg*	Differential backscatter phase	***Not computed if radID=1***
elev	[nx, ny, nz]	*deg*	Elevation angle from horizontal (zenith=90 deg)	
azim	[nx, ny, nz]	*deg*	Azimuth angle (EAST=0 deg, NORTH=90 deg)	
range	[nx, ny, nz]	*m*	Radar range	
rad_freq	[one]	*GHz*	Radar frequency	Configuration variable (copied)
rad_beamwidth	[one]	*deg*	Radar antenna beam width	Configuration variable (copied)
rad_range_resolution	[one]	*m*	Radar range resolution	Configuration variable (copied)
rad_ixc	[one]	-	Index of position in x (x_scene coordinate) direction of radar origin	Configuration variable (copied)
rad_iyc	[one]	-	Index of position in y direction (y_scene coordinate) of radar origin	Configuration variable (copied)
rad_zc	[one]	*m*	Radar height	Configuration variable (copied)
height	[nx, ny, nz]	*m*	Height	*WRF variable (copied or routinely calculated)*
wcont	[nx, ny, nz]	*kg m^{-3}*	Water content	*WRF variable (copied or routinely calculated)*
x_scene	[nx]	*m*	Scene extent in E-W direction	
y_scene	[ny]	*m*	Scene extent in S-N direction	
mpl_wavel (cloud, ice, drizzle)	[one]	*nm*	MPL wavelength	Computed if mplID >0
mpl_back_obs	[nx, ny, nz]	*[m sr]$^{-1}$*	MPL observed backscatter (cloud+ice(+drizzle)+aerosol+atm.molecular)	Computed if mplID >0

(cloud, ice, drizzle)				
mpl_back_true (cloud, ice, drizzle)	[nx, ny, nz]	*[m sr]$^{-1}$*	MPL true backscatter (cloud+ice(+drizzle)+aerosol+atm.molecular)	Computed if mplID >0

Table 9: List of CR-SIM output variables reported only in the main output file (for the total hydrometeor content)

VARIABLE	DIMENSION	UNITS	DESCRIPTION	Comment
ceilo_back_obs	[nx, ny, nz]	*m^{-1} sr^{-1}*	Attenuated cloud lidar true backscatter	***Computed if ceiloID=1***
ceilo_back_true	[nx, ny, nz]	*m^{-1} sr^{-1}*	Cloud lidar true backscatter	***Computed if ceiloID=1***
ceilo_ext	[nx, ny, nz]	*m^{-1} sr^{-1}*	Cloud lidar extinction coefficient	***Computed if ceiloID=1***
lidar_ratio	[nx, ny, nz]	-	Cloud lidar ratio	***Computed if ceiloID=1***
ceilo_first_cloud_base	[nx, ny]	*m*	Height of the first cloud base observed by ceilometer	***Computed if ceiloID=1***
Zmin	[nx, ny, nz]	*dBZ*	Radar sensitivity limitation with range	
temp	[nx, ny, nz]	*deg C*	Temperature	*WRF variable (copied or routinely calculated)*
rho_d	[nx, ny, nz]	*kg m^{-3}*	Dry air density	*WRF variable (copied or routinely calculated)*
u	[nx, ny, nz]	*m s^{-1}*	U horizontal wind component	*WRF variable (copied or routinely calculated)*
v	[nx, ny, nz]	*m s^{-1}*	V horizontal wind component	*WRF variable (copied or routinely calculated)*
w	[nx, ny, nz]	*m s^{-1}*	Vertical air velocity	*WRF variable (copied or routinely calculated)*
arscl_cloud_mask	[nx, ny, nz]	*0 or 1*	Cloud mask from radar, mpl, ceilo_first_cloud_base	*Computed if arsclID=1*
arscl_cloud_source_flag	[nx, ny, nz]	*1,2,3, or 4*	Instrument source flag for cloud detections: 1: Clear according to radar and MPL; 2: Cloud detected by radar and MPL; 3: Cloud detected by radar only; and 4: Cloud detected by MPL only	*Computed if arsclID =1*
arscl_cloud_layer_base_height	[nx, ny, n_layers]	*m*	Base heights of cloud layers for up to 10	*Computed if arsclID =1*

arscl_cloud_layer_top_height	[nx, ny, n_layers]	*m*	Top heights of cloud layers for up to 10	*Computed if arsclID =1*
model_lwp	[nx, ny]	*kg m $^{-2}$*	Liquid water path (cloud+rain)	*Computed if mwrID =1*
mpl_rayleigh_back	[nx, ny, nz]	*[m sr]$^{-1}$*	MPL molecular backscatter	*Computed if mplID >0*
mpl_wavel	[one]	*nm*	MPL wavelength	*Computed if mplID >0*
mpl_back_obs	[nx, ny, nz]	*[m sr]$^{-1}$*	MPL observed backscatter (cloud+ice(+drizzle)+aerosol+atm.molecular)	*Computed if mplID >0*
mpl_back_true	[nx, ny, nz]	*[m sr]$^{-1}$*	MPL true backscatter (cloud+ice(+drizzle)+aerosol+atm.molecular)	*Computed if mplID >0*
mpl_ext	[nx, ny, nz]	*m^{-1}*	MPL extinction coefficient (cloud+ice(+drizzle)+aerosol+atm.molecular)	*Computed if mplID >0*
mpl_lidar_ratio	[nx, ny, nz]	*sr*	MPL lidar ratio (cloud+ice(+drizzle)+aerosol+atm.molecular)	*Computed if mplID >0*
aero_back_obs	[nx, ny, nz]	*[m sr]$^{-1}$*	MPL aerosol observed backscatter	*Computed if mplID >0 and aeroID=1*
aero_back_true	[nx, ny, nz]	*[m sr]$^{-1}$*	MPL aerosol true backscatter	*Computed if mplID >0 and aeroID=1*
aero_ext	[nx, ny, nz]	*m^{-1}*	MPL aerosol extinction coefficient	*Computed if mplID >0 and aeroID=1*
aero_lidar_ratio	[nx, ny, nz]	*sr*	MPL aerosol lidar ratio	*Computed if mplID >0 and aeroID=1*

4 CR-SIM STRUCTURE

The **CR-SIM** algorithm flow chart is shown in Figure 2. The main algorithms are depicted in blocks. The algorithm processes as depicted.

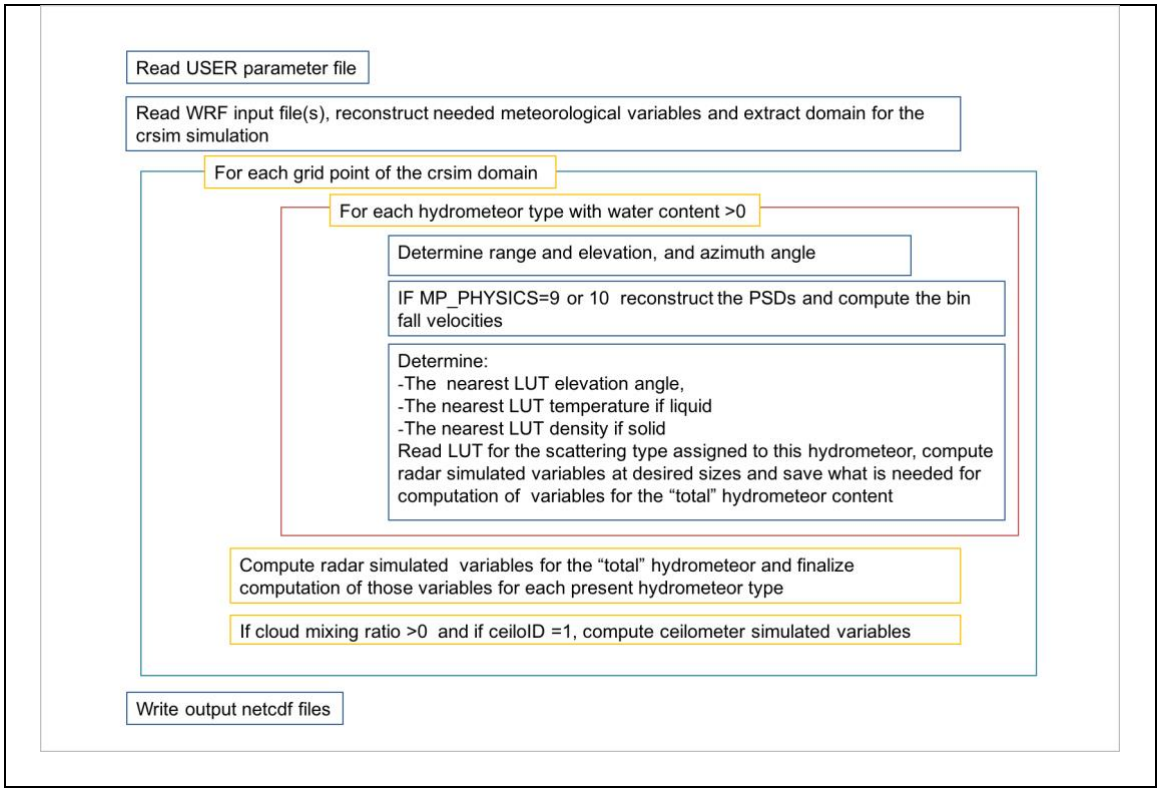

Figure 2: CR-SIM algorithm flow chart

An example of the WRF input and the CR-SIM output variables at 3 *GHz* is shown in Figure 3.

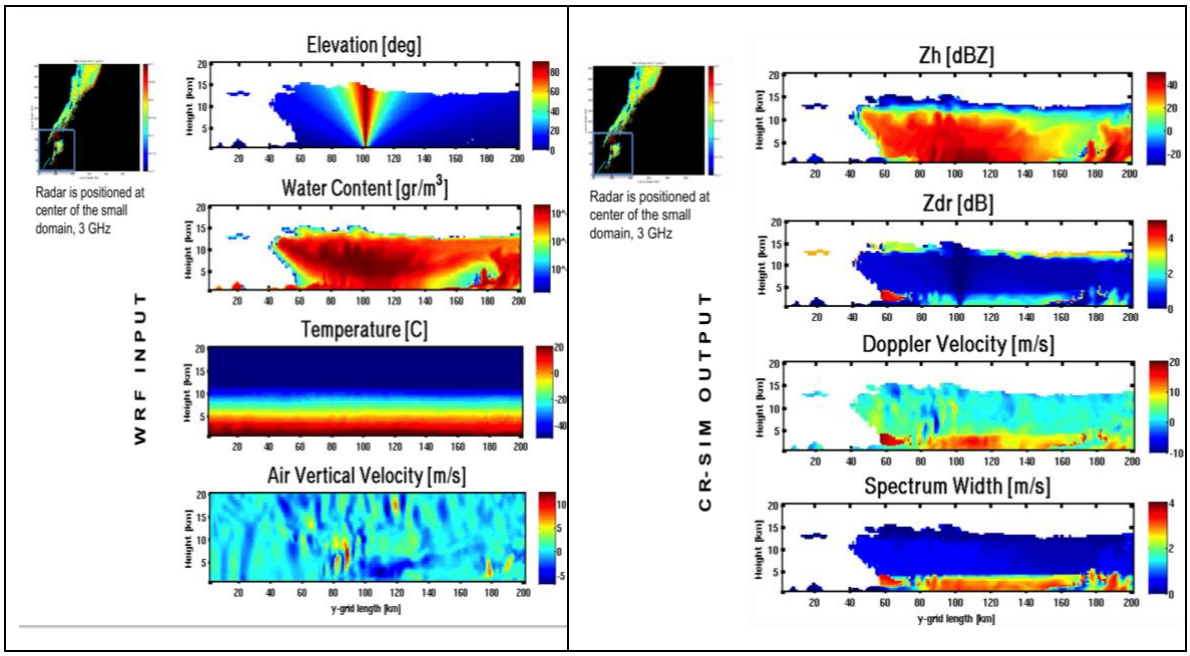

Figure 3: Example of the WRF input and the CR-SIM output variables at 3 *GHz*.

4.1 The Input WRF scene

The **CR-SIM** forward simulator is tailored to read the output format (NetCDF) and variables names produced by the **WRF v.3.9** model using microphysical options MP_PHYSIC=8, MP_PHYSIC=9, MP_PHYSIC=10, MP_PHYSIC=20, or MP_PHYSIC=50, **ICON** model using MP_PHYSICS=30, **RAMS** model using MP_PHYSICS=40, **SAM** model using MP_PHYSICS=70 or MP_PHYSICS=75, or **CM1** model using MP_PHYSICS=80.

The WRF model outputs the state variables defined in the Registry file, and these state variables are used in the model's prognostic equations. Some of these variables are perturbation fields; therefore, the following procedure for reconstructing meteorological variables is performed:

$$P[Pa] = \overline{P} + P'$$

$$T[K] = (300. + q') \left(\frac{P}{100000.} \right)^{\frac{287.}{1004.}}$$

$$h[m] = \frac{PHB + PH}{9.81}$$

where P is the total pressure, T is the total temperature, θ' is the perturbation potential temperature ("*T*" in the input WRF data file), h is the geopotential height, *PHB* and *PH* are the base-state and perturbation geopotentials. Variables with subscript " ' " represent perturbations and those with " $\overline{\ }$ " the base-state values. Values of h are linearly interpolated at centers of mass, at which pressure, temperature and mixing ratios of water vapor and hydrometeor species are defined.

The density of dry air ρ_d is the inverse of the variable "*ALT*", if this variable is provided in the WRF NetCDF file. If not provided, it is calculated using the definition of the water vapor mixing ratio and equations of state for water vapor and dry air:

$$r_d \left[\frac{kg}{m^3} \right] = \frac{P - \frac{P q_V}{e + q_V}}{R_d T}$$

where q_v is water vapor mixing ratio, R_d=287 $J\ kg^{-1}K^{-1}$ is the individual gas constant for dry air and the constant ε ($\equiv R_d/R_v$) = 0.622. The term $(P\ q_v) / (\varepsilon+q_v)$ represents water vapor pressure in *Pa*.

4.2 Two-moments Microphysics schemes

In the 'regular' WRF NetCDF file, the mixing ratio ($kg\ kg^{-1}$) and total number concentration (kg^{-1}) are provided for hydrometeor types prescribed by the microphysical package used.

4.2.1 MP_PHYSIC=9 – Milbrandt and Yau double-moment scheme

This scheme (Milbrandt and Yau, 2005a and 2005b) consists of six hydrometeor categories: cloud droplets, rain, cloud (pristine) ice, snow (large crystals and aggregates), graupel (moderate-density graupel formed from heavily rimed ice or snow) and hail (high density hail and frozen raindrops). The scheme predicts:

-mixing ratios: Q_c, Q_r, Q_i, Q_s, Q_g and Q_h in $kg\ kg^{-1}$
-number concentrations: N_c, N_r, N_i, N_s, N_g and N_h in kg^{-1}

where subscripts *c*, *r*, *i*, *s*, *g* and *h* stand for cloud, rain, ice, snow, graupel and hail, respectively.

The mass-size relationship is given as $m=a_m D^{b_m}$. Except for ice, all hydrometeors are assumed to be spherical, with $a_m=\pi\rho_h/6$, where ρ_h is the fixed size-independent density, or bulk density. Ice crystals are assumed to be bullet rosettes and have $a_{m_i}= 440\ kg\ m^{-b_{mi}}$. There are two options for snow category: spherical snow with $\rho_s=100\ kg\ m^{-3}$ and not-spherical snow with $a_{m_s}= 0.1597\ kg\ m^{-b_{ms}}$. Hydrometeor densities ρ_h are independent per size for all categories, with the exponent b_m=3, except in the case of not-spherical snow for

which b_m=2.078. The parameters of mass-size relationship for each hydrometeor's specie are given in Table 10.

The generalized gamma distribution is assumed for each hydrometeor:

$$N(D) = N_T \frac{n}{\Gamma(1+a)} \lambda^{n(1+a)} D^{n(1+a)-1} \exp\left(-(\lambda D)^n\right)$$

where N_T is the total number concentration, intercept, λ is the slope parameter, v and α are dispersion parameters and Γ is the gamma function. Note that here, the spectral index μ is defined as $\mu=v\ (1+\alpha)$ - 1. The distribution parameters v and α are given in Table 10.

Expressions for λ and N_T, needed to recover the particle size distribution, are given by:

$$\lambda[m^{-1}] = \left[\frac{\Gamma\left(a+1+\frac{b_m}{n}\right)}{\Gamma(a+1)} \frac{a_m N}{Q}\right]^{\frac{1}{b_m}}$$

$$N_T[m^{-4}] = N\, r_{d_{air}}$$

where Q and N are prognostic hydrometeor mass mixing ratio and number concentration, respectively.

The fall velocity size relationships for all hydrometeors except cloud are specified in a form: $V_f(D)= f_c\ a_v D^{bv}$, where $f_c = (\rho_{surf}/\rho)^k$ is the correction factor for air density with exponent k. The values for prefactor a_v, the exponent b_v and the exponent k in the expression for particle terminal velocity are given in Table 10. The air density at sea level is ρ_{surf} is computed for the first model level. For cloud droplets, the fall velocity is assumed negligible.

Table 10: Parameters in the mass-size and velocity size relationships and the distribution parameters in Milbrandt and Yau double-moment scheme

Hydrometeor	b_m [-]	ρ_h [$kg\ m^{-3}$]	a_v [$m^{1-b_v}\ s^{-1}$]	b_v [-]	k[-]	v[-]	α[-]
Cloud	3	1000.0	0	0	0	3	1
Rain	3	1000.0	149.1	0.5	0.5	1	2
Ice	3	$6/\pi$ 440.0	71.34	0.6635	0.5	1	0
snow spherical	3	100.0	11.72	0.41	0.5	1	0
snow not spherical	2.078	$6/\pi$ 1.597					
graupel	3	400.0	19.3	0.37	0.5	1	0
hail	3	900.0	206.89	0.6384	0.5	1	3

4.2.2 MP_PHYSIC=10 - Morrison double-moment scheme

This scheme (Morrison et al., 2005, Morrison et al., 2009) consists of five hydrometeor categories: cloud droplets, rain, cloud (pristine) ice, snow (large crystals and aggregates), and graupel (moderate density graupel). The scheme predicts:

-mixing ratios: Q_c, Q_r, Q_i, Q_s, and Q_g in $kg\ kg^{-1}$
-number concentrations N_r, N_i, N_s and N_g in kg^{-1}

where subscripts *c*, *r*, *i*, *s* and *g* stand for cloud, rain, ice, snow and graupel, respectively. For cloud droplets, number concentration N_c is fixed (=250 cm^{-3}).

The mass-size relationship is given as $m=a_m D^{b_m}$. All particles are assumed spherical, with fixed size independent densities per hydrometer class. Since all particles are assumed spherical, b_m=3, and $a_m=\pi\rho_h/6$, where ρ_h is the hydrometer density. The values of ρ_h are

given in Table 11. The Gamma distribution with a fixed shape factor is assumed for each hydrometeor distribution:

$$N(D) = N_0 D^m e^{-\lambda D}$$

where N_0 is the intercept, μ is the spectral index and λ is the slope. For ice, rain, snow, and graupel μ=0, so in fact, the exponential distribution is assumed. For cloud, μ is determined in function of droplet number concentration N_c and density of dry air, according to Martin et al. (1994).

Expressions for λ and N_0, needed to recover the particle size distribution, are given by:

$$\lambda\,[m^{-1}] = \left[\frac{\Gamma\left(\alpha + 1 + \frac{b_m}{\nu}\right)}{\Gamma(\alpha+1)} \; \frac{a_m N}{Q}\right]^{\frac{1}{b_m}}$$

$$N_T[m^{-3}] = N \, \varrho_{d\,air}$$

where Q and N are prognostic hydrometeor mass mixing ratio and number concentration, respectively and Γ is the gamma function.

The fall velocity size relationships for all hydrometeors except cloud are specified in a form: $V_f(D) = f_c a_v D^{bv}$, where $f_c = (\rho_{surf}/\rho)^k$ is the correction factor for air density with exponent k. The values for prefactor a_v, the exponent b_v and the exponent k in the expression for particle terminal velocity are given in Table 11. The air density at sea level is ρ_{surf} is computed for reference level 850 *mb* with T=273.15 *K*. For cloud droplets, the dependence on environment conditions follows from Stokes' law through the dynamic viscosity of air $a_v = g\rho_w/(18\mu_{air})$, where g is acceleration of gravity, ρ_w is density of liquid water, and μ_{air} is dynamic viscosity of air. The dynamic viscosity of air is calculated as a function of temperature.

Table 11: Parameters in the mass-size and velocity size relationships in Morrison double-moment scheme

hydrometeor	b_m [-]	ρ_h [$kg\ m^{-3}$]	a_v [$m^{1-b_v}\ s^{-1}$]	b_v [-]	k[-]
cloud	3	997.0	$g\ \rho_w$ / (18. μ_{air}(T))	2.0	-
rain	3	997.0	841.99667	0.8	0.54
ice	3	500.0	700.0	1.0	0.35
snow	3	100.0	11.72	0.41	0.54
Graupel	3	400.0	19.3	0.37	0.54

4.2.3 MP_PHYSIC=8 – Thompson scheme

This scheme (Thompson et al., 2008) consists of five hydrometeor categories: cloud droplets, rain, cloud (pristine) ice, snow (large crystals and aggregates), and graupel (moderate density graupel). The scheme predicts:

-mixing ratios: Q_c, Q_r, Q_i, Q_s, and Q_g in $kg\ kg^{-1}$
-number concentrations N_r and N_i in kg^{-1}.

The Gamma distribution is assumed for each hydrometeor distribution, and its generalized gamma distribution is used as introduced in section 4.2.1, except snow. For cloud droplets, cloud ice, and rain, same as Milbrandt and Yau scheme and Morrison scheme, the slope parameter λ and the intercept parameter N_0 are calculated by:

$$\lambda = \left(\frac{\pi \rho_h}{6} \frac{N}{Q} \frac{\Gamma(\mu+3+1)}{\Gamma(\mu+1)} \right)^{1/3}$$

$$N_0 = \frac{N \rho_{d_{air}} \lambda^{\mu+1}}{\Gamma(\mu+1)}$$

where ρ_h is hydrometeor density given in Table 12. For cloud ice and rain, $\mu_{i,r} = 0$. For cloud droplets, number concentration N_c is fixed (=100 cm^{-3}), and the shape parameter μ_c is set or calculated as:

$$\mu_c = \min\left(15, \frac{10^9}{N_c} + 2\right)$$

For snow, the following number density distribution is applied:

$$N(D) = \frac{M_2^4}{M_3^3}\left[\kappa_0 \exp\left(-\frac{M_2}{M_3}\lambda_0 D\right) + \kappa_1\left(\frac{M_2}{M_3}D\right)^{\mu_s}\exp\left(-\frac{M_2}{M_3}\lambda_1 D\right)\right]$$

where M_n is the *n*th moment of the distribution $M_n = \int D^n N(D) dD$, and $\kappa_0 = 490.6$, $\kappa_1 = 17.46$, $\lambda_0 = 20.78$, $\lambda_1 = 3.29$, and $\mu_s = 0.6357$. For graupel, $\mu_g = 0$, and λ and N_0 are calculated by:

$$\lambda = \left(\frac{\pi\rho_h}{6}\frac{10^6\Gamma(3+1)}{Q}\right)^{1/(3+1)}\left(\frac{\Gamma(\mu+3+1)}{\Gamma(\mu+1)\times\Gamma(3+1)}\right)^{1/3}$$

$$N_0 = \max\left[10^4, \min\left(\frac{200}{Q}, 5\times10^6\right)\right]$$

The hydrometeor fall velocity relation follows Ferrier (1994),

$$V_f(D) = \left(\frac{\rho_{surf}}{\rho}\right)^{1/2} a_v D^{b_v} e^{-f_v D}$$

The mass-size relationship is given as $m=a_m D^{b_m}$. All particles are assumed spherical (except snow) with fixed size independent densities per hydrometer class. Since particles are assumed spherical, $b_m=3$, and $a_m=\pi\rho_h/6$, where ρ_h is the hydrometer density. The values of constants in fall velocity relationship and mass-size relationship are given in Table 12.

Table 12: Parameters in the mass-size and velocity size relationships in Thompson scheme

hydrometeor	a_m [-]	b_m [-]	ρ_h [$kg\ m^{-3}$]	a_v [-]	b_v [-]	f_v [-]
cloud	$\pi\rho_h/6$	3	1000.0	0.316946×10^8	2.0	0.0
rain	$\pi\rho_h/6$	3	1000.0	4854	1.0	195
ice	$\pi\rho_h/6$	3	890.0	1847.5	1.0	0
snow	0.069	2	100.0	40	0.55	100
graupel	$\pi\rho_h/6$	3	500.0	442	0.89	0

4.2.4 MP_PHYSIC=50 – predicted particle properties (P3) scheme (one-category ice)

In this new bulk scheme (Morrison and Milbrandt, 2015; Morrison et al., 2015; Milbrandt and Morrison, 2016), a standard two-moment, the two category approach is used for liquid-phase components (cloud and rain), while for ice, a single ice-phase category or double ice-phase category is represented by several physical properties that evolve freely in time and space. In CR-SIM, we incorporate the single ice-phase category scheme and calculate PSDs and radar variables for four ice particle categories separately: small ice, unrimed ice, partially-rimed ice, and graupel.

For liquid phase, P3 scheme provides mass mixing ratios (Q_c and Q_r, $kg\ kg^{-1}$) and number concentrations (N_c and N_r, kg^{-1}). Here subscripts *c* and *r* stand for cloud and rain, respectively. Note that a prescribed cloud number concentration N_c is used ($200 \times 10^6\ m^{-3}$) in current P3 scheme, while prognostic N_c is planned to be included in next CR-SIM versions. For ice phase, the scheme predicts four ice mixing ratio variables, including total ice mass mixing ratio (Q_i, $kg\ kg^{-1}$), rime ice mass mixing ratio (Q_{rim}, $kg\ kg^{-1}$), rime ice volume mixing ratio (B_{rim}, $m^{-3}\ kg^{-1}$), and ice number concentration (N_i, kg^{-1}). Based on those prognostic variables, several predicted properties are derived, such as rime mass fraction ($F_r = Q_{rim}/Q_i$) and (bulk) rime density ($\rho_r = Q_{rim}/B_{rim}$, $kg\ m^{-3}$).

The PSD for each type of particle is represented by gamma distribution:

$$N'(D) = N_0 D^{\mu} e^{-\lambda D}$$

where D is the maximum particle diameter, and N_0, λ, and μ are the intercept, slope, and shape parameters, respectively. For cloud droplets, μ follows the observations of Martin et al. (1994). For rain, μ changes as a function of λ following the disdrometer observations in Cao et al. (2008): μ=-0.0201λ^2+0.902λ-1.718. For ice, μ is based on the in-situ observations in Heymsfield (2003): μ=0.0019$\lambda^{0.8}$-2. To get the size distribution parameters N_0 and λ for each type of particle requires to solve the equations related to the prognostic number concentration N and mass mixing ratio Q:

$$N = \int N'(D)dD = \int N_0 D^{\mu} e^{-\lambda D} dD$$
$$Q = \int m(D)N'(D)dD = \int m(D)N_0 D^{\mu} e^{-\lambda D} dD$$

where $m(D)$ is the m–D relationship ($m=aD^b$) which should be specified over the size distribution.

For cloud droplets and rain (spherical): $m=\pi\rho_w D^3/6$, where ρ_w is the liquid water density. Since the parameters in m–D relationships remain constant across the PSD, the N_0 and λ can be calculated analytically using equations above.

For ice particles, the m–D relationship varies in time and space and over the range of particle sizes, which can be calculated using the predicted and the prognostic quantities. In CR-SIM, PSDs and m–D relationships are estimated for the four ice particle categories separately. For small ice particles, which are assumed as spheres, with density of bulk ice ρ_i (=917 $kg\ m^{-3}$), the m–D relationship is expressed as: $m=\pi\rho_i D^3/6$. After growing by vapor diffusion and/or aggregation as larger unrimed crystals, the m–D relationship is given as: $m=0.0121D^{1.9}$ (which followed Brown and Francis 1995, but the coefficient was modified based on Hogan et al. 2012). When crystals are partially rimed, they follow a power-law relationship: $m = \left(\frac{0.0121}{1-F_r}\right) D^{1.9}$, where F_r is the rime mass fraction. Once the particle is 'filled in' with rime, the particle is considered to be spherical graupel, with an effective density ρ_g that is predicted and varies locally in time and space, following a m-D relationship as $m = \pi\rho_g D^3/6$.

In the scheme, a continuous PSD is used for ice. The PSD is partitioned into four regions representing the four ice categories based on the various *m–D* relationships described above. Therefore, PSD parameters cannot be derived analytically for the four categories separately, and an integration of incomplete gamma functions has to be considered across the different regions of the PSD. The ice PSD parameters were calculated as a function of ρ_r, F_r, and mixing ratio (personal communications with Dr. J. Fan and Dr. H. Morrison) and are given in look-up tables. The look-up tables are located in aux/P3 directory.

The fall velocity relationship is given by power-law relationship, $V_f(D) = a_v D^{b_v}$, except for cloud droplets. For cloud droplet, the dependence on environment conditions follows from Stokes' law through the dynamic viscosity of air μ_{air}, so $a_v = g\rho_w / (18\mu_{air})$, where g is acceleration of gravity, ρ_w is density of liquid water. The dynamic viscosity of air is calculated as: $1.496\times10^{-6}\ T^{1.5}/(T+120)$, where T is the air temperature. Rain drop speed is expressed using three different power-law relationships (Gunn and Kinzer, 1949; Beard, 1976; Simmel et al. 2002) for different size ranges. When $D < 134.43\ \mu$m, $V_f(D) = 4.5795 \times 10^3((\pi/6 \times 997 \times D^3) \times 10^3)^{2/3}$;When $134.43\ \mu m > D > 1511.64\ \mu m$, $V_f(D) = 4.962 \times 10((\pi/6 \times 997 \times D^3) \times 10^3)^{1/3}$; When $D > 1511.64\ \mu m$, $V_f(D) = 1.732((\pi/6 \times 997 \times D^3) \times 10^3)^{1/6}$. For small ice and unrimed ice, the coefficients a_v and b_v are derived following Mitchell and Heymsfield (2005) based on the *Re–X* relationship, where *Re* is the particle Reynolds number and *X* is the Best (Davies) number (related to the ratio of the particle mass to its projected area). Therefore, the calculation of the projected area $A(D) = a_A D^{bA}$ for ice particles is needed. Under the assumption of sphere, the particle projected areas of small ice particle and graupel can be given as: $A = \pi D^2/4$. For unrimed nonspherical ice, the *A–D* relationship parameters are empirically derived from ice particle observations from Mitchell (1996). For partially rimed crystals, a simple linear weighting is assumed between the value for graupel and unrimed ice as a function of F_r. The air density modification of particle fall speeds for rain (ice) follows Heymsfield et al. (2007), with a factor of $(\rho_0/\rho)^{0.54}$, where ρ_0 is a reference air density calculated at 1000 *hPa* (600 *hPa*) at 273.15 *K* (253.15 *K*).

Table 13: Parameters in the mass-size and velocity size relationships in P3 scheme

hydrometeor	a_m [-]	b_m [-]	ρ_h [$kg\ m^{-3}$]	V_f
cloud	$\pi\rho_h/6$	3	1000.0	$V_f(D) = g\rho w \frac{\square}{\square}(18\mu air)D^2$
rain	$\pi\rho_h/6$	3	1000.0	When D < 134.43 μm, $V_f(D) = 4.5795 \times 10^3((\pi/6 \times 997 \times D^3) \times 10^3)^{2/3}$; When 134.43 μm > D > 1511.64 μm, $V_f(D) = 4.962 \times 10((\pi/6 \times 997 \times D^3) \times 10^3)^{1/3}$; When D > 1511.64 μm, $V_f(D) = 1.732((\pi/6 \times 997 \times D^3) \times 10^3)^{1/6}$.
small ice	$\pi\rho_h/6$	3	917.0	Mitchell and Heymsfield (2005)
unrimed ice,	0.0121	1.9	-	Mitchell and Heymsfield (2005)
partially-rimed ice	$\frac{0.0121}{1-F_r}$	1.9	-	Mitchell and Heymsfield (2005)
graupel	$\pi\rho_h/6$	3	Predicted variable	Mitchell and Heymsfield (2005)

4.2.5 MP_PHYSICS=30 - ICON model with Seifert and Beheng 2-moment microphysics scheme

The ICOsahedral Non-hydrostatic atmosphere model (ICON) is a German regional model (Cotton et al. 2003). The CR-SIM can simulate all variables for ICON with the Seifert and Beheng 2-moment microphysics scheme as MP_PHYSICS=40. The input data file should include same variables as WRF data, and environmental variables are calculated as well as WRF.

The Seifert and Beheng 2-moment scheme (Seifert and Beheng 2006) consists of six hydrometeor categories: cloud droplets, rain, cloud (pristine) ice, snow (large crystals and aggregates), graupel, and hail. The scheme predicts:

-mixing ratios: Q_c, Q_r, Q_i, Q_s, Q_g, and Q_h in kg kg^{-1}

-number concentrations N_c, N_r N_i, N_s, N_g, *and* N_h in kg^{-1}.

The Gamma distribution is assumed for each hydrometeor distribution, and its generalized gamma distribution as a function of mass (M) is used, except rain.

$$N(M) = Ax^{\nu} \exp\left(-\lambda M^{\mu}\right)$$

The coefficients A and λ can be expressed by the number and mass densities:

$$A = \frac{\mu N}{\Gamma\left(\frac{\nu+1}{\mu}\right)} \lambda^{\frac{\nu+1}{\mu}} \text{ and } \lambda = \left[\frac{\Gamma\left(\frac{\nu+1}{\mu}\right)}{\Gamma\left(\frac{\nu+2}{\mu}\right)} \frac{Q}{N}\right]^{-\mu}$$

The mass-size relation is defined by a simple power law of the following form:

$$\mathrm{D} = a_m M^{b_m}$$

Regarding the rain drops, there is a diagnostic ν used outside of clouds. Because of μ=1/3 for rain, the rain drop distribution follows a gamma distribution in D:

$$N(D) = N_0 D^{\eta} \exp\left(-\lambda D\right)$$

Calculation of μ_e follows Seifert (2008, JAS).

$$\mu_e = \begin{cases} 6 \tanh\left[C_1\left(D_m - D_{eq}\right)\right]^2 + 1, & D_m \le D_{eq} \\ 30 \tanh\left[C_2\left(D_m - D_{eq}\right)\right]^2 + 1, & D_m > D_{eq}, \end{cases}$$

then

$$\lambda = [(\mu_e + 3)(\mu_e + 2)(\mu_e + 1)]^{1/3} {D_m}^{-1},$$

$$\mathrm{N}_0 = \frac{\mathrm{N}_r}{\Gamma(\mu_e + 1)} \lambda^{(\mu_e + 1)}$$

where c_1 = 4 mm^{-1}, c_2= 1 mm^{-1}, and D_{eq}=1.1 mm. D_m is the mean volume diameter obtained by the mass-size relation $D_m = a_m (Q/N)^{b_m}$.

The mean hydrometeor density ρ_h is calculated from mean particle mass (Q/N) and D_m.

$$\rho_d = \frac{6}{\pi D_m} \frac{Q}{N}$$

The fall velocity size relationships for all hydrometeors are specified in a form: $V_f(M) = f_c\, a_v\, M^{bv}$, where $f_c = (\rho_{surf}/\rho)^k$ is the correction factor for air density with exponent k.

Table 14: Parameters in the mass-size and mass-velocity, and size relationships for MP_PHYSICS=30 (Seifert and Beheng, 2006; A. Hansen, personal communication)

hydrometeor	v	μ	a_m [-]	b_m [-]	a_v [m s^{-1} kg^{-bv}]	b_v [-]	k [-]
cloud	1.0	1.0	0.124	1/3	3.75x10^5	2/3	1
rain	0.0	1/3	0.124	1/3	159.0	0.266	0.5
ice	0.0	1/3	0.835	0.39	317.0	0.363	0.5
snow	0.0	0.5	5.13	0.5	27.7	0.216	0.5
graupel	1.0	1/3	0.142	0.314	40.0	0.230	0.5
hail	1.0	1/3	0.1366	1/3	40.0	0.230	0.5

4.2.6 MP_PHYSICS=40 - RAMS model with 2-moment microphysics scheme

The CR-SIM with MP_PHYSICS=40 accepts the Regional Atmospheric Modeling System (RAMS; Cotton et al., 2003) model data with 2-moment microphysics. The RAMS data format is HDF5. Although variable names of RAMS data are different from those of WRF, the variables required for simulation are calculated as the following procedure (P. Marinescu, personal communication).

4.2.6.1 RAMS environmental variables

The variables that are needed for the CR-SIM calculations can be diagnosed from the RAMS standard output. RAMS prognoses non-dimensional pressure (π), and the RAMS standard output files include the variables ("PI"+"PC"), which simply scales π by the specific heat of air at constant pressure (c_p, 1005 J kg^{-1} K^{-1}).

Pressure can be solved from the PI variable in the RAMS output, as follows:

$$P\ (hPa) = p_0 * \left(\frac{(PI + PC)}{c_p}\right)^{\frac{c_p}{R_d}}$$

where p_0 = 1000 hPa, c_p = 1005 J kg^{-1} K^{-1}, and R_d = 287 J kg^{-1} K^{-1}.

RAMS standard output also includes potential temperature ("THETA" in the RAMS output), which can be used to diagnose temperature (T) as follows:

$$T\ (K) = \frac{PI}{c_p} * THETA$$

Dry air density (ρ_d) can be diagnosed using the diagnosed pressure and temperature and the water vapor mixing ratio variable in the RAMS standard output ("RV") via the equations of state for water vapor and dry air:

$$\rho_d \left(\frac{kg}{m^3}\right) = \frac{P - \frac{P * RV}{\mathcal{E} + RV}}{R_d * T}$$

where $\mathcal{E}$ = 0.622 and represents the ratio of dry and moist gas constants.

4.2.6.2 RAMS Two-Moment Microphysics Scheme

The RAMS microphysics scheme implemented here is the two-moment, bin-emulating, bulk microphysics scheme (Walko et al., 1995; Meyers et al., 1997; Saleeby and Cotton, 2004; Saleeby and van den Heever, 2013). As a bin-emulating scheme, the assumed hydrometeor distributions are converted into discrete bins for the calculation of various microphysical processes. The CR-SIM accepts the 2-moment microphysics scheme. RAMS prognoses and tracks eight hydrometeor categories: cloud, drizzle, rain, pristine ice, snow, aggregates, graupel and hail. The scheme predicts

- mixing ratios: Q_c, Q_d, Q_r, Q_p, Q_s, Q_a, Q_g, Q_h in kg kg^{-1} (kg kg$_{\text{dry air}}^{-1}$)
- number concentrations: N_c, N_d, N_r, N_p, N_s, N_a, N_g, N_h in kg^{-1} (kg$_{\text{dry air}}^{-1}$)

where the subscripts c, d, r, p, s, a, g, h represent cloud, drizzle, rain, pristine ice, snow, aggregates, graupel, and hail, respectively.

The mass-size relationship is given by $m(D) = a_m D^{b_m}$. The values for the factors a_m and b_m are provided in Table 15 for each hydrometeor category. All diameters (D, D_n) have units of meters, and the minimum and maximum diameters for each hydrometeor category are provided in Table 16. Hydrometeor density is related to mass via the following formula:

$$\rho_h \left[\frac{kg}{m^3}\right] = \frac{6a_m}{\pi} D^{b_m - 3}$$

The generalized gamma distribution is assumed to represent the size distribution of each hydrometeor:

$$N(D) \left[\frac{\#}{kg\ m}\right] = \frac{N_t}{\Gamma(\nu)} \left(\frac{D}{D_n}\right)^{\nu-1} \frac{1}{D_n} \exp\left(-\frac{D}{D_n}\right)$$

where N_t is the total number concentration $\left(\frac{\#}{kg}\right)$, D is the hydrometeor diameter (m), Γ is the gamma function, ν is the gamma distribution shape parameter, and D_n is the gamma distribution characteristic diameter (m). D_n is related to the mass mixing ratio and number concentrations via the following equation:

$$D_n = \left(\frac{Q}{N_t * a_m} \frac{\Gamma(\nu)}{\Gamma(\nu + b_m)}\right)^{\frac{1}{b_m}}$$

The fall velocity relationship is given by $V_f(D)[m\ s^{-1}] = f_c a_v D^{b_v}$. The values for a_v and b_v are provided for each hydrometeor species in Table 15. Note: cloud droplets are not allowed to fall in the RAMS model, and therefore, therefore, a_v and b_v are not provided in Table 15. f_c is a dimensionless factor that accounts for air density effects on the fall velocity and is given by $f_c = \left(\frac{0.7}{\rho_d}\right)^{0.362}$.

Table 15: Parameters for the mass-size and velocity-size relationships and the gamma distribution in the RAMS, two-moment microphysics scheme.

Hydrometeor	$\boldsymbol{\nu}$	$\boldsymbol{a_m}$ $\left(\boldsymbol{kg\ m^{-b_m}}\right)$	$\boldsymbol{b_m}$	$\boldsymbol{a_v}$ $\left(\boldsymbol{m^{1-b_v}\ s^{-1}}\right)$	$\boldsymbol{b_v}$
cloud	4	524	3	--	--
drizzle	4	524	3	3173	2
rain	2	524	3	149	0.5
pristine ice	2	110.8	2.91	5.77E+05	1.88
snow	2	2.74E-03	1.74	188.146	0.933
aggregates	2	0.496	2.4	3.084	0.2
graupel	2	157	3	93.3	0.5
hail	2	471	3	161	0.5

Table 16: Minimum and maximum diameters for each hydrometeor category.

Hydrometeor	$\boldsymbol{Minimum\ Diameter\ (m)}$	*Maximum Diameter (m)*
cloud	2.00E-06	5.00E-05
drizzle	6.50E-05	1.00E-04
rain	1.00E-04	5.00E-03
pristine ice	1.50E-05	1.25E-04
snow	1.00E-04	1.00E-02
aggregates	1.00E-04	1.00E-02
graupel	1.00E-04	5.00E-03
hail	8.00E-04	1.00E-02

4.2.7 MP_PHYSICS=75 - SAM model with Morrison 2-moment microphysics scheme

The CR-SIM with MP_PHYSICS=75 accepts the output from System for Atmospheric Modeling (Khairoutdinov and Randall 2003) simulations with Morrison 2-moment microphysics. The SAM simulation output includes two types of data. One is 3D (or 2D) data including U, V, W, P, T, hydrometeor mixing ratio and number density, and water vapor mixing ratio; the other is time series of vertical profile data including dry air density. Since the SAM is an anelastic model, the air density profile does not change with time. CR-SIM inputs those data files which are specified in the command line as "input_file_1 (WRFInputFile)" and "input_file_2 (WRFmpInputFile)," respectively, as described in section 2.3, but the profile data ("input_file_2") is optional. If the profile data is not given, air density is calculated from P and T from the 3D data. The microphysics part of this option is same as MP_PHYSICS=10 described in 4.2.2.

Hydrometeor mixing ratio variables from the SAM with Morrison 2-moment microphysics are rain water (QR), cloud ice (QI), snow (QS), non-precipitating hydrometeor (cloud water + cloud ice, QN), and precipitating hydrometeor (rain + snow QP). Therefore, cloud water mixing ratio (QC) is derived from QN – QI, and graupel mixing ratio (QG) is from QP – QR – QS.

4.2.8 MP_PHYSICS=80 – NCAR CM1 model with Morrison 2-moment microphysics scheme

The CR-SIM with MP_PHYSICS=80 accepts the output from NCAR Cloud Model 1 (CM1, Bryan and Fritsch 2002) simulations with Morrison 2-moment microphysics. The CM1 simulation output variables needed for CR-SIM are similar to WRF; including U, V, W, P, potential temperature, hydrometeor mixing ratio and number density, and water vapor mixing ratio. Temperature (T) and dry air density (ρ_d) are calculated in CR-SIM (see section 4.6.2.1). Height information is included in the CM1 output. Hydrometeor mixing ratio variables from the CM1 with Morrison 2-moment microphysics and the microphysics are identical to MP_PHYSICS=10.

4.3 Spectral microphysics schemes

Bin models that explicitly calculate evolution of the particle size resolution are nor widely used in 3-D cloud and climate models with a large number of grid cells due to a significant computational cost. When they are used, some balance has to be made in order to reduce associated cost expense. This balance is usually achieved by reducing the number of sizes for which the explicit microphysics is calculated. In the fast spectral-bin microphysical scheme (Fan et al., 2012), the number of hydrometeor categories is reduced by combining akin species into one spectrum. In addition, bin models operate with bins that progressively increase with diameter of hydrometeors. The small number of sizes and too large size bins may not be suitable for adequate modeling od radar variables, due to strong resonances in electromagnetic scattering which may occur at some diameter ranges. Those resonance ranges can be quite strong and narrow and may not be captured in the case of coarse resolution. This would in turn result in the low accuracy of computed radar variables, which could be in some cases significantly biased. Ryzhkov et al. (2011) have suggested that at C band, the bin resolution coarser than, for example, 0.5 *mm* could be

tolerable for the particle sizes above 10 *mm* and this only in the size ranges free of resonance effects.

4.3.1 MP_PHYSIC=20 – the fast spectral-bin microphysics scheme for WRF

In the fast spectral-bin microphysical (the fast SBM) scheme (Fan et al., 2012) with MP_PHYSIC=20, three hydrometeor categories are provided: water droplets, low-density ice and high-density ice. In the first hydrometeor category, the threshold size is 100 μm between droplets and raindrops. Ice and snow are combined into one size spectrum, low-density ice. The smaller ice particles with sizes less than 100 μm are assumed to be crystals, while larger particles are assigned to snow. As in the case with water droplets, the bin number that divides ice and snow is equal to 18. The third hydrometeor category is the high-density ice representing the graupel and hail with one size distribution without separation.

Bin mixing ratios of those three categories are provided in the WRF SBM NetCDF file for in total 43 mass-doubling size bins (the mass of a particle m_k in the k bin is determined as $m_k=2m_{k-1}$):

ff1i01-**ff1**i43	*kg kg*$^{-1}$	for cloud/rain bins
ff5i01- **ff5**i43	*kg kg*$^{-1}$	for ice/snow bins
ff6i01- **ff6**i43	*kg kg*$^{-1}$	for graupel-hail bins

Bin number concentration N_{ff} (D_j) per unit volume of air is obtained by:

$$N_{ff}\left(D_j\right)=\frac{ff\left(D_j\right)}{m_j}\,r_{d_{air}}$$

where D_j is the bin diameter in meters, the subscript j represents the bin number, m_j is the bin mass in kilograms and ρ_{dair} is the density of dry air in $kg\ m^{-3}$.

In the CR-SIM redistribution of those 3 hydrometeor categories to five hydrometeor species (cloud, rain, ice, snow and graupel/hail) is performed, in order to link the microphysical output with scattering look-up tables (see Section 4.4). Note that cloud and ice have 17 bins each, rain and snow are distributed in 16 bin-sizes each, while the graupel category has 33 bins. Density of graupel is fixed to 400 $kg\ m^{-3}$ for all sizes. Density of ice and snow decreases with size so that the smallest particles have the density of pure ice and the largest aggregates with diameters reaching 20 *mm* have a low density around 35 $kg\ m^{-3}$. Some characteristics of the fast SBM hydrometeor categories are given in Table 17.

The radii, densities and fall velocities of hydrometeors are provided as an input in separate ASCII files. Those files have to be in specified format, and are located in aux directory: aux/SBM_20/.

Table 17: Some characteristics of the fast SBM hydrometeor categories

Hydrometeor category in SBM	Hydrometeor subcategory in CR-SIM	Radius range	Num of sizes	Min Bin size	Max Bin size	Density [$kg\ m^{-3}$]	Fall velocity range [ms^{-1}]
Water droplets	***cloud***	2 μm - 80.6 μm	17	0.25 μm	21 μm	1000	$5x10^{-4}$ – 0.52
	rain	101.6 μm - 3.3 *mm*	16	26.4 μm	21 μm	1000	0.71 - 9.0
Low-density ice	***ice***	2.1 μm - 99 μm	17	0.54 μm	32.6 μm	900 -> 540	$2x10^{-4}$ – 0.21
	snow	131.6 μm - 9.9 *mm*	16	42.1 μm	2.2 *mm*	460 -> 35	0.26 – 1.4
High-density ice	***graupel/hail***	2.7 μm – 4.4 *mm*	33	0.7 μm	0.9 *mm*	400	$4x10^{-4}$ – 4.0

4.3.2 MP_PHYSIC=70 – the bin microphysics scheme for SAM

The Tel Aviv University (TAU) two-moment bin microphysics scheme for liquid droplets (cloud and rain) for SAM (Tzivion et al. 1987; Feingold et al. 1996) is incorporated

(MP_PHYSIC=70). Since this scheme has been operated as double moments, CR-SIM inputs number and mass for each size bin.

The bin boundaries and bin sizes are specified in a input file (referred as WRFmpInputFile). Below is an example of input text file:

```
MICRO_TAUBIN: bin information
      index  mass (g)  diameter (cm)  radius (cm)
-----  1   0.160E-10   0.313E-03   0.156E-03 -----
  bin  1
-----  2   0.320E-10   0.394E-03   0.197E-03 -----
  bin  2
-----  3   0.639E-10   0.496E-03   0.248E-03 -----
  bin  3
-----  4   0.128E-09   0.625E-03   0.313E-03 -----
  bin  4
-----  5   0.256E-09   0.787E-03   0.394E-03 -----
  bin  5
-----  6   0.511E-09   0.992E-03   0.496E-03 -----
  bin  6
-----  7   0.102E-08   0.125E-02   0.625E-03 -----
  bin  7
-----  8   0.205E-08   0.157E-02   0.787E-03 -----
  bin  8
-----  9   0.409E-08   0.198E-02   0.992E-03 -----
  bin  9
----- 10   0.818E-08   0.250E-02   0.125E-02 -----
  bin 10
----- 11   0.164E-07   0.315E-02   0.157E-02 -----
  bin 11
----- 12   0.327E-07   0.397E-02   0.198E-02 -----
  bin 12
----- 13   0.654E-07   0.500E-02   0.250E-02 -----
```

…

These bins are separated into cloud and rain categories in CR-SIM. The numbers of bins for cloud and rain are 12 and 24, respectively. These numbers can be changed by modifying a subroutine “hydro_info_samsbm” in crsim_subrs.f90.

Mean diameter at each bin (D_i) should be calculated using mass (M_i) and number concentration (N_i) at each bin.

$$D_i = [(M_i / N_i) * \rho_d / \rho * (3.0 / 4.0 / \pi)]^{1/3} * 2$$

$$D_i = \mathrm{MAX}(d_i, \mathrm{MIN}(d_{i+1}, D_i))$$

Here, particle density ρ is assumed to be 1000 kg m^{-3}. d_i and d_{i+1} represent diameter bin boundaries, and ρ_d represents air density in kg m^{-3}.

Particle fall velocity is calculated as a function of particle mass in a form: $V_{f\,i} = a_v M_i^{\,bv} \times 0.01$, where M_i is particle mass, which is provided as bin data in g. The unit of $V_{f\,i}$ is $m\ s^{-1}$. Coefficients a_v and b_v vary with particle size:

a_v = 0.45795E+6 and b_v = 2.0 / 3.0 for 3 μm < D <= 100 μm;

a_v = 4.962E+3 and b_v = 1.0 / 3.0 for 100 μm < D <= 800 μm;

a_v = 1.732E+3 and b_v = 1.0 / 6.0 for 0.8 mm < D <= 4.03 mm; and

a_v = 917.0 and b_v = 0.0 for D > 4.03 mm.

CR-SIM optionally accepts the profile data as "input_file_3 (ProfileInputFile)" of section 2.3, to get air density data. If the profile data is not given, air density is calculated from P and T from the "input_file_1 (WRFInputFile)."

4.4 Look-up tables

The solution of the scattering problem of a single particle reduces to the computation of the amplitude scattering matrix ***S*** that relates the scattered field to the incident field. The measureable radar variables can be expressed in function in term of particle backward and forward amplitudes. The elements S_{ij} of the 2x2 scattering matrix depend on the directions of incidence and scattering of the electromagnetic wave as well as on the size, morphology, and composition of the particle. The indices "*i"* and "*j"* indicate all the possible combinations of the polarizations *h* and *v*. Note that:

- There are the two conventions for the defining the referent system: 1) the **f**orward **s**cattering **a**lignment convention or FSA where the direction of observation is fixed to that of the wave (used, for example, for the amplitude and phase matrix components in Mishchenko's T-matrix code) and 2) the **b**ack**s**catter **a**lignment convention or BSA where the view direction is fixed to that of the transmitting radar antenna (used in definitions of polarimetric radar measurements except forward scattering parameters involving attenuation and phase shift)

- For monostatic radars (i.e., radars where one single antenna transmits and receives electromagnetic waves and are limited to measurements at the exact backscattering direction), the cross-polarization elements of the scattering matrix are identical (S_{hv} = S_{vh})$_{\mathrm{BSA}}$

- For spherical particles, the radar sees the same section whatever polarization *h* of *v* is used $S_{hh} = S_{vv} = S_{sphere}$, and $S_{hv} = S_{vh} = 0$

- For non-spherical particles S_{hh} and S_{vv} are not equal and, furthermore S_{hv} and S_{vh} are not equal to zero. However, if we assume that every single particle is uniformly oriented with a zero canting angle (i.e., with their axes of symmetry vertically aligned with respect to the direction of incidence of the transmitted radar signal), S_{hv} and S_{vh} continue to be 0.

Complex scattering amplitudes S_{ij} of the 2x2 scattering matrix are calculated using Mishchenko's T-matrix code for a non-spherical particle at a fixed orientation (available online on http://www.giss.nasa.gov/staff/mmishchenko/t_matrix.html). Following Ryzhkov et al. (2011), it is assumed that the scattering characteristics of arbitrarily oriented particles can be expressed via the scattering amplitudes f_a and f_b corresponding to the principal axes of spheroid when the electric vector of illuminated electromagnetic wave is directed along the spheroid axes *a* and *b* respectively. Each hydrometeor is characterized by its equivalent volume diameter $D=(ab^2)^{1/3}$, where *a* is the symmetry axis of spheroid and *b* is its transverse axis. In this convection, for oblate hydrometeor, $a < b$. The scattering amplitudes f_a and f_b correspond to S_{vv} and $-S_{hh}$ computed by Mishchenko's T-matrix code, respectively ($f_a \equiv S_{vv}$; $f_b \equiv -S_{hh}$). The minus sign in expression for f_h is to account for the switching from the FSA to BSA convention.

The T-matrix code requires knowledge of equivalent volume diameter *D*, axis ratio, radar wavelength λ, dielectric constant, directions of the incident and scattered waves and the particle orientation parameters as input parameters. All hydrometeors are modeled as oblate spheroids. Radar polarimetric variables depend on particle orientation, and since the distributions of particle orientations are not obtained from the cloud model, they have to be determined separately. For all hydrometeors, the scattering amplitudes are calculated assuming mean canting angle equal to zero degrees. Possible choices of the distributions of particle orientations are: 1) fully chaotic orientation, 2) random orientation in the horizontal plane and 3) two-dimensional aximmetric Gaussian distribution of orientations. Those are special cases for which simple expressions for angular moments can be obtained,

as described in Ryzhkov 2001. As in Ryzhkov et al. (2011), we assume that most of the atmospheric hydrometeors have oblate shapes characterized by 2D Gaussian distribution of orientations with zero mean canting angle and the angular moments. The width of canting angle distributions is different for various species of hydrometers. The default values for σ are 10° for cloud, rain, and ice, and 40° for dry snowflakes, unrimed ice, partially rimed ice, graupel and hail. The choice of angular moment distribution and the width of canting angle distribution per hydrometeor specie can be specified in the User CRSIM Configuration File.

Each medium is characterized by refractive index $\mathbf{Re}(n)+j\,\mathbf{Im}(n)$, where $\mathbf{Re}(n)>0$ and $\mathrm{Im}(n)>0$ if the $\mathbf{exp}(-j\omega t)$ convention is used. Refractive index of water and solid ice depend on temperature and radar wavelength. Ice particles, snow, graupel, unrimed ice, partially rimed ice and hail are assumed to be dielectrically dry and are represented as mixtures of air and solid ice. Thus, the refractive index of dielectrically dry hydrometeors depends on relative mixture of air and solid ice, or, in other words, on hydrometeor density and is computed using Maxwell Garnett (1904) mixing formula.

The complex scattering amplitudes for equally spaced particle sizes are pre-computed and stored in the look-up tables (LUTs) using the Mishchenko's T-matrix code for a non-spherical particle at a fixed orientation (Mishchenko, 2000). A hydrometeor class for which the look-up tables were pre-built by setting a fixed number of assumptions prior to running the T-matrix is referred as the “scattering type”. Each hydrometeor species present in the WRF output has to be assigned to the corresponding scattering type in the Configuration File. There is in total 13 scattering types present in LUTs. For each scattering type, the complex scattering amplitudes are pre-calculated for the total of 91 elevation angles from 0° to 90° with a spacing of 1°, five radar frequencies: 3 *GHz*, 5.5 *GHz*, 9.5 *GHz*, 35 *GHz* and 94 *GHz*, different temperature ranges for liquid hydrometeors, different possibilities of particles densities for solid hydrometeors and few different assumptions about particle aspect ratios. The canting angle in all cases is 0°. The main characteristics of pre-built LUTs are summarized in Table 18. For MP_PHYSICS=40, drizzle and aggregate categories are considered as cloud and snow, respectively.

Table 18: CR-SIM scattering look-up tables

Hydrometeor type	Scattering type	Diameter range	N of diameters	Temperature [° C]	Density [gr cm^{-3}]	Shape
cloud	**cloud**	1 μm-250 μm	250	[-30° 20°] every 2°	1	spherical
rain	**raina**	100 μm – 9 mm	446	[0° 20°] every 2°	1	Oblate according to Andsager et al. (1999)
	rainb					Oblate according to Brandes et al. (2002)
ice	**ice_ar0.20**	1 μm-1.5 mm	300	-30°	[0.4-0.9] every 0.1 $gr\ cm^{-3}$	Oblate with aspect ratio fixed to 0.2
	ice_ar0.90					Oblate with aspect ratio fixed to 0.9
	Smallice (P3 only)				0.001, 0.9	spherical
snow	**snow_ar0.60**	100 μm -5 cm	500	-30°	[0.1-0.5] every 0.1 $gr\ cm^{-3}$ 0.01, 0.05	Oblate with aspect ratio fixed to 0.6
graupel hail	**Graupel (P3 graupel only)**	5 μm - 4 cm	401	-30°	[0.01-0.09] every 0.01 $gr\ cm^{-3}$ [0.1-0.6] every 0.05 $gr\ cm^{-3}$	spherical
	graupel_ar0.80	100 μm -5 cm	501		0.4,0.5,0.9	Oblate with aspect ratio fixed to 0.8
	graupel_ar0.60					Oblate with aspect ratio fixed to 0.6
	gh_ryzh					Oblate with aspect ratio as in Ryzhkov et al. (2011)
unrimed ice (P3 only)	**unrimedice_ar 0.40**	5 μm - 4 cm	401	-30°	0.001, 0.005	Oblate with aspect ratio fixed to 0.4
	unrimedice_ar 0.60				[0.01-0.09] every 0.1 $gr\ cm^{-3}$]	Oblate with aspect ratio fixed to 0.6
	unrimedice_ar 0.80					Oblate with aspect ratio fixed to 0.8
	Unrimedice				[0.1-0.8] every 0.05 $gr\ cm^{-3}$	spherical
partially rimed ice (P3 only)	**partrimedice_ar0.40**	5 μm - 4 cm	401	-30°	[0.01-0.09] every 0.01 $gr\ cm^{-3}$ [0.1-0.6] every 0.05 $gr\ cm^{-3}$	Oblate with aspect ratio fixed to 0.4
	partrimedice_ar0.60					Oblate with aspect ratio fixed to 0.6
	partrimedice_ar0.80					Oblate with aspect ratio fixed to 0.8
	Partrimedice					spherical

All particles are modeled as dielectrically dry spheroids. For spherical particles (cloud), the aspect ratio is equal to one. We define here the aspect ratio as a ratio of minor

axis to major axis. Raindrops are simulated as oblate spheroids whose aspect ratio changes with size, according to:

1. Brandes et al. (2002)
   $ar = 0.9951 + 0.02510\ D - 0.03644\ D^2 + 0.005303\ D^3 - 0.0002492\ D^4$,
   with D expressed in millimeters

2. Andsager et al. (1999)
   $ar = 1.0048 + 0.0057\ D - 2.628\ D^2 + 3.682\ D^3 - 1.677\ D^4$,
   with D expressed in centimeters

A fixed aspect ratio is used for ice:

1. spherical small ice particles
2. 0.9 for near spherical pristine ice particles
3. 0.2 for simple models of plate-type ice crystals, e.g. for stellar or dendritic crystals which orient themselves by their long dimension in the horizontal plane

Also, a fixed aspect ratio of 0.6 is used for snow. In general, the aspect ratio for dry snow varies between 0.6 and 0.8 (Straka et al, 2000) but the impact of the aspect ratio of low-density aggregates on radar variables is rather small.

A fixed aspect ratio of 0.4, 0.6 or 0.8 can be specified for the categories of unrimed ice and a partially rimed ice.

There are two possibilities for choice of axis ratio for graupel and hail category:

1. spherical graupel
2. a fixed value of 0.8
3. as in Ryzhkov et al. (2011):

$$ar = 1.0 - 0.02\ D \quad \text{if} \quad D < 10\ mm$$
$$ar = 0.8 \quad \text{if} \quad D > 10\ mm$$

In general, the aspect ratio of dry graupel-hail varies between 0.6 and 0.9 (Straka et al, 2000). There is an argument that the choice of the aspect ratio is not too important due to the tumbling of those particles. Some authors have used a fixed aspect ratio of 0.75 for both snow and graupel.

In order to verify our computations of radar variables, we employed the Mueller-matrix-based code kindly provided by Dr. J. Vivekanandan (Colorado State University) and fully described in Vivekanandan et al. (1991) and Vivekanandan et al. (1993). From the scattering matrix calculated for a given orientation and elevation angle, the sixteen elements of the 4x4 Mueller matrix are constructed. These elements are then averaged over the specified orientation distribution. The canting effects are assumed to be 2σ-truncated Gaussian and random in azimuthal direction. Figures 4 and 5 show selected radar variables for simulated raindrops as a function of elevation angle and particle diameter, at 3 *GHz* and 9.5 *GHz*, respectively, computed by:

a) The method used in the CR-SIM Simulator based on Mishchenko's T-matrix code for a non-spherical particle at a fixed orientation and Ryzhkov's formulas for two-dimensional axisymmetric Gaussian distribution, mean canting angle 0° and σ=10°

b) The Mueller-matrix-based code from Vivekanandan et al. (1991). Orientation function assumed is 2σ truncated Gaussian, with mean canting angle 0° and σ=5°.

In both cases, rain particles are assumed oblate with the aspect ratio according to Brandes et al., 2002. Temperature is fixed to 13°*C* and an arbitrary concentration taken is equal to 1 m^{-3} per size.

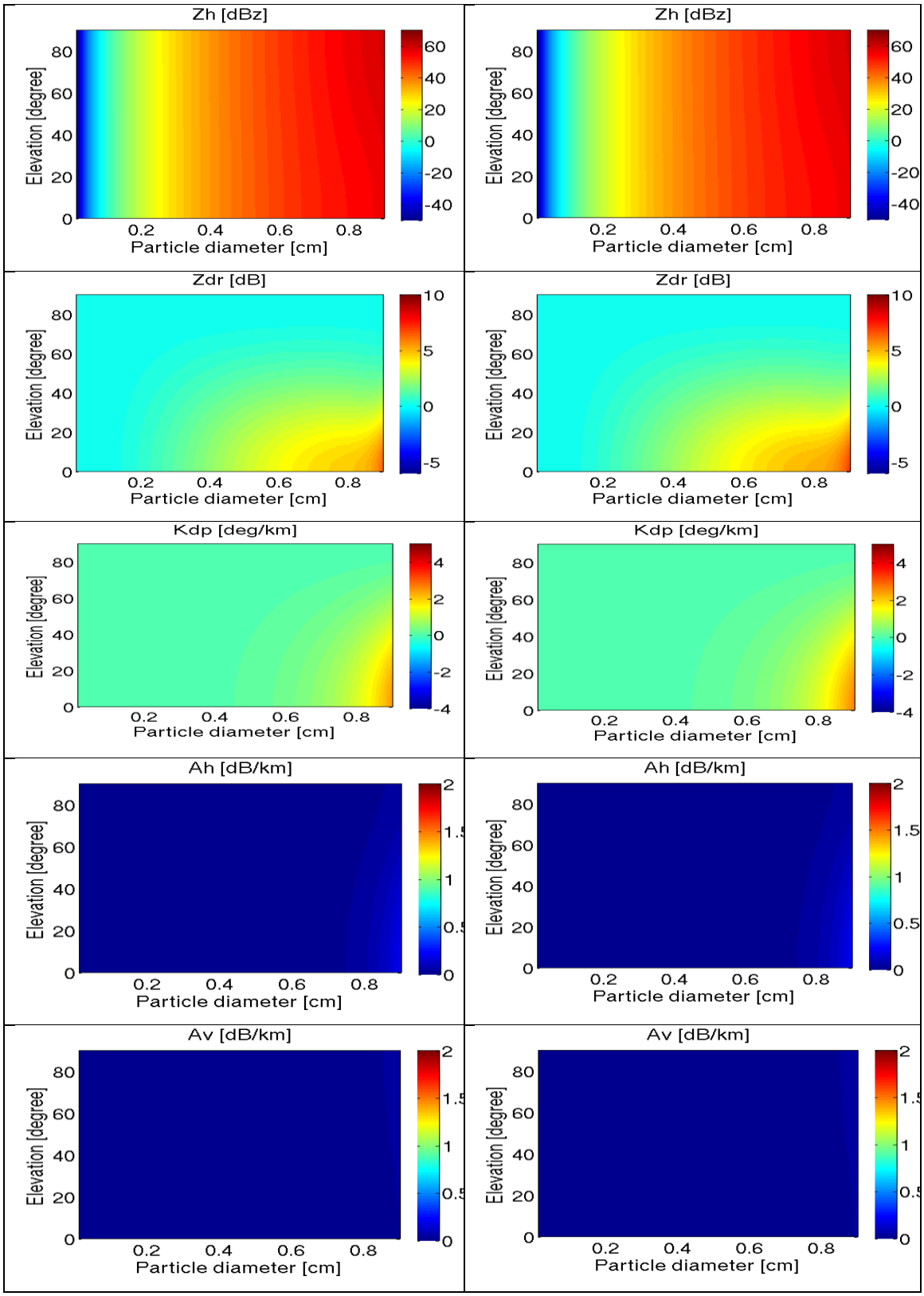
Zh [dBz]
Elevation [degree]
Particle diameter [cm]
Zdr [dB]
Kdp [deg/km]
Ah [dB/km]
Av [dB/km]

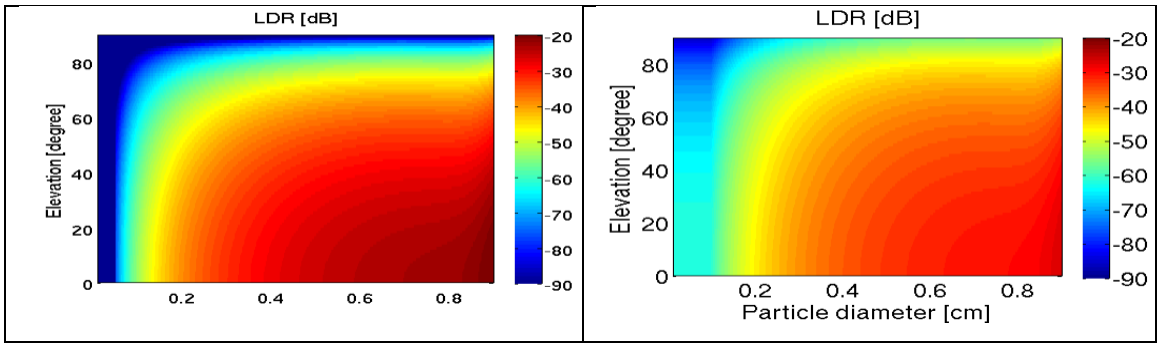

Figure 4: Selected radar variables at 3 *GHz* for simulated raindrops in function of elevation and particle size (diameter of equivolume sphere) computed by a) method used in the CR-SIM Simulator based on Mishchenko's T-matrix code for a non-spherical particle at a fixed orientation and Ryzhkov's formulas for angular moments 2) the Mueller-matrix-based code from Vivekanandan et al. (1991).

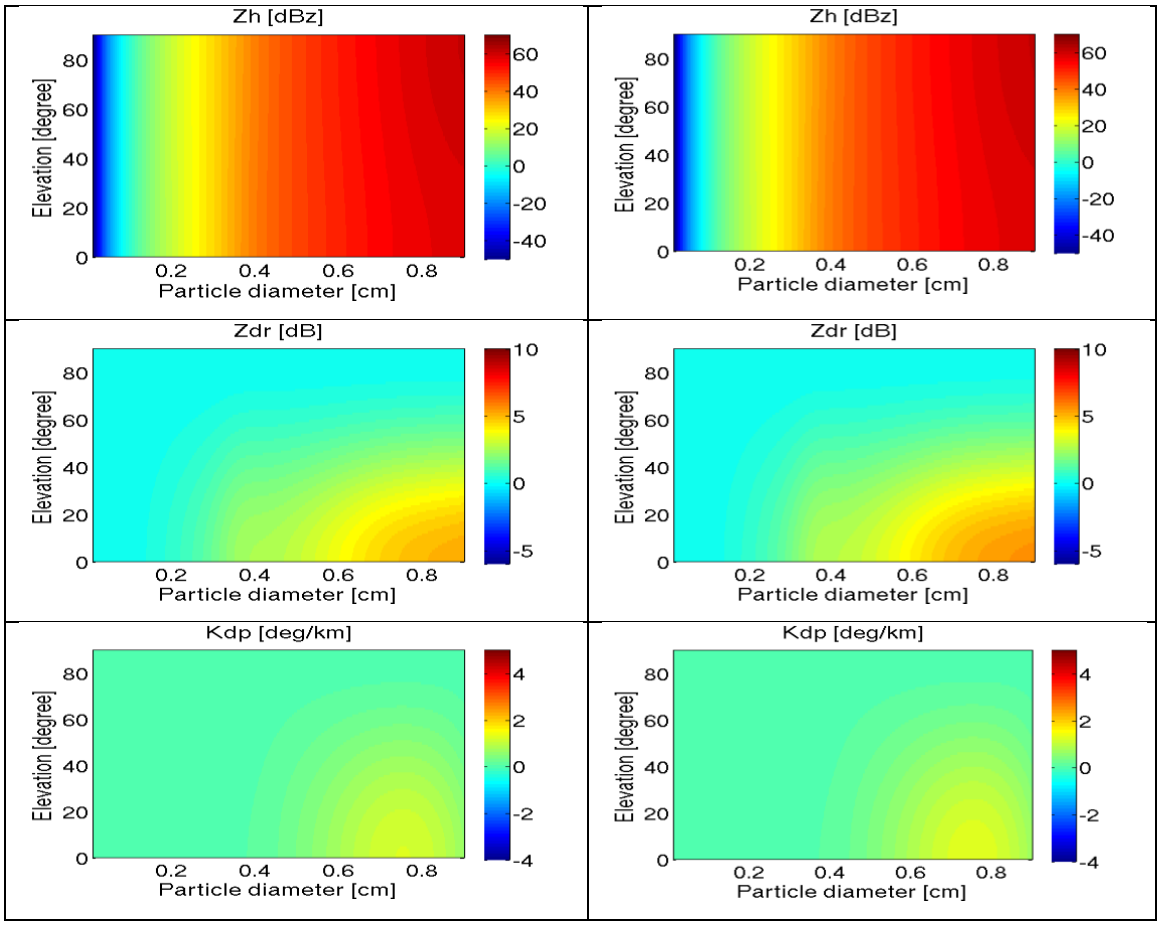

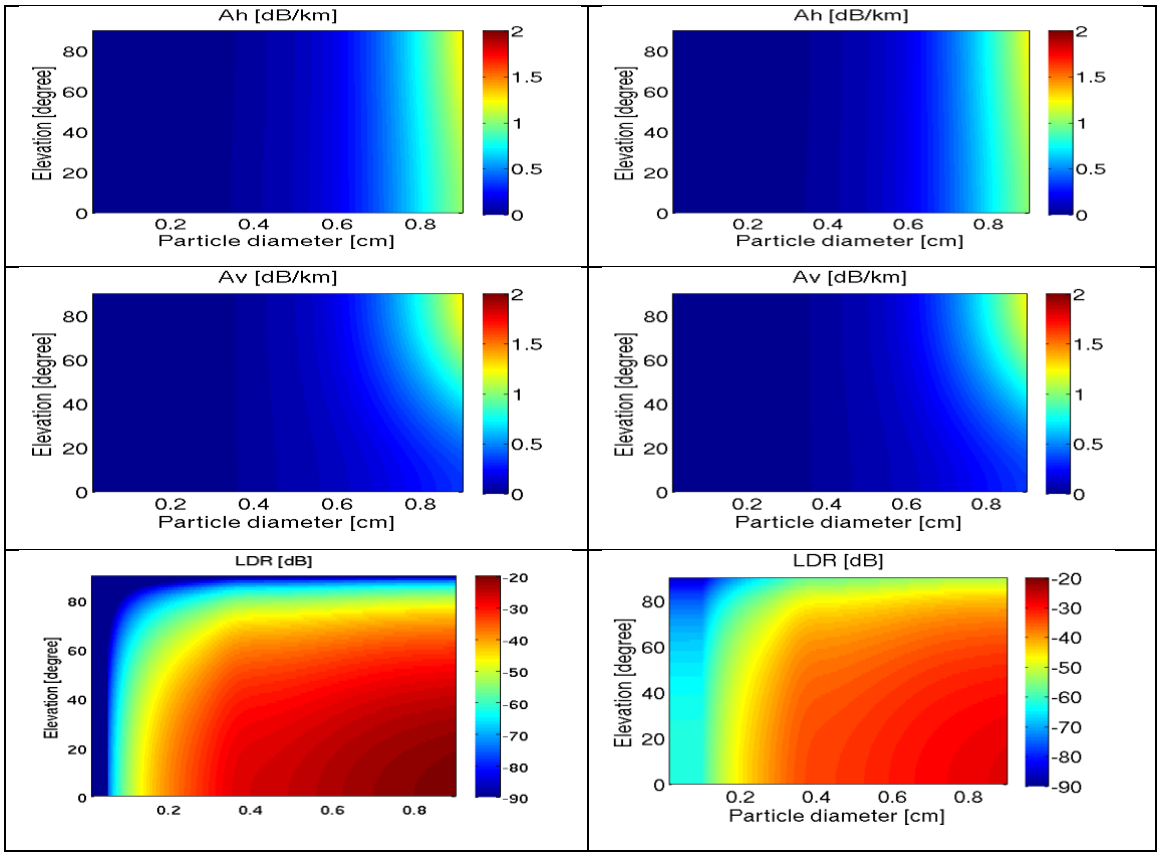

Figure 5: Selected radar variables at 9.5 *GHz* for simulated raindrops in function of elevation and particle size (diameter of equivolume sphere) computed by a) method used in the CR-SIM Simulator based on Mishchenko's T-matrix code for a non-spherical particle at a fixed orientation and Ryzhkov's formulas for angular moments 2) the Mueller-matrix-based code from Vivekanandan et al. (1991).

4.5 Computation of radar variables

The following radar variables can be computed using the outputs of the cloud models:

- Radar reflectivity factor at horizontal polarization, Z_h [$mm^6\ m^{-3}$ or dBZ]
- Radar reflectivity factor at vertical polarization, Z_v [$mm^6\ m^{-3}$ or dBZ]
- Co-polarization radar reflectivity factor, Z_{vh} [$mm^6\ m^{-3}$ or dBZ]. This variable is needed for computation of *LDR*

- Differential reflectivity Z_{DR} [unitless or *dB*] defined as the ratio between the fractions of horizontally polarized backscattering and vertically polarized backscattering. In general, Z_{DR} depends on the shape and on the common orientation degree but it is independent from the number of particles in the radar volume.
- Linear depolarization ratio LDR_h [unitless or *dB*] defined as the ratio of the power backscattered at vertical polarization to the power backscattered at horizontal polarization for a horizontally polarized field. Since *LDR* is a ratio between reflectivities, it is insensitive to the absolute radar calibration. As the cross-polar power is usually two to three orders of magnitude smaller than the co-polar signal, the *LDR* values are affected by noise contamination, propagation effects, and antenna mis-alignments.
- Cross-correlation coefficient RHOhv [unitless] is a measure of a variability of hydrometeor's size, shape, orientation and phase in the resolution volume. If the hydrometeor is "frozen" (i.e., there is no variability) in the radar resolution volume, then the value of cross-correlation coefficient is equal to one. One could expect a significant decrease in the cross-correlation coefficient due to non-sphericity effects, phase composition or if the size of scatterers is in resonant regime.
- Specific differential phase, K_{DP} [$degree\ km^{-1}$] is a comparison of the backward phase difference between the horizontally and vertically polarized waves.
- Differential backscatter phase, δ [degree] defined as the difference between the phases of horizontally and vertical polarized components of the wave caused by backscattering from the objects within the radar resolution volume. The computation of differential backscatter phase is based on Trömel et al (2013).
- Specific attenuation at horizontal polarization, A_h [$dB\ km^{-1}$] or for horizontally polarized waves, represented by forward scattering amplitudes.
- Specific attenuation at vertical polarization, A_v [$dB\ km^{-1}$], or for vertically polarized waves, represented by forward scattering amplitudes.
- Specific differential attenuation, A_{DP} [$dB\ km^{-1}$] is defined as the difference between the specific attenuations for horizontally and vertically polarized waves.

- Mean Radial Doppler velocity, V_D [$m\ s^{-1}$], positive away from the radar (radar notation)
- Mean Vertical Doppler velocity, V_{D_90} [$m\ s^{-1}$], positive upward (radar notation)
- Spectrum width, SW_{TOTAL}. There are six major spectral broadening mechanisms that contribute to the spectrum width SW_{TOT} measurements (Doviak and Zrnic, 2006): contribution due to 1) different hydrometeor terminal velocity of different sizes SW_H, 2) turbulence SW_T, 3) mean wind shear contribution SW_S, 4) cross wind contribution SW_V, 5) antenna motion SW_A, and 6) contributions due to variation of orientation and vibrations of hydrometeor SW_O:

$$SW_{TOTAL} = \sqrt{SW_H^2 + SW_T^2 + SW_S^2 + SW_V^2 + SW_A^2 + SW_O^2}$$

- Contributions SW_A and SW_O are not estimated here and their contributions to SW_{TOTAL} are considered negligible compered to contributions of other terms. Computed and outputted contributions however include SW_H, SW_T, SW_S and SW_V, and the total spectrum width SW_{TOT} is calculated as

$$SW_{TOT} = \sqrt{SW_H^2 + SW_T^2 + SW_S^2 + SW_V^2}$$

- In addition to SW_H for an arbitrary elevation direction θ, also reported is SW_{H_90} representing the spectrum width due to different hydrometeor terminal velocity of different sizes in vertical, such that $SW_{H\_90} = SW_H$ (θ=90°).
- Reflectivity weighted velocity, V_{RW} [$m\ s^{-1}$], (positive downward).
- Radar sensitivity limitation with range Z_{MIN} [dBZ], computed as follows:

$$Z_{MIN}[dBZ] = Z_0\ [dBZ] + 20\ log_{10}(\ r\ [km]\ )$$

where Z_0 is configurable term defined in User Parameter File and par default equal to -50 *dBZ*, while *r* is the radar range in *km*.

- Doppler velocity accounting for instrument moving speed, DV_airborne [$m\ s^{-1}$], where the instrument's moving direction and speed (specified in the configuration file) are accounted.
- Specific attenuation by water vapor, Avap [$dB\ km^{-1}$] is calculated based on the Rosenkranz (1998) result, using the water vapor mixing ratio, temperature, and pressure obtained from the CRM input. The two-way total attenuation, Atot [*dB*

km^{-1}] is also calculated when the user selects a fixed elevation angle = 90º (elev = 90º) as follows.:

$$A_{tot} = \sum_0^r 2(A_h + A_{vap})dr$$

where r is the radar range [km].

$$Z_{hh} = \frac{4\,\lambda^4}{\pi^4\,|K_w|^2}\ \sum_{i=1}^{M}\left[\int_0^{\infty}\left\{\left|f_{bi}^{(\pi)}\right|^2\ -\ 2R_e\left[f_{bi}^{(\pi)^*}\left(f_{bi}^{(\pi)}-f_{ai}^{(\pi)}\right)\right]A_{2i}\ +\ \left|f_{bi}^{(\pi)}-f_{ai}^{\pi}\right|^2 A_{4i}\right\}\ N_i\,(D)\,dD\right] \qquad \left[\frac{mm^6}{m^3}\right]$$

$$Z_{vv} = \frac{4\,\lambda^4}{\pi^4\,|K_w|^2}\ \sum_{i=1}^{M}\left[\int_0^{\infty}\left\{\left|f_{bi}^{(\pi)}\right|^2\ -\ 2R_e\left[f_{bi}^{(\pi)^*}\left(f_{bi}^{(\pi)}-f_{ai}^{(\pi)}\right)\right]A_{1i}\ +\ \left|f_{bi}^{(\pi)}-f_{ai}^{\pi}\right|^2 A_{3i}\right\}\ N_i\,(D)\,dD\right] \qquad \left[\frac{mm^6}{m^3}\right]$$

$$Z_{vh} = \frac{4\,\lambda^4}{\pi^4\,|K_w|^2}\ \sum_{i=1}^{M}\left[\int_0^{\infty}\left\{\ \left|f_{bi}^{(\pi)}-f_{ai}^{\pi}\right|^2 A_{5i}\right\}\ N_i\,(D)\,dD\right] \qquad \left[\frac{mm^6}{m^3}\right]$$

$$Z_{DR} = \frac{Z_{hh}}{Z_{vv}} \qquad [-]$$

$$LDR_h = \frac{Z_{vh}}{Z_{hh}} \qquad [-]$$

$$RHO_{HV} = \frac{\frac{4\,\lambda^4}{\pi^4\,|K_w|^2}\ \sum_{i=1}^{M}\left[\int_0^{\infty}\left\{\left|f_{bi}^{(\pi)}\right|^2\ +\ \left|f_{bi}^{(\pi)}-f_{ai}^{\pi}\right|^2 A_{5i}-f_{bi}^{(\pi)^*}\left(f_{bi}^{(\pi)}-f_{ai}^{(\pi)}\right)A_{1i}-f_{bi}^{(\pi)}\left(f_{bi}^{(\pi)^*}-f_{ai}^{(\pi)^*}\right)A_{2i}\right\}\ N_i\,(D)\,dD\right]}{(Z_{hh}\,Z_{vv})^{0.5}} \qquad [-]$$

$$K_{DP} = \frac{180\,\lambda}{\pi}\ 10^{-3}\ \sum_{i=1}^{M}\left[\int_0^{\infty}\left\{\ R_e\left(f_{bi}^{(0)}-f_{ai}^{0}\right)A_{7i}\right\}\ N_i\,(D)\,dD\right] \qquad \left[\frac{deg}{km}\right]$$

$$\delta = \frac{180\,\lambda}{\pi}\ arg\left[\sum_{i=1}^{M}\left[\int_0^{\infty}\left\{\left|f_{bi}^{(\pi)}\right|^2\ +\ \left[\left|f_{bi}^{(\pi)}-f_{ai}^{(\pi)}\right|^2\right]A_{3i}-\left[f_{bi}^{(\pi)^*}\left(f_{bi}^{(\pi)}-f_{ai}^{(\pi)}\right)\right]A_{1i}-\ \left[f_{bi}^{(\pi)}\left(f_{bi}^{(\pi)^*}-f_{ai}^{(\pi)^*}\right)\right]A_{2i}\right\}\ N_i\,(D)\,dD\right]\right] \quad [deg]$$

$$A_H = \frac{10}{log(10)}\ \ 2\,\lambda\ \ 10^{-3}\sum_{i=1}^{M}\left[\int_0^{\infty}\left\{\ I_m\left(f_{bi}^{(0)}\right)-I_m\left(f_{bi}^{(0)}-f_{ai}^{(0)}\right)A_{2i}\right\}\ N_i\,(D)\,dD\right] \qquad \left[\frac{dB}{km}\right]$$

$$A_V = \frac{10}{log(10)}\ \ 2\,\lambda\ \ 10^{-3}\sum_{i=1}^{M}\left[\int_0^{\infty}\left\{\ I_m\left(f_{bi}^{(0)}\right)\ -I_m\left(f_{bi}^{(0)}-f_{ai}^{(0)}\right)A_{1i}\ \right\}\ N_i\,(D)\,dD\right] \qquad \left[\frac{dB}{km}\right]$$

$$A_{DP} = A_H - A_V \qquad \left[\frac{dB}{km}\right]$$

$$VZ_i = \int_0^{\infty}\left\{\left|f_{bi}^{(\pi)}\right|^2\ -\ 2R_e\left[f_{bi}^{(\pi)^*}\left(f_{bi}^{(\pi)}-f_{ai}^{(\pi)}\right)\right]A_{2i}\ +\ \left|f_{bi}^{(\pi)}-f_{ai}^{\pi}\right|^2 A_{4i}\right\}\ V_{Fi}(D)\ N_i\,(D)\,dD \qquad \left[\frac{mm^6}{m^3}\ \frac{m}{s}\right]$$

$$V_{RW} = \frac{\frac{4\,\lambda^4}{\pi^4\,|K_w|^2}\ \sum_{i=1}^{M}[VZ_i\,]}{Z_{hh}} \qquad \left[\frac{m}{s}\right]$$

$$V_{D\_90} = \frac{\frac{4\,\lambda^4}{\pi^4\,|K_w|^2}\ \sum_{i=1}^{M}[w\,Z_{hh}\ -\ VZ_i\,]}{Z_{hh}} \qquad \left[\frac{m}{s}\right]$$

$$V_D = [u\,cos\varphi\ +\ v\,sin\varphi]\cos\theta\ +\ V_{D\_90}\sin\theta \qquad \left[\frac{m}{s}\right]$$

$$SW_{H\_90} = \sqrt{\frac{4\,\lambda^4}{\pi^4\,|K_w|^2}\,\Sigma_{i=1}^{M}\left[\int_0^{\infty}\left\{\left|f_{bi}^{(\pi)}\right|^2 - 2R_e\left[f_{bi}^{(\pi)^*}\left(f_{bi}^{(\pi)} - f_{ai}^{(\pi)}\right)\right]A_{2i} + \left|f_{bi}^{(\pi)} - f_{ai}^{\pi}\right|^2 A_{4i}\right\}\left(V_{Fi}(D) - \frac{VZ_i}{Z_{hh}}\right)^2 N_i(D)\,dD\right]}{Z_{hh}}} \quad \left[\frac{m}{s}\right]$$

$$SW_H = SW_{H\_90}\,\sin\theta \quad \left[\frac{m}{s}\right]$$

$$SW_{TOT} = \sqrt{SW_H^2 + SW_T^2 + SW_S^2 + SW_V^2} \quad \left[\frac{m}{s}\right]$$

In the equations above, M is the number of different hydrometeor species coexisting in the same spatial resolution volume of the model, and subscript i means index of species. Backward and forward scattering amplitudes are denoted as $f_{a,b}^{(\pi)}$ and $f_{a,b}^{(0)}$, respectively. The subscript * in expression $[\ldots]^*$ denotes conjugation, $R_e[\ldots]$ and $I_m[\ldots]$ represent the real and imaginary part of the complex number, respectively, and $|\ldots|$ means the magnitude of the value between the single bars. The radar wavelength is λ [mm] and the value of dielectric factor for water is $K_w = 0.92$. The scattering amplitudes are given in millimeters. $N_i(D)$ defines the particle size distribution and is number of particles per unit volume of air and unit bin size, given here in $m^{-3}\,mm^{-1}$, with the bin equivolume diameter D in mm. Both the bin fall velocity V_{Fi} and vertical air velocity w are given in meter per second.

The spectrum width contribution due to turbulence SW_T is computed from the following relation:

$$SW_T^2 = \left[\frac{1}{0.72}\left(EDR\;\; r\;\; \sigma_\theta\;\; A^{3/2}\right)\right]^{2/3} \qquad for\;\; \sigma_r \le r\;\; \sigma_\theta,$$

$$SW_T^2 = \sigma_r^{2/3}\;\; 1.35\;\; A\;\; EDR^{\,2/3}\;\; \mathcal{M} \qquad otherwise.$$

In the above equation, EDR is the eddy dissipation ratio in $m^2\,s^{-3}$, A (=1.6) is the universal dimensionless constant generally having values between 1.53 and 1.68, r is the radar range, σ_r = 0.35 δr where δr is the radar range resolution in meters, $\sigma_\theta = \Theta_1 / (4\ ln2)$ with beamwidth Θ_1 in degrees and M is defined as follows:

$$\mathcal{M} = \frac{11}{15} + \frac{4}{15}\;\frac{r^2\;\sigma_\theta{}^2}{\sigma_r{}^2}$$

EDR is calculated using an empirical equation in the papers Pokharel et al. (2017) and Regmi et al. (2017):

$$EDR = 0.238 \times \frac{(TKE - 0.1)^{2/3}}{L}$$

where *TKE* is the input turbulence kinetic energy in $m^2\ s^{-2}$, and *L* is the length scale in *m* estimated by $\sqrt{dx^2 + dy^2 + dz^2}$.

The spectrum width SW_s represents contribution due to wind shear within the radar volume and is decomposed (Doviak and Zrnic, 2006) intro three terms each at orthogonal directions in radar coordinates:

$$SW_S^2 = (\sigma_\theta\, r\, k_\theta)^2 + \left(\sigma_\varphi r\, k_\varphi\right)^2 + (\sigma_r k_r)^2$$

Here $\sigma_\theta = \sigma_\varphi$, and rk_θ, rk_φ and k_r are the components of radial wind shear in spherical coordinates. If $\boldsymbol{V} = u\,\boldsymbol{i} + v\,\boldsymbol{j} + w\,\boldsymbol{k}$ is the wind in the Cartesian coordinate system, then we can write:

$$k_r \equiv \frac{\partial \boldsymbol{V}}{\partial r} = \frac{\partial \boldsymbol{V}}{\partial x}\frac{\partial x}{\partial r} + \frac{\partial \boldsymbol{V}}{\partial y}\frac{\partial y}{\partial r} + \frac{\partial \boldsymbol{V}}{\partial z}\frac{\partial z}{\partial r}$$

$$r\,k_\theta \equiv \frac{1}{r}\frac{\partial \boldsymbol{V}}{\partial \theta^*} = \frac{1}{r}\left(\frac{\partial \boldsymbol{V}}{\partial x}\frac{\partial x}{\partial \theta^*} + \frac{\partial \boldsymbol{V}}{\partial y}\frac{\partial y}{\partial \theta^*} + \frac{\partial \boldsymbol{V}}{\partial z}\frac{\partial z}{\partial \theta^*}\right)$$

$$r\,k_\varphi \equiv \frac{1}{r\sin\theta^*}\frac{\partial \boldsymbol{V}}{\partial \varphi} = \frac{1}{r\sin\theta^*}\left(\frac{\partial \boldsymbol{V}}{\partial x}\frac{\partial x}{\partial \varphi} + \frac{\partial \boldsymbol{V}}{\partial y}\frac{\partial y}{\partial \varphi} + \frac{\partial \boldsymbol{V}}{\partial z}\frac{\partial z}{\partial \varphi}\right)$$

The shear terms in the three orthogonal Cartesian system $k_x = \partial u/\partial x$, $k_y = \partial v/\partial y$ *and* $k_z = \partial w/\partial z$ can be easily computed from the WRF input wind, while the partial derivatives $\partial(x, y, z)/\partial(r, \theta^*, \varphi)$ can be computed from the relations between spherical coordinate system and Cartesian coordinates:

$$x = r\,\cos\varphi\ \sin\theta^*$$

$$y = r\,\sin\varphi\ \sin\theta^*$$

$$z = r\ \cos\theta^*$$

where *r* is the radar range, φ is the azimuth and θ^* is the zenith angle (measured from zenith to horizontal). Note that the radar elevation angle θ is equal to 90 - θ^*, and that $\sin\theta^* = \cos\theta$ and $\cos\theta^* = \sin\theta$. Finally, the shear components along *r*, elevation θ, and azimuth φ direction are computed as follows:

$$k_r = \frac{\partial \boldsymbol{V}}{\partial r} = k_x\ \cos\varphi\ \cos\theta\ + k_y\ \sin\varphi\ \cos\theta + k_z \sin\theta$$

$$r\,k_\theta = \frac{1}{r}\,\frac{\partial \boldsymbol{V}}{\partial \theta^*} = k_x \cos\varphi \sin\theta + k_y \sin\varphi \sin\theta - k_z \cos\theta$$

$$r\,k_\varphi = \frac{1}{r\sin\theta^*}\,\frac{\partial \boldsymbol{V}}{\partial \varphi} = -k_x \sin\varphi + k_y \cos\varphi$$

The contribution SW_V due to cross wind $\boldsymbol{V_{cross}}$ within the radar volume can be expressed as:

$$SW_V^2 = (V_{cross}\,\sigma_\theta)^2$$

where cross wind V_{cross} is computed as:

$$V_{cross} = u \cos\varphi \sin\theta + v \sin\varphi \sin\theta + w\cos\theta\,.$$

Values of angular moments A_{1i}-A_{7i} are obtained from expressions given in Table 19. The corresponding values of Z_h, Z_v, Z_{vh}, Z_{DR} and LDR_h in logarithmic units are obtained as follows:

$$Z_{h,v,vh}[dBz] = 10\log_{10}\left(Z_{h,v,vh}[mm^6 m^{-3}]\right)$$
$$Z_{DR}[dB] = 10\log_{10}\left(Z_{DR}[-]\right)$$
$$LDR_h[dB] = 10\log_{10}\left(LDR_h[-]\right)$$

Note that

$$LDR_v(dB) = LDR_h(dB) + Z_{DR}(dB)$$

where LDR_v is linear depolarization ratio for a vertically polarized field defined as the ratio of the power backscattered at horizontal polarization to the power backscattered at vertical polarization. The elevation and azimuth angles are denoted θ and φ respectively, and u and v are the two components of horizontal wind.

The coefficients A_j are angular moments for three special cases, assuming the mean canting angle equal to zero and an angle between direction of the symmetry axis of the particle and direction of wave propagation perpendicular to polarization plane close to 90°). The horientID in Table 19 is the parameter whose value for each hydrometeor type has to be set in the Configuration File.

Table 19: Simple expressions for angular moment for the three distributions of orientations (from Ryzhkov et al., 2011)

Fully chaotic orientation (horientID=1)	Random orientation in the horizontal plane (horientID=2) -valid assumption for prolate particles (column, needles, etc.)	Two-dimensional axisymmetric Gaussian distribution of orientations (horientID=3) -valid assumptions for oblate particles with zero mean canting angle-
$A_1 = \frac{1}{3}$ $A_2 = \frac{1}{3}$ $A_3 = \frac{1}{5}$ $A_4 = \frac{1}{5}$ $A_5 = \frac{1}{15}$ $A_6 = 0$ $A_7 = 0$	$A_1 = \frac{1}{2}\sin^2 b$ $A_2 = \frac{1}{2}$ $A_3 = \frac{3}{8}\sin^2 b$ $A_4 = \frac{3}{8}$ $A_5 = \frac{1}{8}\sin^2 b$ $A_6 = 0$ $A_7 = -\frac{1}{2}cos^2 b$ where β is the elevation angle	$A_1 = \frac{1}{4}(1+r)^2$ $A_2 = \frac{1}{4}(1-r)^2$ $A_3 = \left(\frac{3}{8} + \frac{1}{2}r + \frac{1}{8}r^4\right)^2$ $A_4 = \left(\frac{3}{8} - \frac{1}{2}r + \frac{1}{8}r^4\right)\left(\frac{3}{8} + \frac{1}{2}r + \frac{1}{8}r^4\right)$ $A_5 = \frac{1}{8}\left(\frac{3}{8} - \frac{1}{2}r + \frac{1}{8}r^4\right)(1-r^4)$ $A_6 = 0$ $A_7 = \frac{1}{2}r(1+r)$ where $r=exp(-2\sigma^2)$, with σ in radians

In the case of two-dimensional axisymmetric Gaussian distribution of orientations, its width has to be specified in the Configuration File. In Ryzhkov et al. (2002) it is assumed that σ is equal to 10° for rain and oblate crystals, and to 40° for dry snowflakes and graupel-hail. Other values of σ can be, as well, found in literature.

As an illustration of CR-SIM capabilities, the three following figures show CFADs of reflectivity weighted velocity with height per hydrometeor class and for the total hydrometeor content at 3 *GHz* (Figure 6), CFADs of vertical Doppler velocity with

reflectivity at different domains and frequencies (Figure 7), and CFADs of vertical Doppler velocity with reflectivity per hydrometeor class at 3 *GHz* (Figure 8).

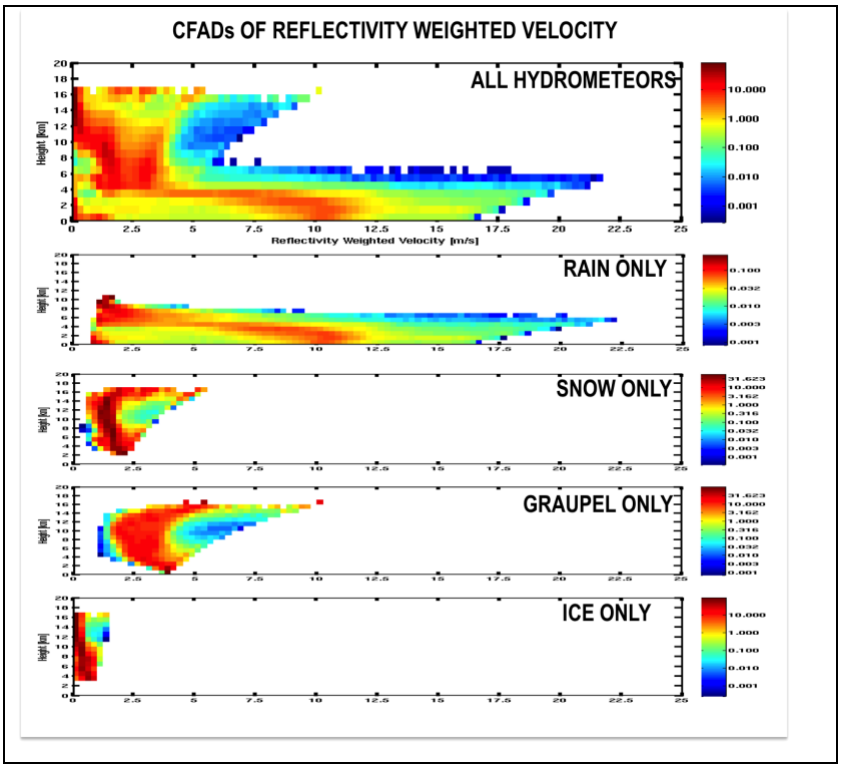

Figure 6: CFADs of reflectivity weighted velocity with height per hydrometeor class and for the total hydrometeor content at 3 *GHz*.

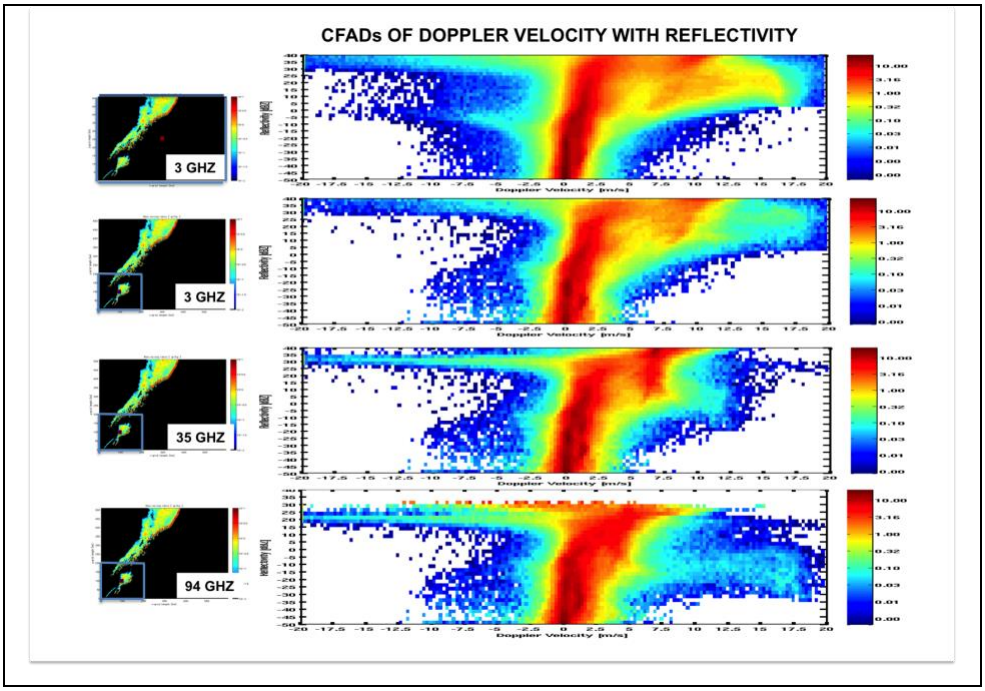

Figure 7: CFADs of vertical Doppler velocity with reflectivity at different domains and frequencies

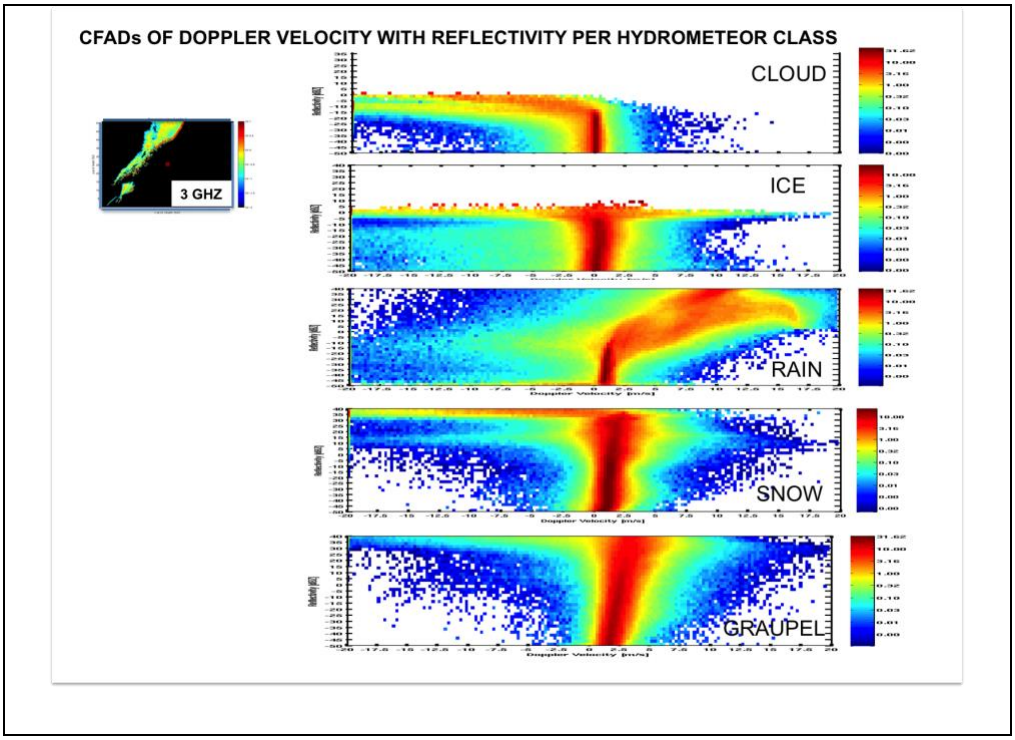

Figure 8: CFADs of vertical Doppler velocity with reflectivity per hydrometeor class at 3 *GHz*.

4.6 Computation of cloud lidar (ceilometer) variables

For spherical droplets, using BHMIE Mie code (Bohrean and Hyffman,1998) the single particle extinction σ_α and backscattering cross sections σ_β are computed for a wavelength of 905 *nm*.

$$\beta_{true} = \sum_i \sigma_\beta (D_i)\ N (D_i)\, \Delta D_i$$

$$\alpha_{ext} = \sum_i \sigma_\alpha (D_i)\ N (D_i)\, \Delta D_i$$

The value of refractive index of water used calculations is $1.327+i\ 0.672\text{x}10^{6}$ (Hale and Querry, 1973). The backscatter observed, β_{obs} observed by cloud lidar at a wavelength of 905 *nm* and at a distance *z* can be written as:

$$\beta_{obs}(z) = \int_0^z \beta_{true}(z)\ \exp\left(-2\,\alpha_{ext}(z)\right)\, dz, \qquad [sr\ m]^{-1}$$

where β_{true} is the true backscatter at height z, and α_{ext} is the extinction coefficient:

$$\beta_{true} = \frac{1}{4\pi} \sum_i \sigma_\beta (D_i)\ N (D_i)\, \Delta D_i \qquad [sr\ m]^{-1}$$

$$\alpha_{ext} = \frac{1}{4\pi} \sum_i \sigma_\alpha (D_i)\ N (D_i)\, \Delta D_i \qquad [sr\ m]^{-1}$$

Along with the true and observed (attenuated) backscatter, lidar ratio *S*, defined as the ratio between the lidar extinction and true backscatter is provided in the main output file.

$$S = \frac{\alpha_{ext}}{\beta_{true}} \qquad [\ -\ ]$$

Also estimated is the first cloud base as observed by ceilometer, based on a method somewhat simplified than one described by O'Connor et al (2004), and this due to simplified nature of simulated lidar measurements when compared to observations.

4.7 Computation of micro pulse lidar (MPL) variables

Users can make an option of MPL wavelength between 353 and 532 *nm* for computation of MPL variables. As similar as the computation of ceilometer variables (section 4.6), the single particle extinction σ_α and backscattering cross sections σ_β for spherical cloud droplets are calculated using BHMIE Mie code (Bohrean and Hyffman,1998), but for wavelengths of 353 and 532 *nm* and output in look-up tables. For ice cloud, σ_α and σ_β for spherical cloud ice particles are calculated and output as similar as cloud droplets, but particle bulk density varies from 100 $kg\ m^{-3}$ to 917 $kg\ m^{-3}$.

The unattenuated backscatter β_{true} and the extinction coefficient α_{ext} are computed as the sum of σ_β and σ_α over the particle size distribution, respectively:

$$\beta_{true} = \frac{1}{4\pi} \sum_i \sigma_\beta (D_i)\ N (D_i)\ \Delta D_i \qquad [sr\ m]^{-1}$$

$$\alpha_{ext} = \frac{1}{4\pi} \sum_i \sigma_\alpha (D_i)\ N (D_i)\ \Delta D_i \qquad [sr\ m]^{-1}$$

Single ice bulk densities according to a selected microphysics scheme are used for the ice particle size distribution.

Observed MPL backscatter includes backscatters from atmospheric aerosols and molecules in addition to hydrometeor backscatter. Standard vertical profiles of atmospheric molecular backscatter β_{mol}, aerosol backscatter β_{aero}, and aerosol extinction coefficient α_{ext_aero} are given by Spinhirne (1993):

$$\beta_{mol} = 2.398 \times 10^{32} \frac{0.01P}{\lambda^{4.0117} T} \qquad [sr\ m]^{-1}$$

$$\alpha_{ext\_aero} = \sigma_0 \frac{(1+a)^2 \exp\left(\frac{z}{b}\right)}{\left[a+\exp\left(\frac{z}{b}\right)\right]^2} + f \frac{(1+a\prime)^2 \exp\left(\frac{z}{b\prime}\right)}{\left[a+\exp\left(\frac{z}{b\prime}\right)\right]^2};\ z > 1000\ \text{m}\ [sr\ m]^{-1}$$

$$\alpha_{ext\_aero} = \sigma_0 \frac{(1+a)^2 \exp\left(\frac{z}{b}\right)}{\left[a+\exp\left(\frac{z}{b}\right)\right]^2} + f \frac{(1+a\prime)^2 \exp\left(\frac{z}{b\prime}\right)}{\left[a+\exp\left(\frac{z}{b\prime}\right)\right]^2} + 0.00005;\ z < 1000\ \text{m (for boundary layer)}\ \ [sr\ m]^{-1}$$

$$\beta_{aero} = \frac{\alpha_{ext\_aero}}{S_p} \qquad [sr\ m]^{-1}$$

The terms σ_0, a, a', b, b', f are constants. For the current model, σ_0 = 0.000025 m^{-1}, a = 0.4, a' = 2981, b = 1600 m, b' = 2500 m, and f = 1.5×10^{-10} m^{-1}. S_p is a constant specified by users in the Configuration file. A general value of S_p is 30.

The attenuated backscatter, β_{atten} at a given frequency at distance z is written as:

$$\beta_{atten}(z) = \int_0^z \beta_{true}(z)\ \exp\left(-2\ \alpha_{ext}(z)\right)\ dz \qquad [sr\ m]^{-1}$$

Similarly, the attenuated aerosol backscatter β_{aero_atten} and the attenuated molecular backscatter β_{mol_atten} are respectively:

$$\beta_{aero\_atten}(z) = \int_0^z \beta_{aero}(z)\ \exp\left(-2\ (\alpha_{ext\_aero}+\alpha_{ext}(z))\right)\ dz \qquad [sr\ m]^{-1}$$

$$\beta_{mol\_atten}(z) = \int_0^z \beta_{mol}(z)\ \exp\left(-2\ (\alpha_{ext\_aero}+\alpha_{ext}(z))\right)\ dz \qquad [sr\ m]^{-1}$$

Observed unattenuated/attenuated MPL backscatters including backscatters from aerosols and molecules are output:

$$\beta_{obs} = \beta_{true} + \beta_{aero} + \beta_{mol} \qquad [sr\ m]^{-1}$$

$$\beta_{obs\_atten} = \beta_{atten} + \beta_{aero\_atten} + \beta_{mol\_atten} \qquad [sr\ m]^{-1}$$

Along with the true and attenuated backscatter, lidar ratio S, defined as the ratio between the lidar extinction and true backscatter is provided in the main output file.

$$S = \frac{\alpha_{ext}}{\beta_{true}} \qquad [\ -\ ]$$

Aerosol lidar ratio S_{aero} is also provided:

$$S_{aero} = \frac{\alpha_{ext\_aero}}{\beta_{aero}} \qquad [\ -\ ]$$

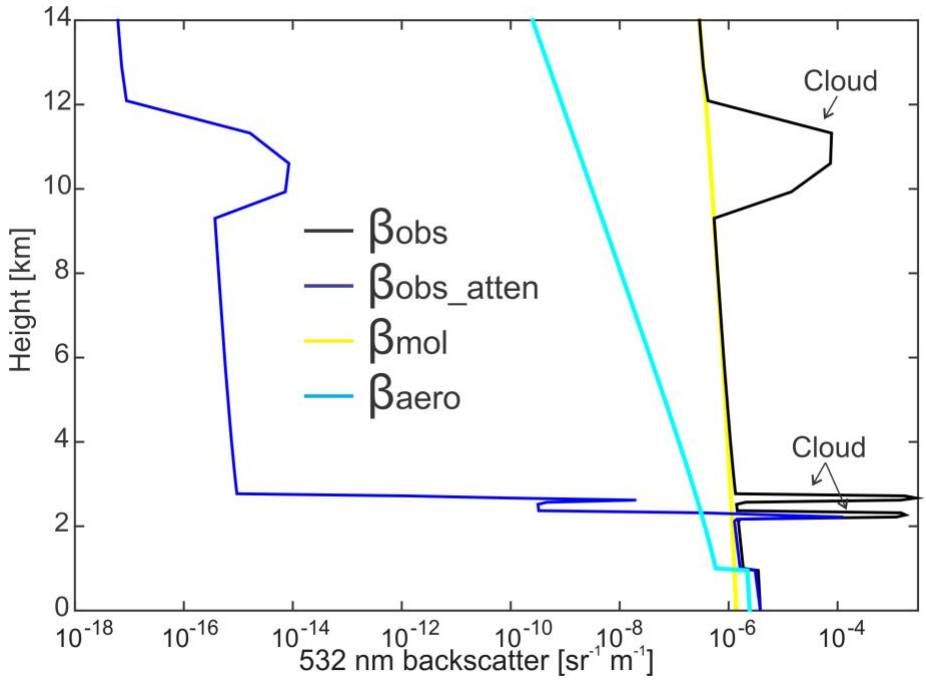

Figure 9: Example of simulated vertical profiles of β_{obs}, β_{obs_atten}, β_{mol}, and β_{aero} at a wavelength of 532 *nm*.

4.8 Computation of Doppler spectra

Computation of Doppler spectra has been implemented since version 3.1.1. Users can make an option of computation of Doppler spectra (spectraID=1) in the configuration file. The computation is based on Kollias et al. (2014). Computed backscattering power and fall velocity at each particle size are converted and interpolated into power at each spectrum velocity bin. Turbulence broadening are considered.

Parameters required for the computation are preset in crsim_mod.f90 as follows.

Integration time: 2.0 s

Pulse repetition frequency (PRF): 600.0 Hz for S band, 1240 Hz for C band, 2000 Hz for X band, 2700 Hz for Ka band, and 7500 Hz for W band

Noise power at 1 km: 0.0001 (linear unit)

Number of FFT points: 256

Nyquist velocity is calculated as [radar wavelength in m] * PRF/4 (m s^{-1}), and the number of spectral averages is [integration time] * PRF / NFFT.

4.9 Computation of surface backscatter

When the radar is steered toward the surface such as airborne radars, backscatter from the earth surface is not ignored. CR-SIM v4.0 includes computations of the surface reflectivity. The surface backscatter generally depends on incident angle and surface condition (e.g., Wu 1990; Freilich and Vanhoff 2003; Li et al., 2005; Battaglia et al. 2017). Over land, the computation of the surface backscatter is parameterized. Based on airborne radar observations, the land surface backscatters were represented as a function of incident angle as shown in Fig. 10. Black and gray lines in Fig 10 represent the observed surface radar backscatter cross section (σ_0) over road and wet snow. Generally, the surface backscatter decreases for coarse surface condition (i.e wet now). CR-SIM v4.0 uses the following equations:

$\sigma_0 = 6.767 \times exp(-0.293\theta) - 0.127\theta - 6.767$ for a coarse surface (purple line)

and

$\sigma_0 = 6.767 \times exp(-0.293\theta) - 0.127\theta + 8.223$ for a flat surface (brown line)

Over ocean, the surface backscatter can depend on sea surface temperature, salinity, and wind speed (Wu 1972; Wu 1990). In CR-SIM, the computation of the normalized radar cross section over the ocean surface is followed by Li et al. (2005), using a scattering model over ocean proposed by Wu (1990). In this method, the ocean surface is assumed isotropic and the surface wave distribution probability density is a function of the surface mean-square slope, $s(v)$. Then the normalized radar cross section over the ocean can be given as:

$$\sigma_0(\theta, v, \lambda) = \frac{|\Gamma_e(0,\lambda)|^2}{s(v)^2 cos^4(\theta)} exp\left[-\frac{tan^2(\theta)}{s(v)^2}\right]$$

where λ is the radar wavelength, v is surface wind speed, and $s(v)^2$is the effective mean square surface slope (Li et al. 2005). The ocean surface effective Fresnel reflection coefficient $\Gamma_e(0,\lambda)$ is computed using a method proposed by Klein and Swift (1977), accounting for a salinity. The default salinity value in CR-SIM is 38 ppt.

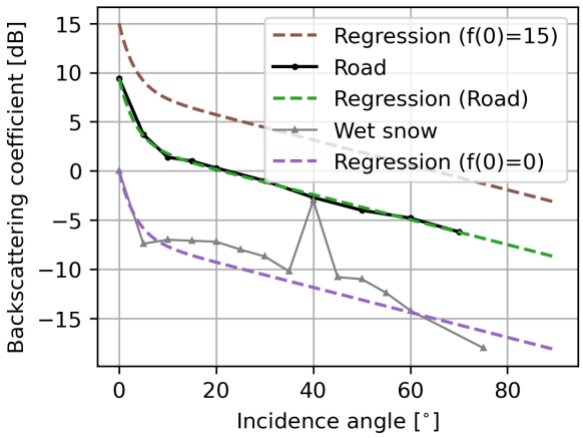

Figure 10: Backscatter coefficients as a function of incidence angle for different surface conditions: flat road (black solid line), wet snow (gray solid line). The green dashed line and purple dashed line represent fitted lines to the flat road and wet snow surface backscatter lines, respectively. Brawn dashed line represents a flat surface condition assumed in CR-SIM.

5 Post Processing: Simulation of Observational Value Added Products

Using simulated radar and lidar variables, the ARM Value Added Products (VAP) are simulated.

5.1 Active Remote Sensing of Clouds (ARSCL) VAP

Cloud location mask is provided from simulated zenith-pointing radar, ceilometer, and MPL measurements, when the ARSCL simulation option (arsclID=1) is selected.
First, observed zenith-pointing radar reflectivity, which takes account of attenuation and radar sensitivity, is estimated. For zenith-pointing radar, total attenuation (A_{tot}) at each gridbox is calculated as twice of sum of specific attenuation (A_h) from surface to a height at each column:

$$A_{tot}(z) = 2\int_0^z A_h(z)\,dz$$

The observed zenith pointing reflectivity Z_{obs} is estimated as subtracting A_{tot} from Z_{hh}:

$$Z_{obs} = Z_{hh} - A_{tot}$$

where if Z_{obs} value is less than radar minimum detectable reflectivity Z_{min}, the value is excluded.

Second, attenuated MPL hydrometeor backscatter (β_{hydro_atten}) is estimated. Since the MPL total backscatter includes aerosol backscatter and molecular backscatter (see section 4.7), β_{hydro_atten} is obtained as subtracting β_{aero_atten} and β_{mol_atten} from β_{obs_atten}. If obtained β_{hydro_atten} is less than the background scatter ($\beta_{aero} + \beta_{mol}$), the value is excluded. Theoretically, when there is hydrometeor attenuation, the background scatter is also decreased. However, in MPL measurements of real atmosphere, attenuated backscatter includes strong noisiness, which makes it difficult to detect hydrometeor signals below the no-attenuated background scatter. Therefore, the no-attenuated background scatter ($\beta_{aero} + \beta_{mol}$) is used as the MPL minimum detectable value in this simulation.

A gridbox is indexed as a 'cloudy' gridbox when Z_{obs} or β_{hydro_atten} has a detectable value, but gridboxes below simulated ceilometer first cloud base are indexed as 'clear'.

Heights of cloud layer base/top are also reported up to 10 cloud layers at each column. Output parameters from the ARSCL simulation is listed in Table 20 and shown in Figure 10.

Table 20: List of dimension and output variables from the ARSCL simulation.

DIMENSION NAMES	Description
nx	Number of grid boxes along the horizontal E-W axis
ny	Number of grid boxes along the horizontal S-N axis
nz	Number of grid boxes along the vertical axis at WRF resolution
n_layers	Number of maximum cloud layers reported

VARIABLE	DIMENSION	UNITS	DESCRIPTION	Comment
arscl_cloud_mask	[nx, ny, nz]	-	Cloud mask from radar, MPL, and ceilometer observations	Flag 0 = 'clear'; Flag 1 = 'cloudy'. Computed if arsclID=1
arscl_cloud_source_flag	[nx, ny, nz]	-	Instrument source flag for cloud detection	Flag 1 = "Clear according to radar and MPL"; Flag 2 = "Cloud detected by radar and MPL"; Flag 3 = "Cloud detected by radar only"; Flag 4 = "Cloud detected by MPL only". Computed if arsclID=1
arscl_cloud_layer_base_height	[nx, ny, n_layers]	*m*	Base height of cloudy layers for up to 10 layers	Computed if arsclID=1
arscl_cloud_layer_top_height	[nx, ny, n_layers]	*m*	Top height of cloudy layers for up to 10 layers	Computed if arsclID=1

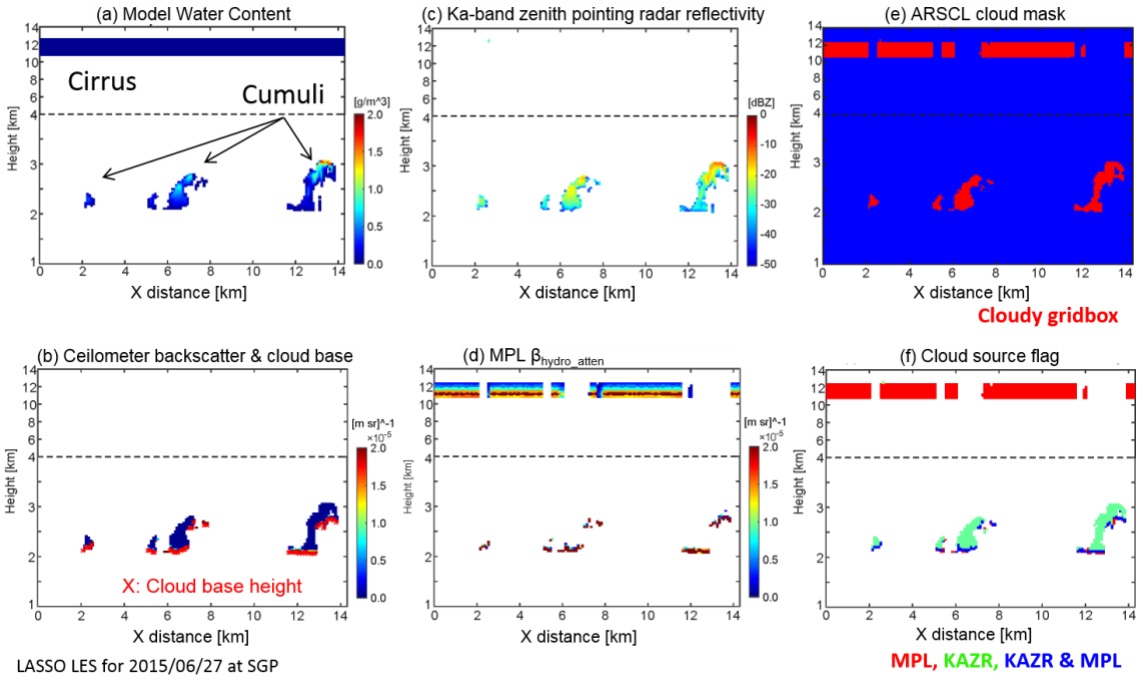

Figure 11: Vertical cross sections of (a) WRF-simulated water content, (b) CR-SIM ceilometer backscatter, (c) CR-SIM Ka-band zenith-pointing radar attenuated reflectivity, (d) CR-SIM MPL attenuated hydrometeor backscatter, (e) CR-SIM ARSCL cloud mask, and (f) CR-SIM ARSCL cloud source flag. Red cross marks in (b) represent ceilometer first cloud bases. Model horizontal grid space is 100 *m*.

5.2 Microwave Radiometer (MWR) Liquid Water Path (LWP)

Microwave radiometer (MWR) measurements can provide liquid water path (LWP) VAD. The field of view of MWR is sometimes larger as it includes more than one gridbox. The CR-SIM optionally calculates MWR-observed LWP taking account of its field of view, when mwrID=1 is selected. Note that this simulation does not calculate MWR scattering, but just considers the field of view.

The MWR field of view (in degrees) can be specified by users in Configuration file. The number of gridboxes included in the horizontal field of view increases with height (Figure 11a). Liquid water contents (LWCs) are averaged over gridboxes within the horizontal field of view using Gaussian weights as a function of distance between the center of the field of view and a gridbox. The MWR LWP is calculated as integration of the weighted average of LWC from the ground to model top at each column. Output parameters from the MWR LWP are listed in Table 21, and example is shown in Figure 11.

Table 21: List of dimension and output variables from the MWR LWP simulation.

DIMENSION NAMES	Description
nx	Number of grid boxes along the horizontal E-W axis
ny	Number of grid boxes along the horizontal S-N axis
nz	Number of grid boxes along the vertical axis at WRF resolution

VARIABLE	DIMENSION	UNITS	DESCRIPTION	Comment
model_lwp	[nx, ny]	$kg\ m^{-2}$	Model liquid water path	Computed if mwrID=1
mwr_lwp	[nx, ny]	$kg\ m^{-2}$	Microwave radiometer liquid water path taking account of field of view	Computed if mwrID=1
number_of_grid points_mwrlwp	[nx, ny, nz]	-	Number of gridboxes within MWR horizontal field of view	Computed if mwrID=1

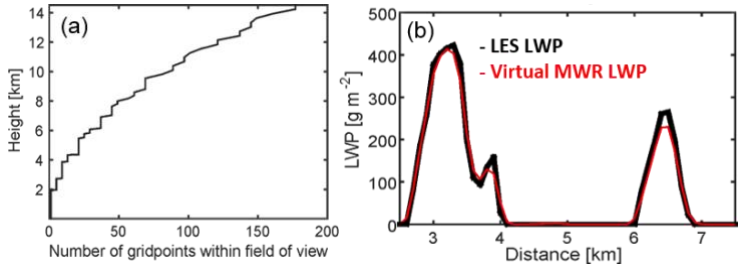

Figure 12: (a) Vertical distribution of number of gridboxes within the MWR field of view of 5.9°, and (b) model-simulated LWP (black) and CR-SIM MWR LWP (red). Model horizontal grid space is 100 m.

6 Change history since the initial release of the model

-version 4.0 (Aug. 2024)

Incorporated water vapor attenuation.
Fixed a bug for computation of SW_t.
Fixed a bug for obtaining pressure values for RAMS.
Add calculations for negative elevation angles.
Add computations of the earth's surface backscatter.
Add computation of Doppler velocity accounting for the instrument's moving speed (DV_airborne).
Fixed some bugs for test runs.
Released through GitHub.
Changed contact persons.

-version 3.3.3

Incorporated CM1 model coupled with Morrison 2-moment scheme.
Fixed bugs for obtaining grid spacings for RAMS and SAM (this affected spectrum width computations).
Fixed an issue occasionally happening when reading WRF Thompson solid hydrometeor species.

-version 3.3.2 (Dec 18, 2019)

Included computation of new radar polarimetric variable cross-correlation coefficient

---

-version 3.3.1 (Sept 09, 2019)

Fixed bug causing the test 1 to periodically pass and fail.

---

version 3.3.0 (Sep 03 2019) publicly released version _

-Aug 2019

Modified computation of the specific attenuation at horizontal and vertical polarizations to include the dependencies of Ah and Av on the angular moments

Improved stability of the software

Corrected inconsistencies when using real instead of double precision variables corrected in all files

The tolerance for all the tests modified from 1.e-10 to 1.e-4

The module wrf_var_mod.f90 copied to module wrf_rvar_mod.f90. Created the new wrf_var_mod.f90 with the same types and subroutines as wrf_rvar_mod.f90 but in double precision. The structures from wrf_rvar_mod.f90 are used for reading the input model data which are then copied and saved to corresponding structures from wrf_var_mod.f90.

Indentation introduced in ReadInpWRFFile.f90 and ReadInpRAMSFile.f90

Work on implementation of observations made by airborne scanning radar

-Jul 2019

Adapted cloud number concentration and mu for rain in P3 for WRF v4.1.

Fixed bug in hydro_icon (max and minimum values for rain mixing ratio at each diameter bin).

Work on implementation of observations made by airborne scanning radar

version 3.2 (Feb 2019) publicly released version _

-Dec 2018

Updated processor version (configure.ac)

Introduced progress messages in percentage

The main code and file crsim_subrs.f90 cleaned and introduced indentation.

-Nov 2018

Fixed bug in test script when reporting if the test passes or fails

Added the new test with RAMS 2-moments microphysical scheme

Modified Makefile.am files so that 'make clean' does not remove configuration files

-Nov 2018

Added a new module phys_param_mod.f90 that should include all the physical parameters and constants used throughout the CR-SIM. The idea is to gradually exclude the use of hard-coded values.

-Nov 2018

Introduced the parameter maxNumOfHydroTypes equal to the maximal number of hydrometeor types allowed (currently 8 for RAMS, MP=40). Corrected dimension for those variables whose dimension was not updated (i.e. was equal to less than maxNumOfHydroTypes)

-Nov 2018

Modified parts of the code with Doppler spectra generator for bulk moment microphysics.

-Oct 2018

Incorporated a retrieval of particle size distribution parameters which are used in the Thompson scheme's reflectivity calculation in WRF instead of those described in Thompson et al. (2008 & 2004)

-Jun 17 2018

Incorporated SAM Morrison 2-moment microphysics (MP_PHYSICS=75).

-May 27 2018

Incorporated Doppler spectra generator.

-Apr 2018

Incorporated SAM warm bin microphysics (MP_PHTSICS=70).

version 3.1 (March 2018) publicly released version

-Mar 17 2018

Fixed bug in subroutine gcf: values an and b are properly defined inside of do loop.

Look-up tables for graupel density 500 kg m-3 added.

-Mar 15 2018

The name of the I/O files removed from the configuration file "PARAMETERS". The model is now invoked via command line arguments.

-Mar 13 2018

Improved automake configuration: written out configure script, automake files and test scripts. Installation of the model is simplified and is achieved via "configure", "make", "make check", "make install" and "make installcheck" steps.

The license changed from GNU LESSER GENERAL PUBLIC LICENSE to **GNU GENERAL PUBLIC LICENSE**.

-Mar 12 2018

The CR-SIM folder structure somewhat modified. Location of the scattering libraries is fixed (share/scrsim/aux/) and all auxiliary files are placed under the aux directory.

-Mar 12 2018

Several bugs fixed, no significant impact on final simulation results.

-Feb 22 2018

Implemented automake configuration and updated Configuration File so that the number of OpenMP threads can be specified by users.

-Oct 30 2017

Incorporated P3 microphysics

version 3.0 (August, 2017) publicly released version

-July 21 2017

Incorporated the RAMS input and its 2-moment microphysics scheme

-July 17 2017

Incorporated the ICON input and its 2-moment microphysics scheme
Modified ceilometer and MPL simulation subroutines to work with z decreasing with index

-June 30 2017

Implemented "__PRELOAD_LUT__" mode and related subroutines are implemented in crsim_subrs.f90. OpenMP parallelization is applied.

version 2.3 (17 07 2017) publicly released version

-June 7 2017

Added the pre-calculated scattering properties of the ice particles in P3 microphysics scheme in /aux/LLUTS3/

-May 20 2017

Added the pre-calculated particle size distribution parameters of the ice particles in P3 microphysics scheme (p3_ice_psd_para_lookup_table.dat)

- May 17 2017

Postprocessing: ARSCL and MWR LWP are implemented.

---

version 2.2 (12 05 2016) publicly released version

- May 17 2017

Fixed Thompson microphysics subroutine (hydro_thompson and get_hydro08_vars).

- Sep 19 2016

Incorporated Thompson microphysics scheme.

- May 12 2016

Included computation of molecular backscatter in MPL measurements.

- May 9 2016

Included computation of aerosol average profile in MPL measurements.

- May 2 2016

  Included computation of micro pulse lidar (MPL) measurements for cloud and ice hydrometeors.

---

version 2.1 (25 04 2016) publicly released version (third release)

- Apr 19 2016

  New variables written in the output NetCDF files: rad_ixc, rad_iyc, rad_zc

- Apr 18 2016

  New variables written in the output NetCDF files: rad_freq, rad_beamwidth and rad_range_resolution

- Apr 18 2016

  Corrected bug in expression for Kazim in subroutine determine_sw_contrib_terms (removed term dcos(elev*d2r) from the expression)

- Mar 26 2016

  Subroutine get_hydro_vars is modified to work for MP_PHYSICS=9. For this reason get_hydro_vars is splitted out to 2 subroutines: get_hydro10_vars and get_hydro09_vars. In the case of Morrisson scheme, a possibility of the input cloud liquid total concentration /=0 is taken into account.

- Mar 26 2016

  In all soubrutines GetPolarimetricInfofromLUT*, when selecting the LUTs densities for hydrometeor isc the line "if (isc==5)" is replaced by "if (isc>=5)" in order to account not only graupel but hail also

---

version 2.0 (23 02 2016) publicly released version (second release)

- Feb 18 2016

  Corrected bug in sign when computing Doppler velocity at elevations different than 90 deg. All velocities are now positive away from the radar (radar notation).

- Feb 17 2016

  Included new variable diff_back_phase in the polarimetric output. Affected structures are mout_var and mrad_var, as well as all the subroutines for allocating, deallocating and nullifying those structures.

- Feb 17 2016

  Included computation od cloud lidar (ceilometer) measurements:

  1. included new configuration parameter ceiloID for whether or not to include cloud lidar measurements
  2. included new structure subroutine lout_var containing the cloud lidar output variables. Also written are new subroutines for allocating, deallocating and nullifying lout variables.
  3. a new subroutine written: GetCloudLidarMeasurements for cloud lidar (ceilometer) simulated measurements
  4. written new optional output variables: lidar observed and true backscatter, extinction coeff., lidar ratio and the first cloud base as observed by ceilometer

- Feb 16 2016

  Added LLUTS3/ceilo/cld_ceilo_905nm_p25.dat data file containing the extinction and backscattering cross sections for spherical particles at 905 nm. The used code for electromagnetic scattering by a single homogenous sphere is the "BHMIE' created by Craig F., Bohren and Donald Ronald Huffman 1983, and available at:
  https://en.wikipedia.org/wiki/Codes_for_electromagnetic_scattering_by_spheres#Codes_for_electromagnetic_scattering_by_a_single_homogeneous_sphere

- Feb 15 2016

Introduced new output variable Z_MIN for the radar sensitivity limitation with range

$$Z\_MIN = ZMIN[dBZ] + 20 \log10 (range[km])$$

1. Included new variable "range" in the rmout structure. Subroutines for allocating, deallocating and nullifying rmout_var variables are accordingly modified. Range is also reported in the output NetCDF file.
2. included new configuration parameter ZMIN, a coefficient in expression for radar sensitivity limitation with range.

- Feb 15 2016

The attribute "missing_value" in the subroutine for writing the NetCDF output is replaced by "_FillValue".

---

version 1.2 (16 01 2016) This version v1.2 is intended for testing prior to official release

---

- Jan 14 - Jan 15 2016:

Included computation of the spectrum width contributions due to turbulence, wind shear in radar volume and cross-wind:

1. included a new variable sw_t in the rmout structure (spectrum width due to the turbulence contribution only). Subroutines for allocating, deallocating and nullifying rmout_var variables are accordingly modified.
2. included new wind shear variables Ku, Kv and Kw to the structure env_var. Subroutines for allocating, deallocating and nullifying env_var variables are accordingly updated.
3. included new variables sw_s and sw_v in the rmout structure (spectrum width due to wind shear in radar volume and due to cross wind, respectively). Subroutines for allocating, deallocating and nullifying rmout_var variables are accordingly modified.
4. included contributions of wind shear and cross-wind to the spectrum width in subroutine determine_sw_contrib_terms. The wind shear computations are added in get_env_vars.
5. included new variables SWt (total spectrum width due to turbulence, wind shear in radar volume, cross-wind and hydrometeor fall velocity) per hydrometeor and SWt_tot (for all hydrometeors) in the rmout structure. Subroutines for allocating, deallocating and nullifying rmout_var variables are accordingly modified. Those new variables are written in the output NetCDF files.
6. Modified subroutine for writing the NetCDF output: changed name of the spect. width variable SPh to SWh (and SPh90 to SWh90) and this is now sp. width due to hydrometeor contribution. Added to the output are: SWt (spectrum width due to turbulence) and SWtot (total spectrum width), and also SWs (spectrum width due to wind chear in radar volume) and SWv (spectrum width due to cross-wind)

- Jan 13 2016:

Fixed bug in reported Zvh. This variable has not been reported in logarithmic but linear units.

- Jan 13 2016:

Included xlat, xlong and tke (turbulence kinetic energy) in the structure env_var. Subroutines for allocating, deallocating and nullifying env_var variables are accordingly updated. Xlat,xlong are also included in the output NetCDF file.

- Jan 13 2016:

New configuration variables Theta1 and dr (beamwidth and range resolution respectively) are added. Also incorporated variables are the ones computed using Theta1 and dr, sigma_theta and sigma_r, needed for the spectrum width computations. See CR-SIM v2.0 or latest User Guide for more details.

- Jan 12 2016:

Added new subroutine "determine_sw_contrib_terms" that will contain computation of the spectrum width due to different contributions. The contribution due to turbulence is codded and verified.

- Jan 12 2016:

Modified subroutine get_env_vars in order to include xlat, xlong and and tke variables

- Jan 12 2016:

  The new parameters in the crsim Configuration file are introduced: the minimum values of the input mixing ratios for hydrometeor species. Mixing ratio values smaller or equal than specified thresholds are set to 0. If MP_PHYSICS=20, in the pixels where computed mixing ratio is <= specified threshold, the input bin total number distributions are set to zeroes. The structure conf_var is modified, as well as subroutine ReadConfParameters.f90.

- Jan 12 2016:

  Modified subroutine get_hydro_vars. Input mixing ratios and total number distributions are set to zero if mixing ratio is lower than the input threshold value and if the input N <0.

- Jan 12 2016:

  Added the "missing_value" attribute (=-999) for most of the output variables in the subroutine WriteOutNetcdf.

- Jan 11 2016:

  Included threshold value Zthr (= -100 dBZ) of minimum reflectivity such that:

  1. if Zhh>Zthr => Zhh,Ah and all Doppler-related variables exist
  2. if Zvv>Zthr => Zvv, Av exist
  3. if both Zhh,Zvv > Zthr => all other polarimetric variables exist (Zvh,Zdr,LDR,Kdp,Zdr).

- Jan 11 2016:

  Control variable hmask is removed as it is now obsolete.

- Jan 08 2016:

  In the WriteOutNetcdf subroutine description attributes for velocity variables are slightly modified to account for change in notation for Doppler velocity output variables.

- Jan 06 2016:

  Change of sign for all velocities. In previous versions velocities are defines as positive downward i.e. towards the radar. Now we follow the radar convention where velocity is positive upward, i.e. away from the radar.

- Jan 05 2016:

  Corrected bug in unrealistic Zdr_tot and LDRh_tot reported in the output (due to incorrectly placed line for change from linear to logarithmic units for rmout%Zhh_tot).

- Jan 04 2016:

  Added few lines at the end of subroutine get_hydro20_vars that remove negative values of the input bin concentrations for MP_PHYSICS==20.

- Jan 04 2016:

  Fixed bug: added few missing lines for writing the u and v variables into the NetCDF files for different species.

- Oct 20 2015:

  Corrected issue with dlog10 (0.d0) appearing in computations

- Oct 15 2015:

  Added air density (density of dry air) to the output list

---

version 1.1 (23 09 2015)

- Sep 15 - Sep 23 2015:

  Following changes are introduced in order to compute the radial Doppler velocity and spectrum width

$$Vr = \cos(el)\,[u\cos(az) + v\sin(az)] + (-w + fvel)\sin(el)$$

1.included horizontal wind variables u and v in the structure env_var. Subroutines for allocating, deallocating and nullifying env_var variables are accordingly modified.
2. included horizontal wind in subroutine get_env_vars. The horizontal wind variables are required to be part of the input WRF file.
3. written a new subroutine "determine_azimuth".The azimuth is needed in expression of forward radial velocity and is written in the output NetCDF file.
4. added a new variable azim in the rmout structure.
5. included new variables in the structure rmout for Doppler velocity and Spectrum Width. Now those variables are computed for both slant and nadir view. Subroutines for allocating, deallocating and nullifying rmout variables are accordingly updated.
6. Changed the order of the output vars in the NetCDF file. The existing Doppler variables are no more vertical but for given elevation and azimuth. Introduced are new variables DV90 and SPh90 for vertical (elevation=90) pointing. Horizontal wind from input is also reported in the output.

- Sep 15 2015:

The bug fixed - change of the filenames of the ice species (ice_ar0.20 and ice_ar0.90) for 5 GHz: the frequency string in the name "fr05.0GHz" is replaced with "fr05.5GHz" for the sake of consistency.

---

version 1.0 (01 05 2015) **The first release of the model**

---

7 References

Andsager, K., K. V. Beard, and N. F. Laird, 1999: Laboratory measurements of axis ratios for large drops. J. Atmos. Sci.,56,2673–2683.

Battaglia, A., M. Wolde, L. P. D'Adderio, C. Nguyen, F. Fois, A. Illingworth, and R. Midthassel, 2017: Characterization of Surface Radar Cross Sections at W-Band at Moderate Incidence Angles. *IEEE Transactions on Geoscience and Remote Sensing*, 55, no. 7, pp. 3846-3859, doi: 10.1109/TGRS.2017.2682423.

Beard, K. V., 1976: Terminal velocity and shape of cloud and precipitation drops aloft. J. Atmos. Sci., 33, 851–864.

Bohren, Craig F. and Donald R. Huffman, Absorption and scattering of light by small particles, New York : Wiley, 1998, 530 p., ISBN 0-471-29340-7, ISBN 978-0-471-29340-8 (second edition)

Brandes, E. A., G. Zhang, and J. Vivekanandan, 2002: Experiments in rainfall estimation with a polarimetric radar in a subtropical environment. J. Appl. Meteor., 41, 674–685

Brown, P. R. A., and P. N. Francis, 1995: Improved measurements of the ice water content in cirrus using a total water probe. J. Atmos. Oceanic Technol., 12, 410–414.

Bryan, G. H., and J. M. Fritsch, 2002: A benchmark simulation for moist nonhydrostatic numerical models. Mon. Wea. Rev., 130, 2917–2928, https://doi.org/10.1175/1520-0493(2002)130,2917:ABSFMN.2.0.CO;2.

Cao, Q., G. Zhang, E. Brandes, T. Schuur, A. Ryzhkov, and K. Ikeda, 2008: Analysis of video disdrometer and polarimetric radar data to characterize rain microphysics in Oklahoma. J. Appl. Meteor. Climatol., 47, 2238–2255.

Cotton, W. R. et al., 2003: RAMS 2001: Current status and future directions, *Meteorol. Atmos. Phys*., 82(1), 5–29, doi:10.1007/s00703-001-0584-9.

Doviak, R. J., and D. S. Zrnic, 2006: Doppler radar and weather observations, 2nd ed., San Diego, Academic Press, Second Addition

Feingold, G., S. M. Kreidenweis, B. Stevens, and W. R. Cotton, 1996: Numerical simulations of stratocumulus processing of cloud condensation nuclei through collision-coalescence, *J. Geophys. Res*., 101(D16), 21,391–21,402, doi:10.1029/96JD01552.

Fan, J., Leung, L. R., Li, Z., Morrison, H., Chen, H., Zhou, Y., Qian, Y., and Wang, Y.: Aerosol impacts on clouds and precipitation in eastern China: Results from bin and bulk microphysics, J. Geophys. Res., 117, D00K36, 2012.

Ferrier, B. S., 1994: A double-moment multiple-phase four-class bulk ice scheme. J. Atmos. Sci., 51,249–280.

Garnett Maxwell, J. C., 1904: Color in metal glasses and in metallic films. Philos. Trans. Roy. Soc. London, A203, 385–420.

Gunn, R., and G. D. Kinzer, 1949: The terminal velocity of fall for water droplets in stagnant air. J. Meteor., 6, 243–244.

Hale, G. M., and M. R. Querry, 1973: Optical constants of water in the 200 nm to 200 m wavelength region. *Appl. Opt.*, 12, 555– 563.

Heymsfield, A. J., 2003: Properties of tropical and midlatitude ice cloud particle ensembles. Part II: Applications for mesoscale and climate models. J. Atmos. Sci., 60, 2592–2611.

Heymsfield, A. J., A. Bansemer, and C. H. Twohy, 2007: Refinements to ice particle mass dimensional and

terminal velocity relationships for ice clouds. Part I: Temperature dependence. *J. Atmos. Sci.*, 64, 1047–1067.

Hogan, R.J., L. Tian, P.R. Brown, C.D. Westbrook, A.J. Heymsfield, and J.D. Eastment, 2012: Radar Scattering from Ice Aggregates Using the Horizontally Aligned Oblate Spheroid Approximation. J. Appl. Meteor. Climatol., 51, 655–671, https://doi.org/10.1175/JAMC-D-11-074.1

Khairoutdinov, M. F., and D.A. Randall, 2002: Similarity of deep continental cumulus convection as revealed by a three-dimensional cloud resolving model. *J. Atmos. Sci*., 59, 2550-2566.

Klein, L. and C. Swift:1977: An improved model for the dielectric constant of sea water at microwave frequencies, IEEE Transactions on Antennas and Propagation, vol. 25, no. 1, pp. 104-111, January 1977, doi: 10.1109/TAP.1977.1141539.

Kollias, P, and S. Tanelli, A. Battaglia, A. Tatarevic, 2014: Evaluation of EarthCARE cloud profiling radar Doppler velocity measurements in particle sedimentation regimes. *J. Atmos. Oceanic Technol.*, 31, 366-386.

Li, L., G. M. Heymsfield, L. Tian, and P. E. Racette, 2005: Measurements of Ocean Surface Backscattering Using an Airborne 94-GHz Cloud Radar—Implication for Calibration of Airborne and Spaceborne W-Band Radars. *J. Atmos. Oceanic Technol*., 22, 1033–1045, https://doi.org/10.1175/JTECH1722.1.

Martin, G. M., D. W. Johnson, and A. Spice, 1994: The measurement and parameterization of effective radius of droplets in warm stratocumulus clouds. J. Atmos. Sci., 51, 1823–1842.

Meyers, M. P., R. L. Walko, J. Y. Harrington, and W. R. Cotton, 1997: New RAMS cloud microphysics parameterization. Part II: The two-moment scheme, *Atmos. Res*., 45(1), 3–39, doi:10.1016/S0169-8095(97)00018-5.

Milbrandt, J. A., and M. K. Yau, 2005a: A multimoment bulk microphysics parameterization. Part I: Analysis of the role of the spectral shape parameter. J. Atmos. Sci., 62, 3051–3064.

Milbrandt, J. A. and H. H. Morrison, 2016: Parameterization of Cloud Microphysics Based on the Prediction of Bulk Ice Particle Properties. Part III: Introduction of Multiple Free Categories. J. Atmos. Sci., 73, 975–995.

Milbrandt, J. A., and M. K. Yau, 2005b: A multimoment bulk microphysics parameterization. Part II: A proposed three-moment closure and scheme description. J. Atmos. Sci., 62, 3065–3081.

Mishchenko M. I. and Travis L. D., 1998: Capabilities and limitations of a current FORTRAN implementation of the T-matrix method for randomly oriented, rotationally symmetric scatterers, J. Quant. Spectrosc. Radiat. Transfer 60, 309–324.

Mishchenko, M. I., 2000: Calculation of the amplitude matrix for a nonspherical particle in a fixed orientation. Appl. Opt., 39, 1026–1031.

Mitchell, D. L., and A. J. Heymsfield, 2005: The treatment of ice particle terminal velocities, highlighting aggregates. J. Atmos. Sci., 62, 1637–1644.

Mitchell, D. L., 1996: Use of mass- and area-dimensional power laws for determining precipitation particle terminal velocities. J. Atmos. Sci., 53, 1710–1723.

Morrison, H., J. A. Curry, and V. I. Khvorostyanov, 2005: A new double-moment microphysics parameterization for application in cloud and climate models. Part I: Description. J. Atmos. Sci., 62, 1665–1677.

Morrison, H., G. Thompson, and V. Tatarskii, 2009: Impact of cloud microphysics on the development of trailing stratiform precipitation in a simulated squall line: Comparison of one- and two-moment schemes. Mon. Wea. Rev., 137, 991–1007.

Morrison, H. and J. A. Milbrandt, 2015: Parameterization of Cloud Microphysics Based on the Prediction of Bulk Ice Particle Properties. Part I: Scheme Description and Idealized Tests. J. Atmos. Sci., 72, 287–311.

Morrison, H., J. A. Milbrandt, G. H. Bryan, K. Ikeda, S. A. Tessendorf, and G. Thompson, 2015: Parameterization of Cloud Microphysics Based on the Prediction of Bulk Ice Particle Properties. Part II: Case Study Comparisons with Observations and Other Schemes. J. Atmos. Sci., 72, 312–339

O'Connor, Ewan J., Anthony J. Illingworth, and Robin J. Hogan. "A Technique for Autocalibration of Cloud Lidar." Journal of Atmospheric & Oceanic Technology 21, no. 5 (2004).

Oue, M. (2024). Radar and Lidar scattering lookup tables for atmospheric hydrometeors using a T-Matrix method and a Mie theory (1.0) [Data set]. Zenodo. https://doi.org/10.5281/zenodo.13345093

Spinhirne, J. D. 1993: Micro Pulse Lidar. IEEE Transactions on Geoscience and Remote Sensing, 31, 48–55.

Simmel, M., T. Trautmann, and G. Tetzlaff, 2002: Numerical solution of the stochastic collection equation comparison of the linear discrete method with other methods. Atmos. Res., 61, 135–148.

Rosenkranz, P. W., 1998: Water vapor microwave continuum absorption: A comparison of measurements and models, *Radio Sci*., 33, 919–928, https://doi.org/10.1029/98RS01182.

Ryzhkov Alexander V., 2001: Interpretation of Polarimetric Radar Covariance Matrix for Meteorological Scatterers: Theoretical Analysis. *J. Atmos. Oceanic Technol.*, 18, 315–328.

Ryzhkov A., M. Pinsky, A. Pokrovsky, and A. Khain, 2011: Polarimetric Radar Observation Operator for a Cloud Model with Spectral Microphysics. *J. Appl. Meteor. Climatol.*, 50, 873–894.

Saleeby, S. M., and W. R. Cotton, 2004: A Large-Droplet Mode and Prognostic Number Concentration of Cloud Droplets in the Colorado State University Regional Atmospheric Modeling System (RAMS). Part I: Module Descriptions and Supercell Test Simulations, *J. Appl. Meteorol*., 43(1), 182–195, doi:10.1175/1520-0450(2004)043<0182:ALMAPN>2.0.CO;2.

Saleeby, S. M., and S. C. van den Heever, 2013: Developments in the CSU-RAMS Aerosol Model: Emissions, Nucleation, Regeneration, Deposition, and Radiation, *J. Appl. Meteorol. Climatol*., 52(12), 2601–2622, doi:10.1175/JAMC-D-12-0312.1.

Seifert, A., 2008：On the parameterization of evaporation of raindrops as simulated by a one-dimensional rainshaft model, *J. Atmos. Sci.* 65, 3608-3619.

Seifert, A. and K. D. Beheng, 2006: A two-moment cloud microphysics parameterization for mixed-phase clouds. Part 1: Model description. *Moteorol. Atmos. Phys*., 92, 45-66.

Straka Jerry M., Zrnić Dusan S., and Ryzhkov Alexander V., 2000: Bulk Hydrometeor Classification and Quantification Using Polarimetric Radar Data: Synthesis of Relations. *J. Appl. Meteor.*, 39, 1341–1372.

Thompson, G., P. R. Field, R. M. Rasmussen, and W. D. Hall, 2008: Explicit forecasts of winter precipitation using an improved bulk microphysics scheme. Part II: Implementation of a new snow parameterization. Mon. Wea. Rev., 136, 5095–5155.

Trömel, Silke; Kumjian, Matthew R; Ryzhkov, Alexander V; Simmer, Clemens; Diederich, Malte. Journal of Applied Meteorology and Climatology 52.11 (Nov 2013): 2529-2548.

Tzivion, S., G. Feingold, and Z. Levin, 1987: An efficient numerical solution to the stochastic collection equation, J. Atmos. Sci., 44, 3139-3149.

Vivekanandan, J., W.M. Adams and V.N. Bringi, 1991: Rigorous approach to polarimetric radar modeling of hydrometeor orientation distributions. *J. Appl. Meteor*., 30, 1053-1063.

Vivekanandan, J., R. Raghavan, and V. N. Bringi, 1993: Polarimetric radar modeling of mixture of precipitation particles. IEEE Trans. Geosci. Remote Sens., 31, 1017–1030.

Walko, R. L., W. R. Cotton, M. P. Meyers, and J. Y. Harrington, 1995: New RAMS cloud microphysics parameterization part I: the single-moment scheme, *Atmos. Res*., 38(1-4), 29–62, doi:10.1016/0169-8095(94)00087-T.

Wu, J., 1972: Sea-Surface Slope and Equilibrium Wind-Wave Spectra. Phys. Fluids, 15 (5), 741–747. https://doi.org/10.1063/1.1693978

Wu, J., 1990: Mean square slopes of the wind-disturbed water surface, their magnitude, directionality, and composition, Radio Sci., 25(1), 37–48, doi:10.1029/RS025i001p00037.